ABSTRACT

Title of dissertation: Propellant Injection Strategy for Suppressing Acoustic Combustion Instability

Qina Diao, Doctor of Philosophy, 2010

Dissertation directed by: Associate Professor Kenneth Yu
Department of Aerospace Engineering

Shear-coaxial injector elements are often used in liquid-propellant-rocket thrust chambers, where combustion instabilities remain a significant problem. A conventional solution to the combustion instability problem relies on passive control techniques that use empirically-developed hardware such as acoustic baffles and tuned cavities. In addition to adding weight and decreasing engine performance, these devices are designed using trial-and-error methods, which do not provide the capability to predict the overall system stability characteristics in advance. In this thesis, two novel control strategies that are based on propellant fluid dynamics were investigated for mitigating acoustic instability involving shear-coaxial injector elements.

The new control strategies would use a set of controlled injectors allowing local adjustment of propellant flow patterns for each operating condition, particularly when instability could become a problem. One strategy relies on reducing the oxidizer-fuel density gradient by blending heavier methane with the main fuel, hydrogen. Another strategy utilizes modifying the equivalence ratio to affect the acoustic impedance through mixing and reaction rate changes. The potential ef-

fectiveness of these strategies was assessed by conducting unit-physics experiments. Two different model combustors, one simulating a single-element injector test and the other a double-element injector test, were designed and tested for flame-acoustic interaction. For these experiments, the Reynolds number of the central oxygen jet was kept between 4700 and 5500 making the injector flames sufficiently turbulent. A compression driver, mounted on one side of the combustor wall, provided controlled acoustic excitation to the injector flames, simulating the initial phase of flame-acoustic interaction. Acoustic excitation was applied either as band-limited white noise forcing between 100 Hz and 5000 Hz or as single-frequency, fixed-amplitude forcing at 1150 Hz which represented a frequency least amplified by any resonance. Effects of each control strategy on flame-acoustic interaction were assessed in terms of modifying the acoustic resonance characteristics subject to white-noise excitation and changes in flame brush thickness under single-frequency excitation.

In the methane blending experiments, the methane mole fraction was varied between 0% and 63%. Under white noise excitation, up to 16% shift in a resonant frequency was observed but the acoustic pressure spectra remained qualitatively similar. For the fixed frequency forcing, the spatial extent of flame-acoustic interaction was substantially reduced. In the other experiments, the equivalence ratio of the control injector was varied between zero and ∞, causing up to 40% shift in a resonant frequency as well as changes in the acoustic pressure spectrum. These results open up the possibility of employing flow-based control to prevent combustion instabilities in liquid-fueled rockets.

Propellant Injection Strategy for Suppressing Acoustic Combustion Instability

by

Qina Diao

Dissertation submitted to the Faculty of the Graduate School of the
University of Maryland, College Park in partial fulfillment
of the requirements for the degree of
Doctor of Philosophy
2010

Advisory Committee:
Associate Professor Kenneth H. Yu, Chair/Advisor
Associate Professor Robert M. Sanner, Co-Chair/Co-Advisor
Professor Ashwani K. Gupta
Assistant Professor J. Sean Humbert
Assistant Professor Ray Sedwick

Dedication

To my dearest grandma and parents for their love and support.

Acknowledgments

I am grateful to all the people who have made this thesis possible and because of whom my Ph.D graduate experience has been one that I will cherish forever.

First of all I would like to sincerely thank my faculty advisor, Dr. Kenneth Yu, for giving me the opportunity to work on this challenging project and for his insightful guidance over the past five years. His enthusiasm and great knowledge have been invaluable in opening my eyes and helping carry out my research. My attitude and ability for research, from which I can benefit for the rest of my life, have been significantly improved with his enormous help and patience.

I am also grateful to my co-advisor, Dr. Robert Sanner, for his deep thoughts, discussions and the helpful comments he has provided regarding this dissertation. All the courses I took with him rank as the best I have had. Dr. Sanner taught us not only by providing knowledge, but also by broadening our views on all control topics. I would like to thank my committee members Dr. Ashwani Gupta, Dr. Ray Sedwick and Dr. Sean Humbert for their invaluable time reviewing this manuscript and for providing critical feedback.

Thanks are due to Dr. Bin Pang for helping me to start my graduate student life in University of Maryland. I am grateful to Dr. Amardip Ghosh for his constant advice and help on this project and all my presentations. He is also a great friend and time with him is always a learning experience. I own my most special thanks to Vijay Ramasubramanian for his patience and encouragement. He always supports me like a family not only on my research but also on my life. I owe many thanks to

David Gers for providing me CFD simulation results and conducting experiments with me for this research.

My colleagues, Camilo Aguilera, Sammy Park, and Colin VanDercreek in the advanced propulsion research lab (APRL) have enriched my graduate life in many ways and deserve a special mention. I would also like to thank my officemates Roland Probst, Neal Smith, Justin Richeson, Jared Grauer and Jamie Meeroff. Additionally, I express my gratitude to Gang Wang, Wei Hu, Min Mao, Chao Liu, Yunsheng Tang, Lian Duan, Donglei Yu, Chen Zhang and Yi Wang for their friendship and support.

I would like to gratefully acknowledge financial support from NASA SVTI with Claudia Meyer as program manager.

Contents

List of Tables

List of Figures

Chapter 1

Introduction

1.1 Background and Motivation

1.1.1 Combustion Instability

Combustion instability poses serious risk to most power and propulsion systems. It has been intensively studied since the 1900s, but is still not completely understood. In most propulsion systems, the combustion processes are never perfectly smooth. A certain amount of unsteadiness in the combustion is always present even though it may be considered steady for analytical purposes. In general, combustion can be considered "smooth" when pressure fluctuations during steady operation do not exceed about $\pm 5\%$ of the mean chamber pressure. Combustion that exceeds this level of pressure fluctuations at random intervals is regarded as rough combustion. The severity of combustion roughness determines its impact during engine operation. If the roughness lies within a certain range, the engine can still operate

successfully. At particular operating conditions, when the fluctuations of pressure and velocity interact with the natural frequencies of the propellant supply system or the chamber acoustics, periodic superimposed oscillations occur. In general, "combustion instability" means a large amplitude oscillation of pressure, which occurs in a organized pattern.

If the combustion oscillations exceed a certain threshold, they can cause detrimental effects, such as excessive pressure vibration forces, mechanical failure of parts, or burn-through of the combustor walls. Such levels of combustion instability can result in combustion system failures and destruction of vehicles or mission failures. However, the existing body of theory and experiment has not provided a sufficiently strong foundation to understand and predict these processes. Current mathematical and computational tools in widespread use have also failed to yield reliable techniques for predicting and controlling such problems. Hence, there are at present only a few guidelines, based on painstaking trial-and-error, available to help designers avoid combustion instabilities. It is therefore important to gain some understanding of the underlying processes and attempt to suppress the combustion instability to tolerable levels.

Combustion instability can be considered an unsteady motion of a dynamical system, which sustains the oscillation behaviors over a broad range of frequencies. The basic mechanisms of combustion instabilities are very similar, although combustion instabilities occur in different types of engines, such as solid rockets, liquid rockets, gas turbines and thrust augmentors or afterburners. Thermo-acoustic instabilities, which are characterized by an interaction between the acoustic field and

periodic heat release, are the major cause of unstable combustion in combustors. The combustion instability only occurs when the combustion processes couple with the gas-dynamical motions, both of which may be stable themselves. However, the entire system including the propellants, the propellant feed systems, the combustion products that support the unsteady motions, and the chamber structure, is unstable.

A combustion system consists of two dynamical systems: the chamber dynamics and the combustion dynamics. The combustion chamber, a confined geometry, possesses certain acoustic properties and acts as an amplifier of acoustical motions. It can be considered analogous to an oscillator, in which the medium supports unsteady wave motions. Thus, the geometry of the chamber and the speed of sound in the flow medium are key factors, which have dominant influence on the acoustic modes. The combustion process is very sensitive to pressure, density, and velocity fluctuations. Flame fluctuation, which is due to burning process, can produce local changes in the properties of flow. Those fluctuations propagate in the medium and convert the local fluctuations to global unsteady behavior in the chamber. A feedback loop exists between the chamber acoustics and combustion dynamics, giving the possibility for unstable oscillations. Figure 1.1 shows a model of the thermal system with unsteady heat release in analogy to a feedback amplifier. In the language of control theory, the oscillator is the medium in the combustion chamber, and the unsteady motion of the combustion dynamics is considered the amplifier. Instabilities will develop under certain conditions, which are addressed by Rayleigh's Criterion. It states that if the heat-release rate from the combustion process is in phase with

pressure oscillations, the system is unstable, and when the heat-release rate is out of phase with the pressure oscillations, the system becomes stable. Rayleigh's Criterion will be discussed in detail in Section 2.1.1. A relatively small part of the available energy is sufficient to produce unacceptably large unsteady motions due to the feedback loop. Unsteady motions do not tend to attenuate easily, mainly because combustion chambers are nearly closed in most applications. This fact suggests that combustion instability can happen even with apparently slight changes in the system.

The mechanism of thermo-acoustic instability is explained here by investigating a flame stabilized in a straight duct, shown in Figure 1.2. The acoustic properties of the pieces of duct upstream and downstream of the flame are characterized by the ducts acoustic impedance. The specific acoustic impedance is a ratio of acoustic pressure, where "acoustic" refers to oscillating component, to flow velocity, defined as

$$Z = \frac{p'}{u'}$$

where p' is pressure oscillation and u' is velocity fluctuation. In Figure 1.2, the upstream specific acoustic impedance is defined by $Z_1 = \frac{p'_1}{u'_1}$ and the downstream specific acoustic impedance is defined by $Z_2 = \frac{p'_2}{u'_2}$. The characteristic impedance of a medium for acoustic waves is analogous to the index of refraction of a transparent medium for light waves. It is important in the determination of acoustic transmission and reflection at the boundary of two materials having different acoustic impedances. When combustion is present, the fluctuating heat release is mainly affected by the

acoustic velocity. The volume expansion associated with the heat release will act as a source term for the acoustic velocity. The dependence of the heat release on the acoustic velocity is given by a transfer function F

$$F = \frac{q'}{u_1'}$$

where q' is the heat release oscillation. The volume expansion is proportional to the heat release, and this proportionality is given by a constant k

$$\triangle u' = kq' = kFu_1'$$

The relationship between the acoustic impedances and the flame transfer function is given in a block diagram, shown in Figure 1.3.

The chamber acoustic characteristics depend on the tube geometry and may be combined in one transfer function representing the geometry of the system:

$$G = \frac{-Z_2}{Z_1 + Z_2}$$

Figure 1.4 shows the thermo-acoustic feedback system for the duct flame, which includes combustion chamber acoustics, represented by G and the heat release process, including F and k. Considering the case without combustion, correspondingly $F = 0$, the dynamics of the system only include the chamber acoustics G. If there are no acoustic losses in the volume or on the boundaries of the ducts, this system is a pure acoustic resonator, which exhibits harmonic oscillations. It is marginally stable, which means a finite perturbation at one of the resonance frequencies will neither grow nor decay, but will be maintained infinitely. When combustion is present, it adds the feedback modification to the pure acoustic resonator system (by making

F non-zero). The combustion factor determines the system stability. Either acoustic impedance or flame dynamics can be manipulated to obtain a stable feedback loop.

1.1.2 Combustion Instability and Control in Liquid Rocket Engines

The problem of instabilities in liquid rockets has received great attention since 1930. For the combustion in liquid rocket engines, the chief mechanisms are associated with the propellant feed system; the injection system; the processes required for conversion from liquid to gas; and combustion dynamics. The possibility of instabilities occurring during development of a new device must always be recognized and anticipated. Treating combustion instabilities is part of the cost for developing liquid rockets.

The current and useful way to suppress combustion instability in liquid rocket engine is hardware modifications based on trial-and-error testing, which is time consuming and expensive. For example, during the development of the F-1 engine from October 1962 to September 1966, more than 3200 full-scale tests were involved. Approximately 2000 of those tests were conducted to address the problems arising with combustion instability. Effort to understand the basic physics of the instability through the laboratory-scale or sub-scale tests is necessary for the design and development of the liquid rocket engine. Significant complications in liquid rocket engines are introduced by the flow and mixing of reactants, which occurs in the region near

the injectors. Thus interaction between flames and the flowfield near the injector plays a key role to causing combustion instability in liquid rocket engines. This work will study the flame-acoustic interaction near the injector in the laboratory scale model combustors.

Typical methods of addressing combustion instability in liquid rocket engines are the installation of baffles, resonators, or acoustic liners that suppress the formation of resonant acoustic wave structures in the chamber. The essential point is to force the resonance to occur in frequency ranges where the driving mechanisms are inadequate to sustain oscillations, or to directly damp the mechanical energy of unsteady motions. These are fixed hardware modifications made to the basic physical configuration of the system, designed and implemented based on empirical experience. Combustion instability is typically a critical issue only at some particular operating conditions, but hardware modifications must be carried through the whole mission. Thus, such devices impose an undesirable penalty. From this research, a novel combustion instability control method is suggested. Metal baffles and similar devices may be replaced by specifically-modulated propellant injectors. These controlled injectors can be used as standard injectors (*i.e.* stoichiometric) during stable operation. Once the combustion tends to become unstable, the controlled injectors would be modulated to steadily emit a different flow composition, which would act like a baffle, thereby altering the acoustic characteristics of the combustor.

1.2 Technical Objectives

The present work studies acoustically-driven combustion instability and the overall goal is to explore the feasibility of a new control methodology for LOX-LH2 rocket engines using shear coaxial injectors. The technical objectives are as follows:

1. Study the basic physics of flame-acoustic interaction involving shear-coaxial injector flow-field.
   (a) Examine the characteristic response of flames subject to the standing wave resonance modes.
   (b) Assess the interaction between the flame fronts and acoustic traveling waves.
   (c) Investigate the effect of the fuel density by using CH_4-H_2 blended fuel on flame-acoustic interaction with standing waves and acoustic traveling waves during the onset of combustion instability.
2. Develop flow-based control approaches for combustion instability suppression, which may replace the hardware-based passive-control approaches currently being used.
   (a) Investigate the feasibility of control flame-acoustic interaction by injection with different reactants at the hardware baffles location.
   (b) Study the experimental approaches to characterize the control authority for the new flow-based methodology.

3. Assess and analyze the potential effectiveness of these new approaches.

   (a) Examine the approach with CH_4-H_2 blended fuel in the specially-modulated injector in the double-element injector model combustor.

   (b) Investigate the approach of using the original reactants, modifying the equivalence ratio at the specially-modulated injector by altering the mass flowrate of the individual reactants.

1.3 Scope of Present Work

This work experimentally investigates basic mechanisms of flame-acoustic instabilities near the injectors and the feasibility of replacing hardware baffles with controlled flow injection in two laboratory-scale combustors employing shear coaxial injectors. Rocket engines intended for flight typically have hundreds of coaxial injectors on the injector plates, while only one or two injectors are studied in this work due to facility limitations. Two-dimensional cross-section models of the injectors are used, as they offer ease of diagnostics, making it possible to study the relevant processes with multiple detailed measurements. The experiments are limited to gaseous oxygen and gaseous fuel mixtures, not just because of facility limitations but also in an effort to minimize any complexity associated with atomization and vaporization coupling. Because flames are formed between vaporized propellants in shear-coaxial injectors, the use of non-cryogenic propellants in this study is not expected to affect the essential features of the flame-acoustic coupling. In the experimental setup the combustion chamber is open to the atmosphere due to safety consideration, while

working rocket engines operate with high pressures,up to 100 bar. The result

The model combustors have an acoustic driver unit mounted transversely, which supplies the acoustic pressure necessary to simulate the flame acoustic interactions that could occur near the injector plate of a typical liquid rocket engine. The input signal to the acoustic driver can be manipulated to obtain the flame response to different pressure wave patterns. Band-limited white noise gives a flame interaction with standing waves, *i.e.* acoustic modes. In contrast, single forcing frequency excitation produces a traveling wave response. Since the acoustic output of the driver unit is limited, the experimental conditions are scaled-down, guaranteeing similar levels of acoustic excitation compared to natural turbulent fluctuations of fluids. Consequently, the design in this work maintains some dominant aspects of fluid behavior which happen in rocket engines and the analysis and results obtained from this study should provide a better understanding of the problem under consideration.

Passive control is currently the most popular and practical control method for combustion instability in liquid rocket engines. Among all passive control methods, baffles are a widely accepted design practice for overcoming or preventing high-frequency instability. In this work, a new approach is suggested to simulate the effect of the baffles by using selective controlled flow injection during operation. Two different methods for employing controlled injectors were investigated. One method used a specialized fuel consisting of CH_4-H_2 blend in the controlled injector, while the other uses the same fuel as in the constant-flow injector, but changed the injectant flow rates. For the first approach, the goal was to characterize the response

of acoustically-excited hydrogen-methane-oxygen flames as a function of mixture composition with CH_4 mole fraction from 0% to 63%, corresponding to oxidizer-fuel density ratio from 16 to 3. For the second approach, only the equivalence ratio between the fuel and oxidizer was varied from 0 to ∞ at the controlled injector while retaining only H_2-O_2 as fuel and oxidizer.

In this dissertation, Chapter 2 gives the background and previous studies about combustion instability, as well as control methods related to the current work. Chapter 3 presents the new control methodology of modifying the reactant injection to simulate the effect of baffles. Chapter 4 describes the experimental setup and approaches used in this study. Chapter 5 shows the effect of fuel density by introducing CH_4-H_2 blended fuel on the flame-acoustic interaction in the single-element injector combustor to assess the feasibility of the control methods proposed in Chapter 3. Chapter 6 demonstrates the effectiveness of the two different ways of modifying flow injection for the new control methodology in a double-element injector combustor. Chapter 7 concludes the findings of this research and provides suggestions for future work to apply this control methodology to flight-worthy liquid rocket engines.

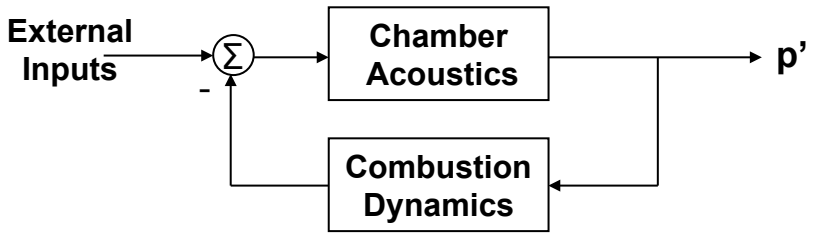

Figure 1.1: Schematic diagram of thermo-acoustic interaction as a feedback loop.

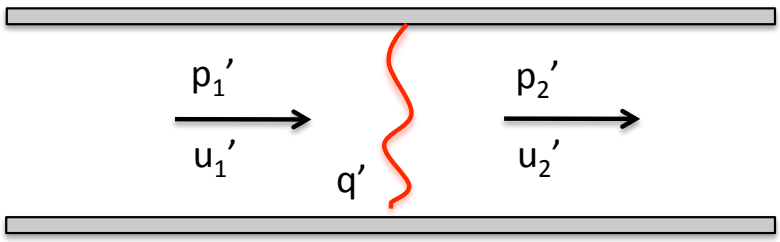

Figure 1.2: Flame stabilized in a straight duct.

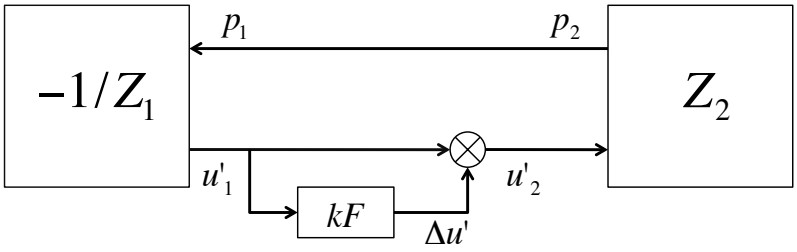

Figure 1.3: Thermo-acoustic block diagram of duct flame.

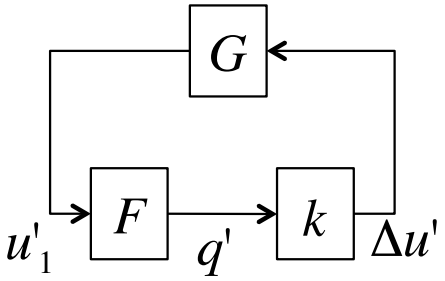

Figure 1.4: Feedback cycle between heat release and combustion chamber acoustics for duct flame.

Chapter 2

Literature Review

2.1 Combustion Instability

2.1.1 Mechanisms of Combustion Instability

Thermo-acoustic combustion instabilities have been widely studied over a long time because they lead to performance degradation and structural damage. These instabilities have been observed in a variety of combustion applications, including liquid and solid rocket engines [1, 2, 3, 4, 5, 6], ramjet engines [7, 8, 9, 10, 11, 12], jet engine afterburners [13, 14], and land-based turbine engines [15]. Although these are different propulsion systems and applications, the mechanism of these instabilities is similar, namely the interaction between flames and acoustics.

Lord Rayleigh was one of the first scholarly investigators of thermo-acoustic instability to develop a theoretical treatment of it as part of his research on the excitation of acoustic waves by heat addition in chambers in 1878 [16]. He stated:

"If heat be periodically communicated to, and abstracted from, a mass of air vibrating (for example) in a cylinder bounded by a piston, the effect produced will depend upon the phase of the vibration at which the transfer of heat takes place. If heat be given to the air at the moment of greatest condensation, or to be taken from it at the moment of greatest rarefaction, the vibration is encouraged. On the other hand, if heat be given at the moment of greatest rarefaction, or abstracted at the moment of greatest condensation, the vibration is discouraged".

This explanation for the presence of combustion instability is referred to as "Rayleigh's Criterion", which is the most widely used tool for understanding the susceptibility of a combustor to instability. Rayleigh addressed only the conditions under which unsteady heat addition can encourage oscillations in the feedback loop with acoustic pressure waves.

The mathematical representation of the Rayleigh's criterion was first proposed by Putnam and Dennis [17, 15] as

$$\int_{T_o} q'(t) \cdot p'(t) dt > 0 \tag{2.1}$$

where T_o represents the time period of one oscillation cycle, $q'(t)$ is the instantaneous heat release oscillation and $p'(t)$ is the instantaneous pressure fluctuation. If the heat-release rate $q'(t)$ from the combustion process is in phase with pressure oscillations $p'(t)$, the system is unstable, and when the heat-release rate is out of phase with the pressure oscillations, the system becomes stable. The Rayleigh Index $G(x)$ is a mathematical way to quantify the coupling between unsteady heat release and acoustic pressure fields, and is defined as

$$G(x) = \frac{1}{T_o} \int_{T_o} q'(x,t) \cdot p'(x,t) dt \tag{2.2}$$

If $G(x) > 0$, the oscillations will grow, and if $G(x) < 0$, damping occurs. Rayleigh's Criterion is the basis of analysis for thermoacoustic combustion instabilities and is evaluated using the Rayleigh Index over one cycle of instability.

Putnam has made the most extensive use of Rayleigh's Criterion in practical situations. His book and papers give many examples of applying the Criterion as an aid to making design changes to avoid oscillations generated by heat release, particularly in power generation and heating systems.

The nonsteady release of heat in the combustor, coupled with acoustic waves, is often also convected hydrodynamically through the flowfield. Therefore, the heat release is not only a function of time, but also of space. The theoretical analysis of flame-acoustic interaction is very difficult due to the spatial dependence on the turbulence structure of the velocity flow field. To take into account this behavior, a more appropriate form for the Rayleigh criterion is given by Zinn in [18]

$$\int_{T_o} \int_V q'(x,t) \cdot p'(x,t) dv dt \geq \int_{T_o} \int_V \sum Li(x,t) dv dt \tag{2.3}$$

where V is the volume of chamber and $Li(x,t)$ is the i-th damping process (*e.g.*, viscous dissipation, heat release, acoustic radiation).

For the mathematical representation of Rayleigh's Criterion, Culick [19] also provided a significant contribution by deriving an expression for the energy addition to the acoustic mode. It can be summarized by the conservation equations of a tube with a superimposed localized heat release zone to represent the dynamic behavior

of a combustion chamber as shown in Figure 2.1.

Assuming the flow is inviscid, stationary, perfect, and has negligible thermal conductivity to the surroundings, the reactive gas dynamics conservation equations for this one-dimensional flow in the longitudinal direction of the combustor are Continuity:

$$\frac{\partial \rho}{\partial t} + \frac{\partial (\rho u)}{\partial x} = 0 \tag{2.4}$$

Momentum:

$$\rho \frac{\partial u}{\partial t} + \rho u \frac{\partial u}{\partial x} + \frac{\partial p}{\partial x} = 0 \tag{2.5}$$

Energy:

$$\rho \frac{\partial e}{\partial t} + \rho u \frac{\partial e}{\partial x} = -p \frac{\partial u}{\partial x} + q \tag{2.6}$$

and the Equation of State:

$$p = \rho R T \tag{2.7}$$

where t is time, x is space, ρ is density, u is velocity, p is pressure, e is specific internal energy, q is the heat release rate per unit volume, R is the gas constant, and T is temperature.

Since only the small perturbation behavior at the onset of the instability is under consideration here, the system can be linearized by separating the variables into their mean value and small perturbation components.

$$p(x,t) = \bar{p}(x) + p'(x,t) \tag{2.8}$$

$$u(x,t) = \bar{u}(x) + u'(x,t) \tag{2.9}$$

$$\rho(x,t) = \bar{\rho}(x) + \rho'(x,t) \tag{2.10}$$

$$q(x,t) = \bar{q}(x) + q'(x,t) \tag{2.11}$$

where the overbar denotes the mean part of a variable and the prime denotes the perturbation part of a variable.

By substituting the separated variables into the conservation equations and noticing that the mean flow should also satisfy the above three conservation equations, the governing equations for the perturbations can be simplified to the following two equations:

$$\bar{\rho}\frac{\partial u'}{\partial t} + \bar{\rho}u\frac{\partial u'}{\partial x} + \rho' u\frac{\partial \bar{u}}{\partial x} + \frac{\partial p'}{\partial x} = 0 \tag{2.12}$$

$$\frac{\partial p'}{\partial t} + u\frac{\partial p'}{\partial x} + \gamma\bar{p}\frac{\partial u'}{\partial x} + \gamma p'\frac{\partial \bar{u}}{\partial x} = (\gamma - 1)q' \tag{2.13}$$

Multiplying Equation 2.12 by u' and Equation 2.13 by $p'/(\gamma\rho')$, and combining these two equations, the change of acoustic energy inside the combustion chamber can be summarized as

$$\frac{\partial}{\partial t}[\varepsilon] + \bar{u}\frac{\partial}{\partial x}[\varepsilon] = \frac{\gamma - 1}{\gamma}\frac{p'q'}{\bar{p}} - \frac{\partial \bar{u}}{\partial x}[\rho' u'\bar{u} + \frac{p'^2}{\bar{p}}] - \frac{\partial}{\partial x}(u'p') - \frac{u'p'}{\gamma\bar{p}}\frac{\partial p'}{\partial x} \tag{2.14}$$

where

$$\varepsilon = \frac{1}{2}\bar{\rho}u'^2 + \frac{1}{2}\frac{p'^2}{\gamma\bar{p}} \tag{2.15}$$

and ε represents the acoustic energy density. The first term is the kinetic acoustic energy and the second one is the potential acoustic energy. Similar to other oscillating systems, the periodic conversion from one form of energy to the other sustains the oscillatory behavior.

The right hand side of Equation 2.14 represents the acoustic sources. When considering only those cases in which the heat release becomes the dominating source of acoustic energy generation, the above equation can be reduced to

$$\frac{D\varepsilon}{Dt} = \frac{\gamma - 1}{\gamma}\frac{p'q'}{\bar{p}} + \text{higher order terms} \tag{2.16}$$

Integrating Equation 2.16 and disregarding the higher order terms, the change in acoustic energy of a combustor due to the coupling between heat release fluctuations q' and pressure fluctuation p' during one period T_o can be introduced as:

$$\Delta E \approx \frac{\gamma - 1}{\gamma}\int_V dv \int_t^{t+T_o} \frac{p'q'}{\bar{p}} dt \tag{2.17}$$

So, if the natural fluctuations in the combustion and flow dynamic processes are such that both p' and q' move in the same direction so that $\Delta E > 0$, the pressure oscillations will grow and resonant instability will occur. On the other hand, if p' is out of phase with q', the oscillations will be damped out.

Another complete analysis of the criterion which includes linear and non-linear thermoacoustic oscillations for chambers of any shape was done by Culick [20]. The work investigated the influence of q' and dq'/dt on creating an acoustic wave and concluded the similarity of the Rayleigh criterion and the principle of linear stability in approximate analysis. Also, this analysis showed the similarity between the effects of an oscillating heat source and the effect of an oscillating piston in generating waves.

Recently, with the development of sensing technology, many research groups have been making direct experimental observations in laboratory systems to check

the validity of the Criterion's implications. The key assumption is that radiation by certain intermediate species in reactions (OH* and CH* are the most common identifiers) can be interpreted as a measure of the rate of chemical reactions taking place and hence of the rate at which energy is released. Simultaneous measurements of radiation in a system and the pressure oscillation can be obtained for calculating the local Rayleigh Index. The results qualitatively assess the extent to which the oscillations are being driven by the energy released in the combustion field. The first report of simultaneous measurements of pressure and radiation allowing confirmation of Rayleigh's Criterion appeared in a Ph.D. dissertation by Sterling [21, 22]. In Sterling's work longitudinal instabilities were studied in a dump combustor, and the integral of ΔE over the volume of the chamber was used as a measure of the severity of oscillations. In this work, the local Rayleigh Index will be calculated by simultaneous pressure measurements and OH* chemiluminescence measurements to gain insight into flame-acoustic interaction.

A great deal of publications on the topic of combustion instability were put forth in the latter half of the twentieth century. In 1960, Gaydon and Wolfhard [23] reviewed earlier literature on the topic of unstable flames. Mechanisms by which flames could trigger and amplify or suppress acoustic waves were studied and discussed by Toong, *et al.*[24]. Further, Toong, *et al.* noted that both linear and non-linear flame-acoustic interaction modes were possible. As treatment of combustion instability in the literature grew, occurrences in different types of combustion applications initially received treatment as domain-specific issues. For example, Price [25], Marxman and Wooldridge [26], and Sirignano [27] specifically discussed

combustion instability in solid rocket engines. On the other hand, Thring [28] considered combustion oscillations in industrial applications and classified these oscillations into the categories of combustion roar, acoustic oscillations, and Helmholtz resonator oscillations. In his comments regarding Thring's paper, Zinn [28] made the observation that the types of instabilities discussed bore similarity to instabilities observed in solid and liquid rocket engines, and suggested a universal classification system for the instabilities seen amongst various combustion systems. Papers on combustion instability in gas turbines, such as Kydd's [29], were also common.

In a book published in 1985, Williams [30] provided in-depth explanations of combustion instabilities in rocket engines, both liquid and solid, detailing amplification and attenuation mechanisms. The discussion included topics such as hydrodynamic and diffusive instabilities, nonlinear effects, and oscillatory burning in liquid rocket engines. Additionally, 233 references on combustion instability were cited. Laverdant, *et al.*[31] performed an analysis starting with the conservation equations for mass, momentum, energy, and species, arriving at an expression for the pressure perturbation in a combustion chamber with two source terms. Hydrodynamic processes leading to in-phase pressure and heat-release oscillations were elaborated on by Candel [32]. Kendrick, *et al.* [33] predicted acoustic modes and mode shapes in a laboratory dump combustor through the use of a one-dimensional acoustic model. The effect of species generation on combustion instability was considered by Sreenivasan and Raghu [34], as an extension of work published by Chu [35] in 1965.

2.1.2 Combustion Instability in Liquid Rocket Engines

During the initial development of rocket motors, many failures were caused by combustion instabilities and the topic became of central importance. Reviews of the early work on rocket instabilities were established by Crocco and Cheng [2, 36, 37, 38]. Initially, there was a focus on the effect of "time lag", *i.e.* the inherent delay between the introduction of a particular volume element of propellant into the combustion chamber and the subsequent heat release associated with that element [39]. Within the time lag framework, the coupling between oscillations in the propellant feed systems and combustion instability was studied by many, including Gunder and Friant[40], Yachter [41], and Summerfield [39]. Crocco considered high-frequency instability using the notion of a combination of constant time lag and time-varying lag dependent on chamber conditions [42, 43].

Early experimental work, *e.g.*, that of Berman and Cheney [44], involved the use of methods such as photographic observation through window slits. Berman and Cheney's experiments allowed the observation of small disturbances developing into high-amplitude waves with frequencies approaching the resonant frequencies of the combustor. The optical data were correlated with pressure measurements in work by Ellis *et al* [45]. Optical methods were further used to study transverse mode instabilities by Ellis [46]. At NASA's Lewis Research Center, Male, Kerslake, and Tischler conducted optical studies of screaming combustion in liquid rocket engines[47]. In these NASA Lewis studies, high wall heat transfer rates were observed, consistent with today's empirical experience with transverse instability modes. Interaction

between longitudinal and transverse oscillation modes was also witnessed.

Several key findings were made in Maslen and Moore's work [48], wherein the effects of damping in a cylindrical combustion chamber were considered analytically. The results indicated that if viscosity were neglected, large-amplitude waves could exist in the form of the spinning tangential mode. Strong transverse waves were found to potentially have highly destructive strength if coupled with energy input from unsteady combustion. Osborn and Bonnell [49] performed experiments to ascertain the effects of chamber pressure, chamber geometry, and propellant chemistry on combustion instability. With some propellants, it was found that when the chamber was lengthened to the point that longitudinal instabilities were possible, the stability of the transverse modes exhibited a distinct change in behavior. Additionally, for propellants having greater heat-release rates, the instability region tended to grow.

In 1960, Pickford *et al.* [50] employed the concept of available energy to attempt calculations of stability behavior from prior understanding of the physical and chemical nature of the propellants, the injection process, and related parameters. Reardon used Crocco's time-varying lag theory to examine high-frequency transverse modes in liquid rocket engines [51]. Both theoretical and experimental findings indicated standing tangential modes were more stable than spinning tangential modes.

A full-scale M1 liquid O_2-H_2 rocket chamber was studied by Barsotti *et al.*[52]. Their experiments showed the fuel-to-oxidizer injection velocity ratio heavily influenced the chamber stability. Increasing the hydrogen injection temperature, as well

as the velocity ratio, promoted greater operating stability. In 1969, Crocco [38] noted that peak transverse mode oscillation amplitudes tended to occur close to the injector.

Many types of instabilities are described in Putnam [15]. A comprehensive reference on liquid rocket instabilities was assembled in the mid 1970s by Harrje and Reardon [1]. This review provided the analytical models for low and high frequency instabilities, experimental aspects of the study of instability and practical guide to designers focusing on the aspects of excitation and damping. Williams also presented a detailed examination [30] with special attention to studies of laminar flame instabilities.

Modern reviews of combustion instabilities in liquid rocket engines have been comprehensively undertaken by Culick [53] and Candel [32]. Mitchell specifically reviewed the state of analytical modeling efforts, tracing back to the 1970s [54]. Included in Mitchell's discussion was a treatment of contemporary developments in liquid rocket combustion instability modeling. The methods considered included both linear and nonlinear frameworks. Culick and Yang [5] presented a chronological overview of research in liquid rocket combustion instability, covering linear and nonlinear behaviors, as well as examples of combustion instability in operational engines. An explanation of the elementary components in the dynamic combustion system which can result in combustion instability was also included. A basic classification of instabilities was proposed by Barrere and Williams [55].

2.2 Control of Combustion Instability

2.2.1 Passive Combustion Control

Passive control methods [53, 15, 56, 8] are the earliest developed control strategies for combustion instability, and are still the most commonly used methods amongst engine developers. All passive control strategies fall into two major categories. One involves changes in hardware design (*e.g.*, in the composition or types of reactants, injection system, chamber geometry) to reduce the susceptibility of the combustion process to acoustic excitation. The other method removes energy from the sound waves by the use of suitable resonators to introduce a dissipative process, such as Helmholtz resonators, quarter wave tubes, perforated plates, or acoustic liners. The drawback with passive approaches is that they tend to be effective only over a limited range of operating conditions.

A baffle is a structure placed in a combustion chamber in such a fashion as to reduce the amplitude of an unacceptable oscillation. Chapter 8 of the volume by Harrje and Reardon [1] contains an extensive discussion of baffles. More detailed considerations of particular applications and of special characteristics are covered in the references cited. Baffles tend to prevent the transverse modes of oscillation through geometric design. The standing transverse modes of instability, including tangential and radial modes, are depicted in Figure 2.2. The particle paths and the pressure antinodes for the first two tangential and radial modes are shown, as well as three common combined modes: the first tangential-first radial; first tangential-second radial; and second tangential-first radial modes. The shape and

optimum number of blades for any baffle configuration depends primarily on the characteristics of the modes to which the system is most susceptible. Once these are known or anticipated, a configuration of baffles may be chosen to interrupt the motions, thus preventing formation of the mode in question. A variety of baffle configurations used in liquid rockets have been considered, as shown in Figure 2.3.

Mitchell *et al.* [57, 58] investigated the effects of different configurations of baffles on the acoustic field, without consideration of mean flow, using linear theory. The most extensive published calculations for a simple configuration to determine the main nonlinear acoustical effects of baffles were done by Wicker, Yoon, and Yang [59]. It is infeasible to predict from first principles the stability and nonlinear behavior of combustion systems due to intrinsic complexities and inevitable uncertainties in basic information, such as material properties, chemical dynamics, and the turbulent behavior of the flow flied. Hence the theories provide a framework for interpreting observations, both in the laboratory and full-scale devices, to suggest experiments to produce required data, to improve the empirical base for understanding, to formulate guidelines for designing full-scale systems, and to understand the fundamental principles governing the physical behavior. All theoretical work in this field has been carried out in response to observational and experimental results.

Male and Kerslake [60] at NASA Lewis Research Center studied experimentally the effectiveness of longitudinal fins in attenuating transverse mode instabilities in rocket engines. They observed that "lateral oscillations appeared first at the injector end and then spread throughout the chamber". Also at Lewis Research Center, the design criteria and practical considerations of baffles and acoustic absorbers were

explained in detail [56].

With respect to changes in the chamber geometry, Crocco and Sirignano [38] showed that increasing the length of the convergent section of the nozzle could suppress the linear axial oscillations in the rocket chamber. In contrast, the transverse modes were almost ineffectively damped.

The actual performance of a resonator in suppressing the combustion instabilities depends on the resonator geometry and the operating conditions. Harrje *et al.* [61] explored the effectiveness of acoustic cavities. When the passages connecting the cavity with the chamber occurred at the pressure antinodes of a given mode, the effectiveness increased. An increase in effectiveness also occurred when the acoustic cavities were placed closer to the injectors. Laudien *et al.* [62] assessed the effectiveness of both resonators and baffles in a model with cold flow (isothermal flow) and showed that rounded corners at the resonator/combustor connection produce a significant difference from square corners in the acoustic response. Two methods for measuring the damping factor were suggested, including decay rate and bandwidth. The values for the decay rate measured at room temperature will not be the same as those applicable under operating conditions at high temperature and with flow. However, as a qualitative indication, room temperature measurements and observations are extremely useful. Wanhainen *et al.* [63] studied Helmholtz type acoustic damping devices in suppressing high frequency combustion instability in Hydrogen-Oxygen rocket engines. Susceptibility to self-triggering under varying Hydrogen injection temperatures was used as the criterion for assessing stability. The lowest self-triggering temperature liner gave the most stable flame-acoustic interaction.

Also acoustically absorbent chamber walls were found to change the stability limits and even the frequencies of the instability. Sirignano *et al.* [64] showed (for acoustic cavity resonators derived from the Helmholtz resonator principle, typically used to dampen oscillations in a combustor) that a jet is formed at the exit of the channel connecting the combustion chamber with the resonant cavity. The eventual dissipation of the kinetic energy of the jet provides a non-linear damping mechanism whose effectiveness improves with the oscillation amplitude.

More recently Gysling *et al.* [65] examined the use of Helmholtz resonators on a sector rig combustor. Based on both theoretical modeling and experimental data, several design variables, such as the ratio of the resonator to combustor volume, the resonator frequency, and the loss coefficient at the resonator mouth were proven very important in the design of resonators. They successfully demonstrated that using two resonators tuned to two different frequencies can provide damping over a range of frequencies. This is of critical importance since a given engine can experience frequency shifts in resonant modes between different operating conditions. Bellucci *et al.* [66] used a Helmholtz resonator model to design dampers that were added to the silo combustor of a stationary gas turbine. The resonator model included more physical detail for loss mechanisms than in Gysling [65]. Experimental testing was used to establish the model parameters and then design resonators for the actual combustion system, but this paper did not report the resonator performance at other frequencies or operating conditions. Pandalai and Mongia [67] studied the use of acoustic dampers on a lean premixed combustion system. They installed damper tubes, whose length was one-quarter of a wavelength of the combustor

resonant frequency observed from engine tests, upstream of the combustor, just prior to the fuel-air mixer. A perforated plate at the resonator mouth was used to control the resonator impedance. These devices have functioned satisfactorily and have accumulated over 100,000 hours of engine operation in factory testing and commercial operation. Richards summarizes passive methods used to improve the stability of low-emission combustors in stationary power gas turbines [68].

2.2.2 Active Combustion Control

Passive combustion control is an effective approach, but it can restrict the control performance to a narrow operating window. It may be ineffective at the low frequencies at which some of the most damaging instabilities occur, and often changes in hardware design to address such shortcomings are costly and time-consuming. In contrast to passive control, the term "active control" implies control of a system involving expenditure of energy from a source external to the system. Some system input, such as the fuel flow rate or the combustor boundary condition, is varied in response to a system measurement, such as a pressure or heat release signal. Generally, the purpose is to minimize the difference of error between the instantaneous desired and actual behavior of the system so that the interaction between the unsteady heat release and acoustic waves leads to decaying rather than growing oscillations. The control input can be decided either without feedback (open loop control) or with the feedback information about the actual response of the system (closed loop control).

Active control theories were initially conceptually applied by Tsien [69] to suppress the chugging instability in a liquid rocket engine. A combustion model based on a pressure-dependent time lag between the instants of propellant injection and burning was used. The propellant injection rate was modulated through a capacitor controlled by a servomechanism with the feedback of pressure signal. A Nyquist plot was used to determine suitable servo coefficients for intrinsic stability. Marble and Cox [70] and Lee *et al.* [71] also studied similar approaches for the control of low-frequency combustion instabilities in bipropellant liquid rocket engines. Tsien's method of active control was not applied in practice due to the limitations of instrumentation at that time.

In the most recent five decades, active combustion control has been studied intensively as fast-response sensors and actuators have been developed rapidly. Ffowcs-Williams described the concept of "anti-sound" in [72]. The basic idea is to eliminate unwanted oscillations in an acoustic field by means of acoustic interference. Control is achieved by producing waves out of phase with the unwanted oscillations. Although this wave-cancellation technique is applicable to combustion systems in principle, it is not practical to implement on a full-scale combustor because acoustic actuators such as loudspeakers cannot offer energy density comparable to levels present in the oscillatory flow field. At Cambridge University, Dine [73] showed the elimination of flame-acoustic instability in a Rijke tube with a phase-shift controller. The unsteady heat-release rate was measured by CH* chemiluminescence and fed back to a loudspeaker placed near one end of the tube to increase the acoustic energy dissipation from the boundary. The same problem was also studied using a micro-

phone as a sensor, instead of a photo-multiplier [74, 75]. Results indicated that the instabilities could be suppressed over a wide range of phase difference between unsteady oscillations and actuating pressure waves with sufficiently large control gain. These results implied that feasible active control of combustion instabilities is not limited to the anti-sound technique, which would require the control excitation to be precisely out of phase with existing oscillations.

Bloxsidge *et al.* explored the control of low-frequency combustion instabilities in a laboratory jet-engine afterburner [76, 77]. Boundary condition variation was achieved using a variable inlet nozzle area downstream of a choked plate. The peak due to combustion instability in the pressure spectrum was reduced by 20 dB. Lang *et al.* [78] and Poinsot *et al.* [79, 80] used a loudspeaker to control the instabilities in a small laboratory burner with acoustic pressure measurement. The pressure signal, obtained from a microphone located upstream of the chamber, was filtered, phase-shifted, amplified, and then applied to the actuator. Their work demonstrated not only the control system but also that active control techniques can be used effectively to study the initial transient behavior of instabilities.

All the aforementioned active approaches suppress combustion instabilities by mechanical means, such as loudspeakers or moving bodies. However for practical systems containing high energy density, the power requirements of mechanical actuators become prohibitive at larger scales. A more attractive control methodology is to vary the Rayleigh energy sources of oscillatory flow fields by fuel modulation. Langhorne *et al.* [81] experimentally achieved feedback control through modulation of the fuel supply in a laboratory afterburner. The phase-shift controller was de-

signed using Nyquist methods. Unsteady addition of just 3% excess fuel reduced the spectral peak corresponding to the main instability mode by 12 dB. This method offers a promising solution to problems of low-frequency oscillations in full-scale combustors. Chu [82] studied a system consisting of a premixed ducted flame with a pressure transducer upstream of the flame zone and fuel injection system for actuation. An H_∞ robust controller was designed based on the constant flame speed combustion model.

Many active combustion controllers for use on combustion models and laboratory-scale rigs have been reported upon. However, only a few feedback control approaches have been applied to full-scale engines thus far. Only fuel modulation and very simple controller designs were employed in these full-scale demonstrations. In 1988 Moran, *et al.* [83] showed feedback control on the afterburner of a Rolls-Royce RB199 military turbofan engine. High-response electro-hydraulic servo valves were used to spill fuel from the engine, rather than adding it. The modulated fuel was approximately 5-10% of the mean. They designed a simple gain/time-delay controller. The results gave a 12dB reduction in the dominant low "buzz" frequency. Seume *et al.* [84] and Hoffmann *et al.* [85] performed active combustion control on a Siemens heavy duty industrial gas turbine. Actuation was performed by modulating the fuel to the pilot flames using a Moog solenoid valve. The feedback signals were pressure measurements at several locations around the combustor circumference. Simple gain/phase-shift controllers were used. The dominant frequency was reduced by 17 dB. Researchers at United Technologies Research Center [86, 87] also demonstrated active control on full-scale liquid fuel lean premixed combustors. Using a solenoid

valve to modulate the fuel supply, a 16 dB reduction of the dominant mode in a single combustor and a 6.5 dB reduction in a 67.5 degree sector cut from a full combustor annulus were obtained. The adaptive phase-shift controller designed by Neumeier & Zinn [88] was also applied at full scale to a Siemens-Westinghouse Dry Low NOx (DLN) combustor [89]. The dominant mode was reduced by 15 dB and the NOx emissions were reduced by approximately 10%.

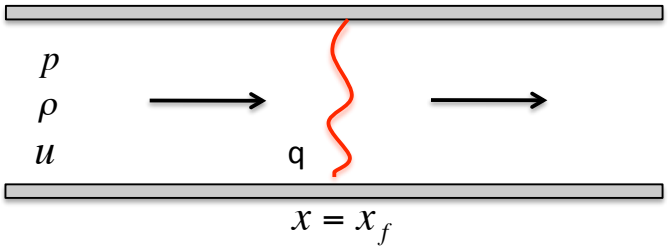

Figure 2.1: Reacting fluid flow with heat added in a tube.

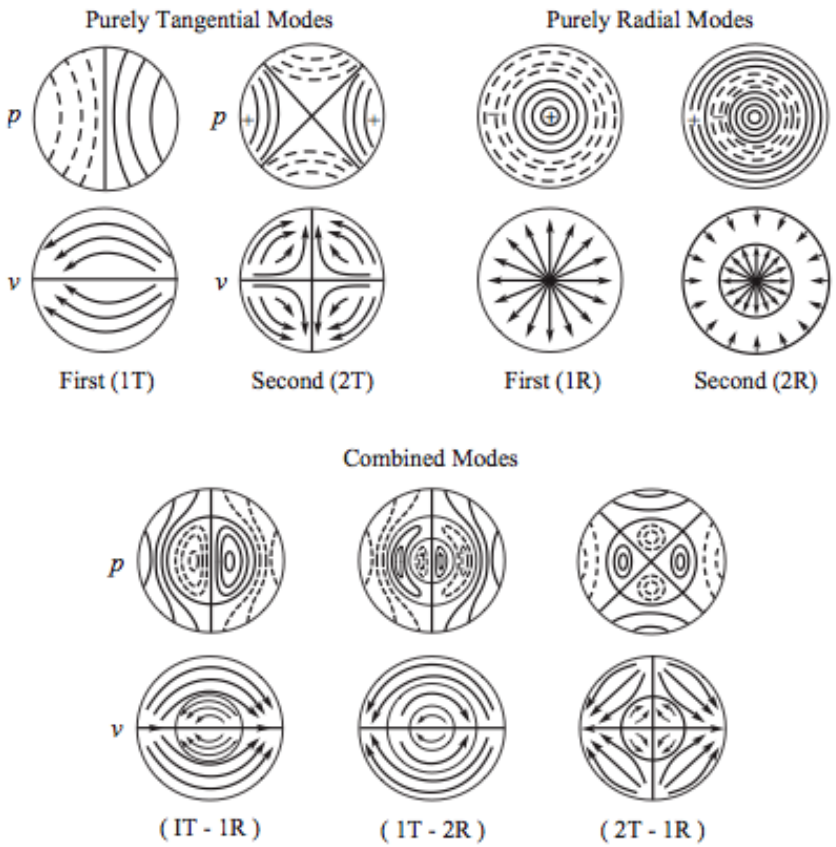

Figure 2.2: The pressure fields for the lowest order modes commonly encountered in circular cylindrical combustion chambers (Figure 8.2.2b of Harrje and Reardon [1]).

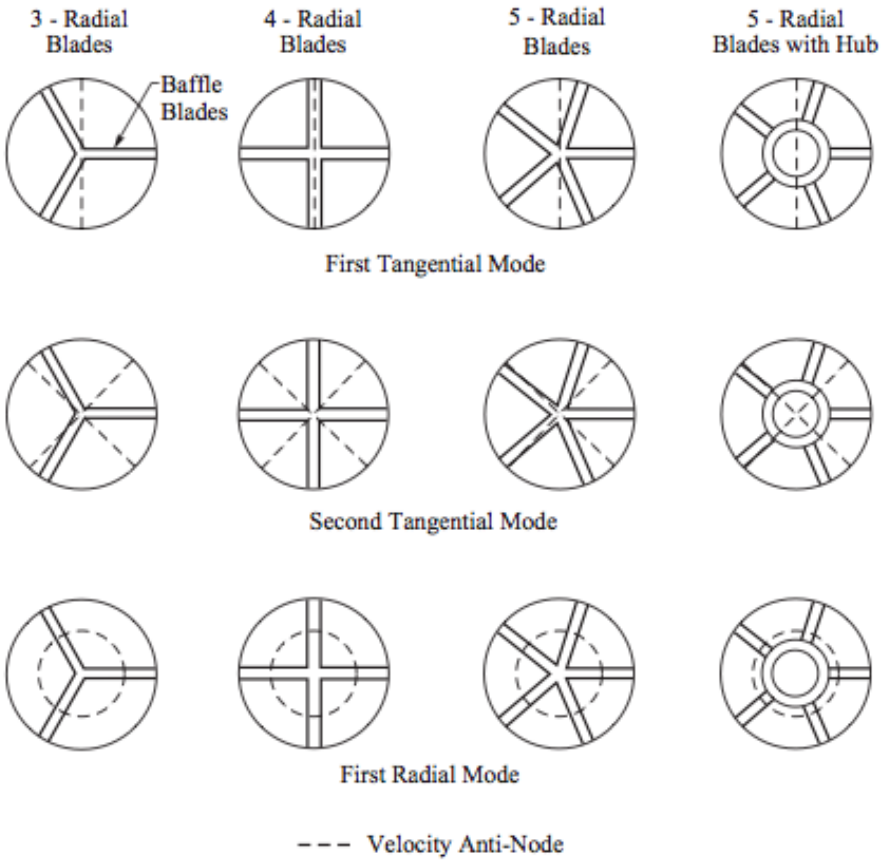

Figure 2.3: Examples of the arrangement and shapes of baffles fixed to the injector face of a liquid rocket(Figure 8.2.2d of Harrje and Reardon [1]).

Chapter 3

Control Methodology and Experimental Strategy

3.1 Prior State-of-the-Art Control Methodologies: Passive Approaches

As previously discussed, combustion instability in liquid Hydrogen-Oxygen rocket engines has been intensively studied for several decades[5, 6, 90]. Such instabilities arise when pressure perturbations within the combustor couple sufficiently in phase with heat release oscillations. When these phenomena occur, they can cause severe increases in heat transfer rates and vibratory mechanical loads, which can eventually lead to catastrophic failure of the engine. For rocket engine designers, the goal is to ensure stable combustion with increasing system pressures and temperatures over a wide range of operating conditions, while decreasing hardware

weight to optimize the overall flight system performance.

Typical methods of addressing combustion instability in liquid rocket engines are the installation of baffles, resonators, or acoustic liners that suppress the formation of resonant acoustic wave structures in the chamber[5, 91]. Baffles are devices that reduce the coupling between the combustion process and the fluid dynamics of the engine system. Another method is to modify the combustion process by changing the injection element characteristics to achieve stable combustion. These methods all fall under the category of passive control techniques, because they are fixed hardware modifications made to the basic physical design of the system. The design of passive control elements is mainly qualitative and empirical, founded on understanding the basic processes. To develop these practical means of passive control, trial and testing are necessary and the only effective way to achieve the desired performance.

Baffles will be discussed in detail here because one application of the current work is to simulate the effect of baffles in suppressing combustion oscillation in the liquid rocket engines. Baffles suppress combustion instabilities by interfering with the formation of the naturally preferred acoustic resonance in the combustion chamber near the injectors. Baffles are physical barriers installed on the injector plate, which divide the region close to injectors to several distinct sectors by changing the boundary conditions. The local acoustic impedance of the baffle is drastically different from the injector with reactants. Each sector has its own acoustic characteristics, preventing the formation of the naturally preferred acoustic modes across the injectors [92]. Figure 3.1 shows the baffles installed in the engine. Even though

there is still the potential to form the naturally preferred modes downstream in the combustor, the acoustic modes of the whole combustor are changed substantially by baffles. The oscillations of the flames interact less with the acoustic resonance modes of the chamber with the baffles installed.

Changes in the acoustic environment effected by baffles can be visualized in the case of a one-dimensional closed tube in Figures 3.2 and 3.3. In the closed tube without baffles, the amplitudes of acoustic pressure oscillations are at their minimum at the closed ends, while the amplitudes of acoustic velocity oscillations are at their maximum. If baffles are installed in locations that are neither the node nor anti-node of the pressure oscillation, the mode shapes are modified. The new mode shapes are determined by the locations of the baffles, which change the acoustic impedance boundary conditions. Different acoustic characteristics are obtained with various baffle configurations. Figure 3.3 shows the pressure and velocity oscillations with baffles at L/3 and 2L/3. However the baffles' acoustic impedance must be substantially different from that the medium in the tube.

Effective design and configuration of baffles require substantial testing and experience. To eliminate instability, baffles must protrude into the chamber enough to be effective. On the other hand, they should not extend too far, otherwise each baffled compartment would act like an individual combustion chamber with its own acoustic characteristics. For example the baffle design for the F-1 engine is shown in Figure 3.4. The whole F-1 engine is about 19 feet long and the diameter of the injector plate is around 3.3 feet, while the baffles extend about 0.25 feet. The amplitudes of the pressure oscillation at the instability frequency are greater than

the mean chamber pressure in the chamber without baffles, while they are about 65% of the mean pressure with baffles.

Baffles are most effective on the transverse acoustic modes of instability which includes tangential and radial modes. Transverse modes are characterized by oscillatory pressure waves and gas-particle motion parallel to the propellant injector face. The first tangential mode is typically the major source of instability, which can be subdued by the downstream extension of the baffles from the injector face. However baffles have little impact on feed-system induced instabilities or longitudinal instability modes. The control methods developed in the current work focus on the transverse mode in the model combustor.

Whereas baffles are fixed hardware modifications made to the basic physical configuration of the system, and designed and implemented based on empirical experience, combustion instability is typically a critical issue only at some particular operating condition. Nonetheless hardware modifications must be carried throughout the whole mission. Thus, such devices impose an undesirable penalty. In this research, a novel combustion instability control method has been identified. Metal baffles and similar devices may be replaced by specifically-modulated propellant injectors.

3.2 Selective Injectant Control Methodology and Experimental Strategy

3.2.1 Control Methodology

The current research aims to damp combustion instability in liquid rocket engines that are nominally designed for Hydrogen and Oxygen propellants. The new combustion instability control strategy is to simulate the effect of baffles by carefully regulating the propellant mixture and quantity in selected injectors. For instance, Figure 3.5 shows a typical configuration, with five radial baffles connected to a hub baffle. Figure 3.6 illustrates a system of "fluidic baffles": controlled injectors replace the hardware baffles. In such a scheme, the specially-regulated injectors would be arranged in a pattern similar to baffles. They can play a similar role as hardware baffles in changing the acoustic characteristics within the combustor if these selective injectors offer a substantially different acoustic impedance from the standard injectors. However, these controlled injectors can be used as standard injectors (i.e. stoichiometric) during stable operation. Once the combustion tends to become unstable at some particular operating conditions, the controlled injectors would be modulated to steadily emit a different flow composition, intended to substantially change the acoustic impedance, thereby altering the acoustic characteristics of the combustor.

Acoustic impedance is the main factor differentiating the controlled injectors from the standard injectors. Varying injectant composition serves to change the

acoustic impedance characteristics of the column of fluid associated with the injector. In turn, the columns with modified acoustic impedance characteristics affect the overall acoustic environment within the combustor. The effectiveness of these changes in suppressing flame-acoustic interaction can be assessed by examining the pressure spectra under forced excitation.

Two different approaches to regulate the propellant injection were investigated to change the acoustic impedance. One approach used a specialized fuel consisting of a H_2-CH_4 mixture in the controlled injector while retaining the same O_2 as standard injectors. However H_2-CH_4 blended fuel may not always be a practical solution, since an extra tank for CH_4 would have to be added to an H_2-O_2 system solely for control purposes. Another possibility consists of using only the original reactants, but operating the controlled injectors at a different equivalence ratio than the majority of the injectors.

For the blended fuel method, modification of the density of the fuel can alter the speed of sound in the fuel and the combustion products, so that the acoustic impedance of the injected fluid is changed. To increase the overall density of the fuel, CH_4 was chosen to be blended with H_2. The density of CH_4 is eight times that of H_2, making it a good candidate by this criterion. Also, CH_4 is comparatively cheap, and plentiful in the Martian environment, making it attractive for future space exploration missions. Among the common hydrocarbons, CH_4 has the best specific impulse. Therefore, CH_4 is selected as a candidate fuel to be used to take advantage of the density difference to change the acoustic impedance of these controlled injectors.

The other approach is to manipulate the mass flow rate of the original reactants, H_2 and O_2. This method removes the complications associated with the supplying the additional CH_4 fuel. In order to determine the potential effectiveness of this approach, the effect of equivalence ratio on the acoustic characteristics of the same multiple-element combustor was also examined. However, there remain some practical issues that require consideration prior to the application of this control method to flight hardware. Turning off the fuel and operating with only O_2 can lead to damage of the combustion chamber walls.

Real-time feedback control would be problematic due to the poor survivability of sensors in the harsh operating environment. Even if suitable sensors could be employed, most active control strategies rely on high-frequency fuel modulation on the order of combustion instability frequencies. It would be difficult and impractical to valve rocket reactant supplies in this fashion. The methods explored in this work do not suffer such disadvantages and provide sufficient flexibility and adaptability to allow their use in many applications.

3.2.2 Experimental Strategy

For the facilities in the Advanced Propulsion Research Lab at the University of Maryland, two model combustors were designed to study the feasibility of the selective injectant control method for liquid rocket engines. Both models are two-dimensional shear coaxial injector combustors. One involved a single injector element, while the other involved two injector elements. Experiments were con-

ducted to characterize the flame-acoustic interaction and study the effect of the fluid injection on the acoustic impedance.

In the single-injector combustor, experiments were conducted to estimate the acoustic impedance variation with injected fuel. The results of these tests indicated the possibility of tailored fluid injection being a good replacement for hardware baffles as shown in Figure 3.3. If the acoustic impedance associated with the modified fluid injection is substantially different from the standard H_2-O_2 operating condition, the modified injection is considered a promising control approach. Pressure spectral measurements taken during combustor operation are good indicators of local acoustic impedances since they are related to the local speed of sound. The effect of the CH_4-H_2 blended fuel on chamber pressure spectra were investigated in the single-injector model combustor.

The selective injection control method was experimentally demonstrated in the double-injector combustor, in which one injector was operated in a standard (stoichiometric H_2-O_2) configuration and the other was specifically-modulated. The baseline case was both injectors operating with stoichiometric H_2-O_2 flow. Various fluid configurations were tested in the specifically-modulated injector. The comparison between each controlled case and baseline case allowed evaluation of the effectiveness of the control method.

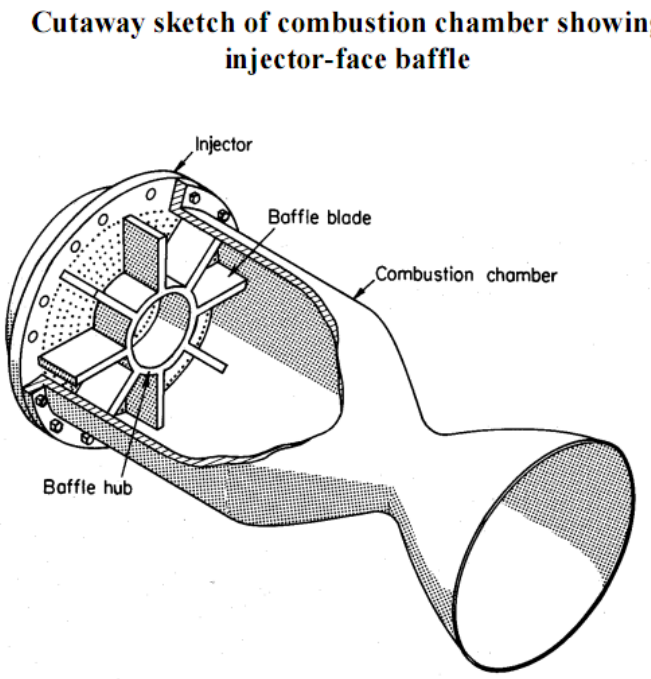

Figure 3.1: Typical baffles are installed in the liquid rocket engine.

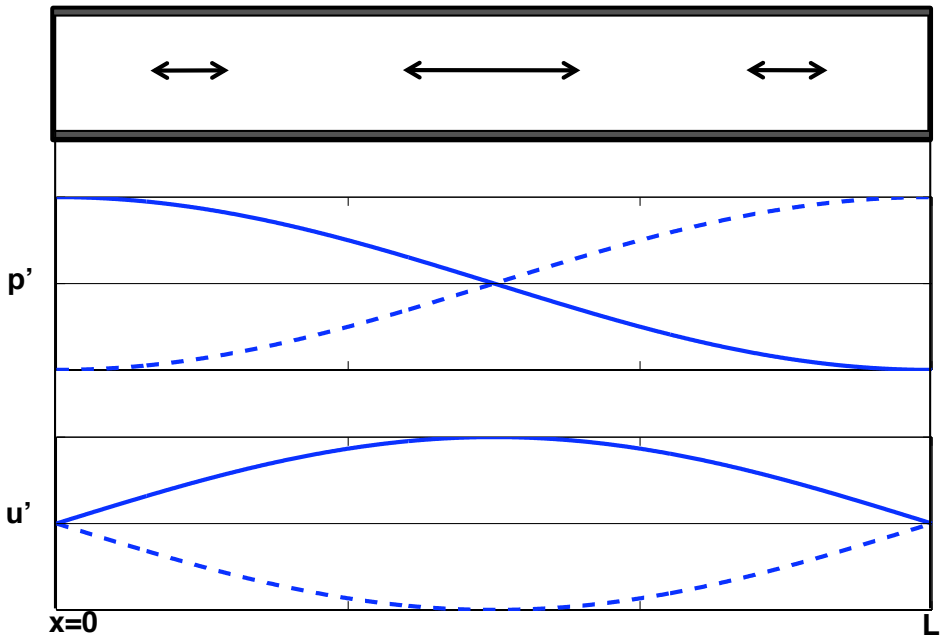

Figure 3.2: Acoustic pressure and velocity distributions for the fundamental mode in a closed tube without baffles.

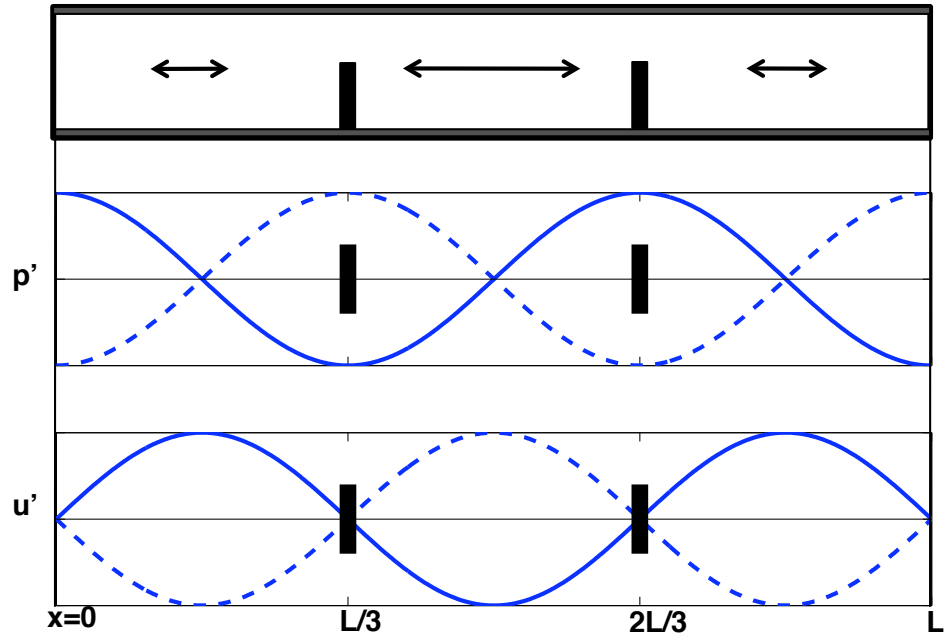

Figure 3.3: Acoustic pressure and velocity distributions for the fundamental mode in a closed tube with baffles placed at L/3 and 2L/3.

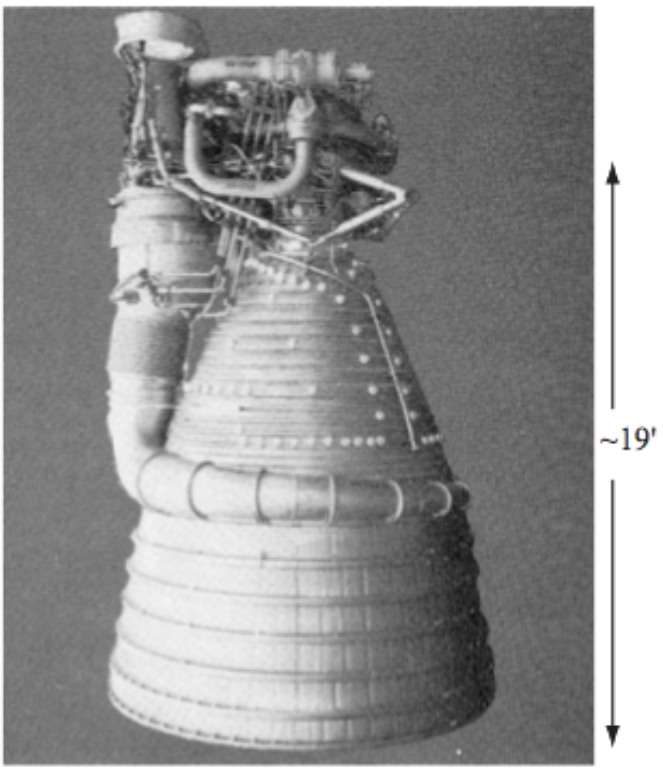

(a) The F-1 engine

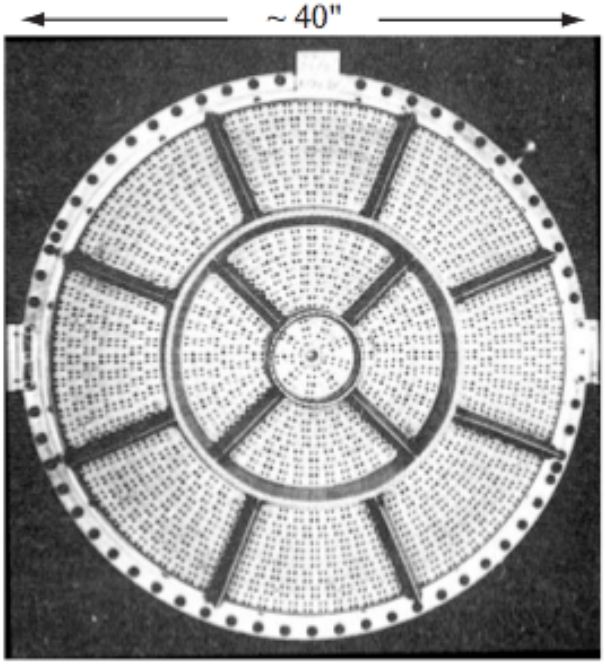

(b) The face of the injector showing the fourteen baffles

Figure 3.4: F-1 engine and baffles on the injector plate (Oefelein and Yang 1993).

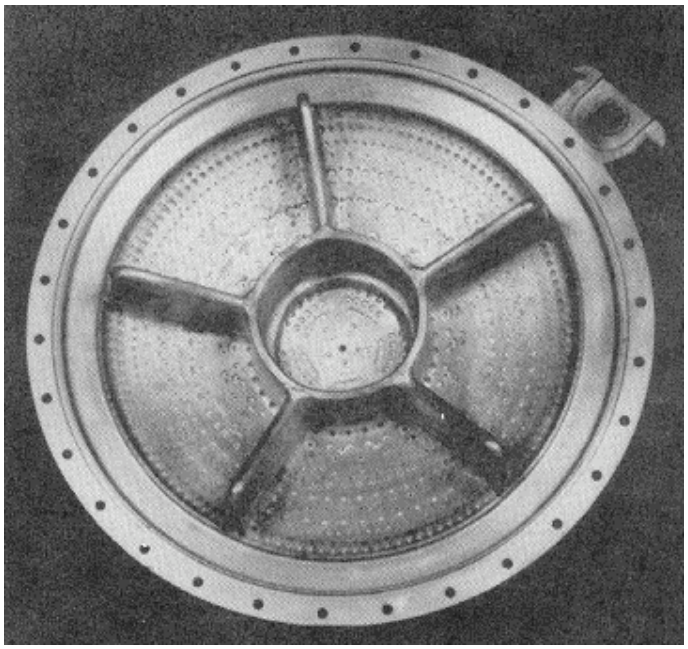

Figure 3.5: Typical baffles on the Apollo SPS engine injector plate.

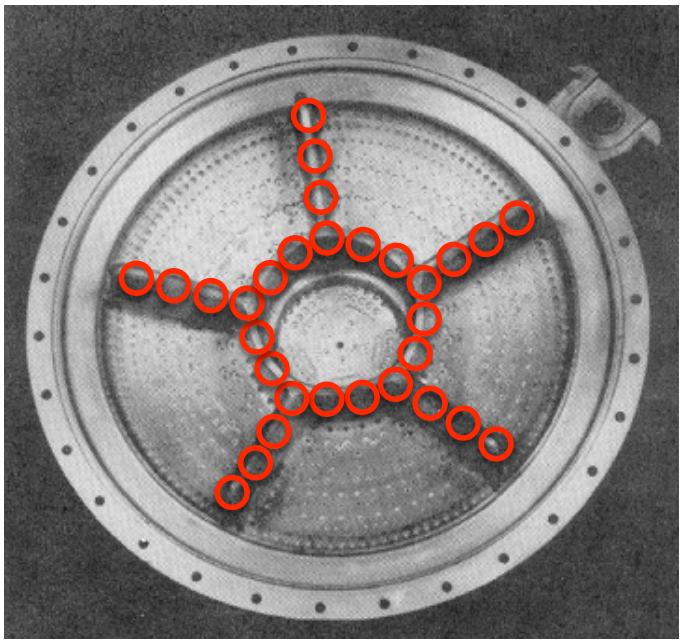

Figure 3.6: Fluidic baffle: replacing the hardware baffle with controlled propellant injectors.

Chapter 4

Experimental Setup and Techniques

4.1 Description of Apparatus

Interaction between turbulent reacting flow and acoustic pressure oscillations is very complicated in the vicinity of the injector in liquid rocket engines. It involves processes associated with periodic atomization and vaporization of the liquid core, unsteady mixing between fuel and oxidizer and flame interactions with traveling and standing pressure waves. It was therefore necessary and important to separate and simplify the flame-acoustic interaction for the current research. Two model shear coaxial injector rigs were designed to conduct flame-acoustic interaction experiments. These model combustors were operated with gaseous oxygen and gaseous fuel, not just because of facility limitations but also in an effort to minimize any complexity associated with atomization and vaporization coupling. Because flames

are formed between vaporized propellants in shear-coaxial injectors even in full-scale LOX-LH_2 rocket engines, the use of non-cryogenic propellants in this study was not expected to affect the essential features of the flame-acoustic coupling. The 2-D models were chosen mainly for ease of diagnostics. A transversely mounted acoustic driver was used to simulate acoustic conditions occurring in the neighborhood of such injectors. As the acoustic output of the driver unit was limited, the model experiments were conducted at scaled-down conditions, ensuring relatively strong levels of acoustic excitation compared to the level of natural turbulent fluctuations.

Two experimental rigs, a single-injector combustor and a double-injector combustor, were designed to study the mechanisms and demonstrate the control effectiveness of the fluidic baffles. Different oxidizer and fuel configurations were applied to the single-injector combustor to investigate the effect on the flame-acoustic interaction. The objective was to understand the physical mechanisms that affect the acoustic stability of shear-coaxial injector flames. The other combustor featured a pair of shear-coaxial injector models, consisting of one controlled injector placed next to a constant-flow GO_2-GH_2 injector. The objective was to quantify the changes in acoustic resonance characteristics and to explore the feasibility of replacing acoustic baffles with a series of controlled injectors.

4.1.1 Combustor Design

Single-Injector Combustor

A schematic drawing of the single-injector combustor setup is shown in Figure 4.1 and 4.2. The combustion chamber is rectangular with 3.5 in. width, 15 in. length, and 0.375 in. depth. The central oxidizer jet is 0.75 in. wide at the base, while the two co-flowing outer jets of fuel are each 0.25 in. wide. The flow configuration for H_2 and O_2 is shown in Figure 4.4. The lip thickness between the center and outer jets is 0.125 in. on each side. The injector end of the combustor was also provided with 0.125 in. slots near the side walls for wall jet injection. Wall jets were only used for igniting the combustor and were turned off once the diffusion flame system between the center and the co-flowing jets was established. A pair of 1 in. thick quartz windows provide optical access of the test section, thereby allowing direct examination of the flame structure as well as chemiluminescence measurements. One of the quartz windows can be replaced with a stainless steel metal window fitted with a number of pressure taps for measuring local pressure fluctuations for studies involving pressure measurements. The tap locations and name designations are shown in Figure 4.5 and also summarized in Table 4.1.

Double-Injector Combustor

The double-injector combustor was designed in a similar pattern to the single-injector combustor. Figure 4.6 is an overall schematic drawing of the double-injector combustor. The combustion chamber is rectangular with 6.0 in. width, 15.0 in.

Table 4.1: Coordinates of various tap locations in single-injector combustor

Tap #	x (in)	y (in)
1	-1.625	0.500
2	-0.500	0.500
3	0.500	0.500
4	1.625	0.500
5	-0.500	0.750
6	0.500	0.750
7	-0.500	2.250
8	0.500	2.250
9	-1.500	3.750
10	-0.500	3.750
11	0.500	3.750
12	1.500	3.750

Table 4.2: Coordinates of various tap locations in double-injector combustor

Tap #	x (in)	y (in)
1	-2.400	0.500
2	0.000	0.500
3	2.400	0.500

length, and 0.5 in. depth. There are two complete injector elements in the combustor. Each element is 1.2 in. wide. In each element, the central oxygen post is 0.6 in., the wall thickness between the center and outer jets is 0.1 in., and the co-flowing outer jets of fuel are each 0.2 in. wide. The center-to-center spacing between the two elements is 2.4 in. The dimensions of the injectors and the flow configuration of H_2 and O_2 flames are shown in Figure 4.9 and 4.10. The side-wall thickness is 1.0 in. Similar to the single-injector combustor, there are 0.1 in. slots for air at the injector end of the combustor near the side walls for wall jet injection. In total, the rig width is 8.0 in. One side of the combustor is a 1.0 in. thick quartz window which provides optical access to the test section. The other side of the combustor is a stainless steel metal window fitted with three pressure taps for measuring local pressure oscillations. The taps are positioned and designated as shown in Figure 4.6 and summarized in Table 4.2. Tap #2 is centered between the two oxidizer posts, and the other two taps are each centered between their respective side walls and outer jets.

4.1.2 Supply System for Fuel and Oxidizer

For both single-injector combustor and double-injector combustor experimental setups, test gases of hydrogen, oxygen, and methane were supplied from high-pressure gas cylinders. The flow rates were metered using choked orifices. Stainless steel honeycomb sections were placed in the injector tube to provide uniform inlet velocity profiles and reduce the turbulence level at the injector exit. Setra pressure transducers (Setra model - 206) were used to monitor the upstream stagnation pressures of the metering orifices and the pressure values were read directly from Setra Datum 2000 metering units. Pressure and choked orifice area values were used to calculate mass flow rates. Electrically operated, normally-closed Parker Skinner valves with 0.25 in orifices were used for switching purposes on the gas supply lines.

For experiments in which transient behavior was characterized, fuel lines were modulated by two HR Textron R-DDV (Rotary-Direct Drive Valve) linear proportional servo-valves (Part 27A50FV1E02). The limited angle, rotary torque motor drives a valve spool directly through an "eccentric" which is built into the motor shaft. Rotary operation of the motor results in a linear spool motion which modulates fluid flow through the cylinder ports of the valve. The R-DDV servo-valve utilizes an integrated electronic controller which is packaged into the motor enclosure. The controller compares spool position, which is monitored by an electronic device within the motor, with the input command signal. The resulting difference generates a current signal which drives the motor to the commanded position. This signal is electronically enhanced to provide optimum valve performance and

linearity. The command signal of 0-10 volts is used to linearly control each servo-valve's effective open area. This property is used to control the mass flow rate of the compressible gas, by holding the supply pressure constant. However, the servo valves have some inevitable leakage even when the command signal is 0 volts. Thus, normally-closed Parker Skinner valves were still used upstream to turn off the gas flows completely.

4.1.3 Acoustic Excitation System

The model injector setup was acoustically forced using a 100 watt maximum power compression driver with a nominal impedance of 16 ohms, mounted on one side of the combustion chamber. Controlled pressure waves were applied through a 1 in by 0.125 in rectangular slot on the side wall. The acoustic driver had a range of optimal operability between 100 Hz to 100,000 Hz.

A Wavetek 40 MHz Universal Waveform generator was used to excite the chamber acoustically at various frequencies and amplitudes. This signal generator provided various monotone and swept signals which were amplified through a Bogen C-100 amplifier and fed into the compression driver. For the experiments where broadband signals and band-limited white noise signals were required, LabVIEW-based signal generators were also used. The average power used was 9 W for white noise forcing and 12.5 W for fixed-frequency forcing.

4.1.4 Data Acquisition System

Data acquisition and computer-based experiment control were performed using a Pentium IV PC equipped with a National Instruments PCI-6251 Multifunction DAQ card, which was connected to a BNC 2120 Data Acquisition Board. National Instruments' LabVIEW 8 software was used to initiate the experiment and digitize the measurement signals. A sampling frequency of 20 kHz was used in LabVIEW-based Virtual Instruments.

In order to have maximum control and clarity over the experiment and the data acquisition for transient process tests, a C-based software approach was chosen over the LabVIEW implementations. The COMEDI (COntrol and MEasurement Device Interface) software package was used with the GNU/Linux operating system under a 2.6.20-family kernel. Customized C programs were written and evolved for each type of experiment.

4.2 Test Techniques and Approaches

4.2.1 Acoustic Characterization

Acoustic resonance characteristics were investigated by probing the combustion chamber using white noise acoustic excitation. This was done using a LabVIEW software package to generate band-limited white noise, which was then fed into the compression driver unit. Input acoustic energy from the driver was further amplified or suppressed by flame-generated acoustics and system resonance characteristics.

The resulting output energy spectrum then reflected both the flame stability and acoustic resonance characteristics of the combustion chamber.

The frequency range of the band-limited white noise was 100 Hz - 5000 Hz. A Kistler 211B5 piezoelectric transducer, with a measurement range of 0 to 250 psi, connected to a Kistler 5134A1 Piezotron coupler, was used for dynamic pressure measurements. The transducer was flush-mounted on the side wall at the locations shown in Figure 4.2 and 4.6 using Kistler 228P water-cooled adapters to protect the transducers. The Piezotron coupler allowed filtering and amplification of signal from the sensors. A low-pass filter of 10 kHz and a gain of 100 on the coupler were typically used for examining pressure fluctuations. Data was sampled at rate of 20 kHz. The LabVIEW VI not only performed a runtime FFT on the sampled data but also saved the data in files which were subsequently loaded into and analyzed with FFT codes in MATLAB. About 400 spectra were averaged to obtain the results, which show distinctive spectral peaks corresponding to various acoustic resonance modes.

4.2.2 Rayleigh Index Measurements

When acoustic forcing is applied at a fixed frequency, the Rayleigh index becomes a valuable tool by which flame-acoustic stability can be evaluated. Computation of the Rayleigh index is performed using the simultaneous pressure oscillation p' and heat-release oscillation q' measurements taken over one forcing cycle. Local fluctuating pressures were measured using Kistler 211B5 piezoelectric trans-

ducers flush mounted on the metal window via water-cooled adapters, as described in the previous section. Local heat release fluctuations were estimated using the OH* chemiluminescence technique [79, 13, 93], which utilizes a custom-built setup consisting of a Hamamatsu R3788 photomultiplier tube (PMT) featuring a high-sensitivity Bi-Alkali Photocathode with good spectral response between 185 nm - 750 nm. It was integrated with a 308 nm band-pass filter for measuring the oscillations of the diffusion flames. The sensor viewing area was a 0.44 in. radius circle centered around each pressure tap location. A TENMA Regulated DC Power Supply provided the required 15 V DC for stable PMT operation while a potentiometer allowed adjustable amplification of the voltage signal from the PMT to a level suitable for data acquisition. The chemiluminescence measurements were made at the specified locations on the flame front where dynamic pressure sensor Taps #5 - #11 were located in the single-injector combustor, as shown in Figure 4.2. The PMT is set up on a graduated mounting rail so that the precise position of the sensor area with respect to the injector could be recorded.

To obtain the information from the digitized pressure transducer and PMT signals, a high-pass FIR filter designed in the MATLAB software package's fdatool (Filter Design & Analysis Tool), was used. In experiments where the Rayleigh index was computed, the sampling frequency was 11.5 kHz, which is ten times the forcing frequency at 1150 Hz. The filter's cut-off frequency was 1120 Hz, the order 1578 and it had a pass frequency of 1140 Hz. To eliminate the unwanted phase shift due to simply applying the filter, a zero-phase filter was desired. MATLAB's *filtfilt.m* function was therefore used to effectively turn the given FIR filter into a zero-phase

filter by first filtering the sensor output in the forward direction, then taking the filtered output, reversing it, and re-running the reversed output through the filter. The final filtered sensor output contained the desired amplification or attenuation of the specified frequencies, but no phase shifts.

Once the fluctuating components p' and q' were obtained from the filter routine, they were used in a MATLAB code to calculate the value of the local Rayleigh index during each period. As the sampling frequency was chosen to be ten times the forcing frequency, there were ten data points in each period. Consequently, for each data point, the Rayleigh index was calculated as the sum of the products of pressure oscillation p' and heat release oscillation q' over ten data points prior to and including the current point.

4.2.3 Flow Visualization

OH*/CH* Chemiluminescence Visualizations

Chemiluminescence is often used in experiments to track the heat release oscillation [93]. Optical radiation from free OH* radicals is considered linearly related to the chemical reaction rate, or equivalently, the heat release rate . In this work, a DiCam Pro ICCD camera with a UV lens and a 308 nm band pass filter were used to pick OH* chemiluminescence emissions from the flame. Images with exposure times as low as 8 μs were recorded for instantaneous imaging. For the ensemble averaged images, the camera exposure was increased to the order of 500 ms - 750 ms and a neutral density filter was used along with the bandpass filters to control

the net amount of light falling on the CCD sensor. For the flames involving CH_4, a 430 nm band pass filter was used to detect the CH* chemiluminescence,

High Speed Cinematographic Imaging

To study the transient process, a Photron FASTCAM-Ultima 1024 high speed camera was used to take high speed image sequences of flame front oscillations. These images were used to observe the rollup of the diffusion flame front under transverse acoustic forcing and subsequent pairing and merging of vortices. A desktop PC running the Photron Fastcam software was used to capture and record images. The camera had an acquisition rate of 60-16000 frames per second (monochrome) and shutter speeds from 0.016 ms to 7.8 ms. For the requirements of the current investigation, the high speed camera was operated at a frame rate of 1000 fps with an associated exposure of 1 ms.

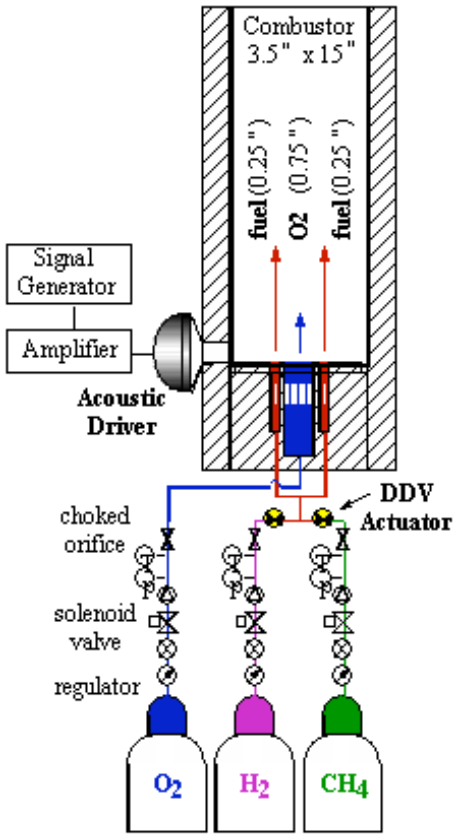

Figure 4.1: Overall setup of the single-injector shear coax combustor.

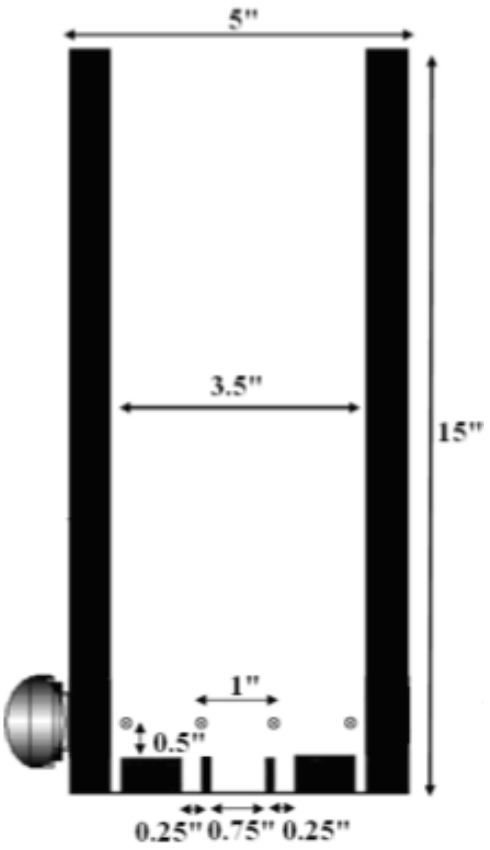

Figure 4.2: Dimensions of the single-injector shear coax combustor.

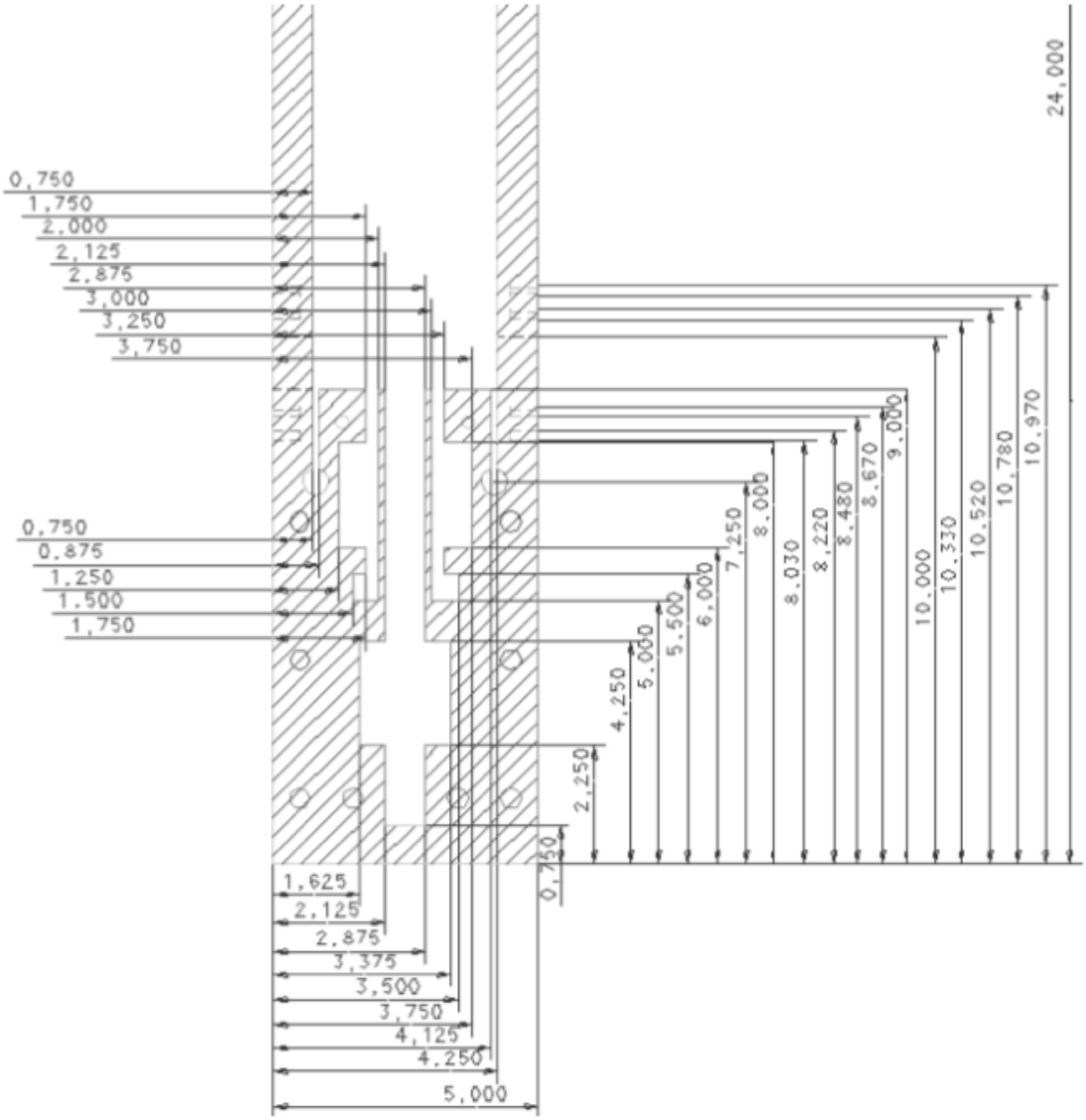

Figure 4.3: Schematic drawing dimensions for the air, oxidizer and fuel inlets to single-injector combustor. Unit:inch.

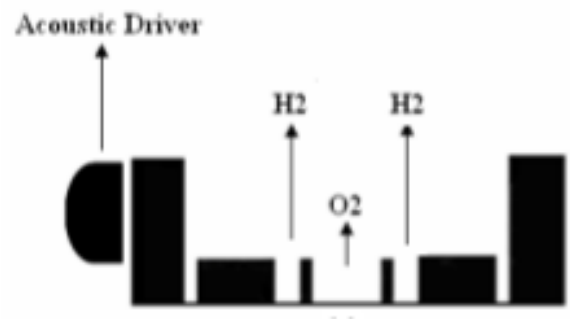

(a) H_2 and O_2 flames

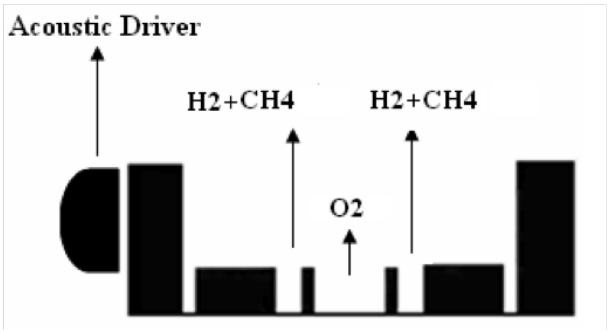

(b) CH_4-H_2 and O_2 flames

Figure 4.4: Flow configuration for H_2-O_2 and H_2-CH_4-O_2 flames in the single-injector combustor.

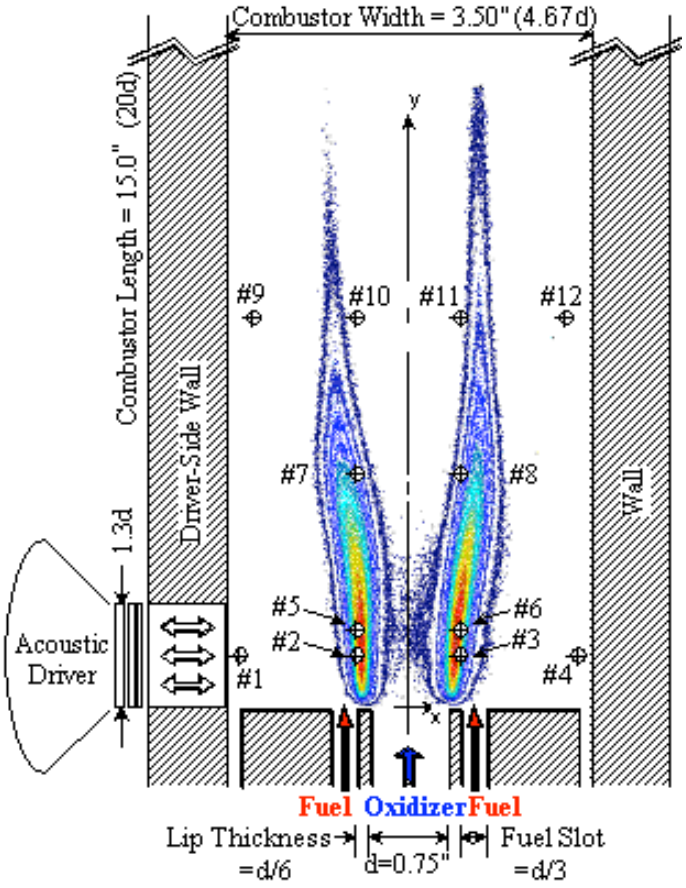

Figure 4.5: A close-up view of the injector flames and tap locations in the single-injector combustor.

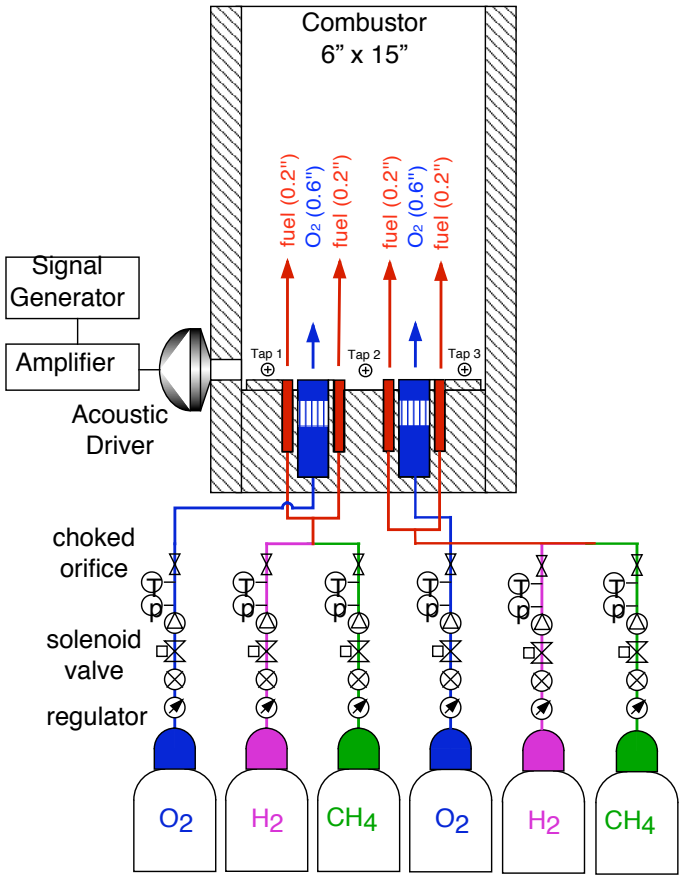

Figure 4.6: Overall setup of the double-injector shear coax combustor.

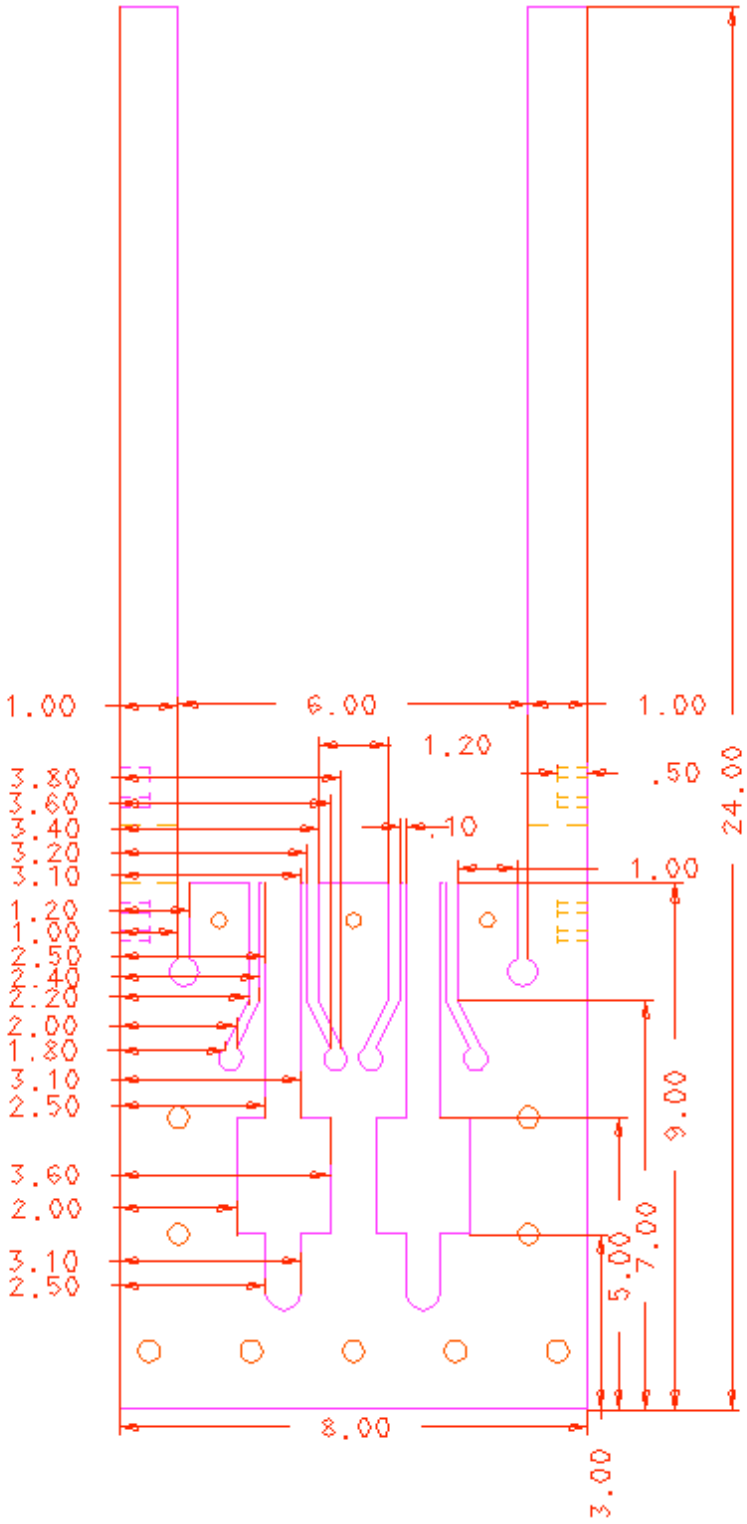

Figure 4.7: Schematic view of the double-injector shear coax combustor for injector dimensions. Unit:inch.

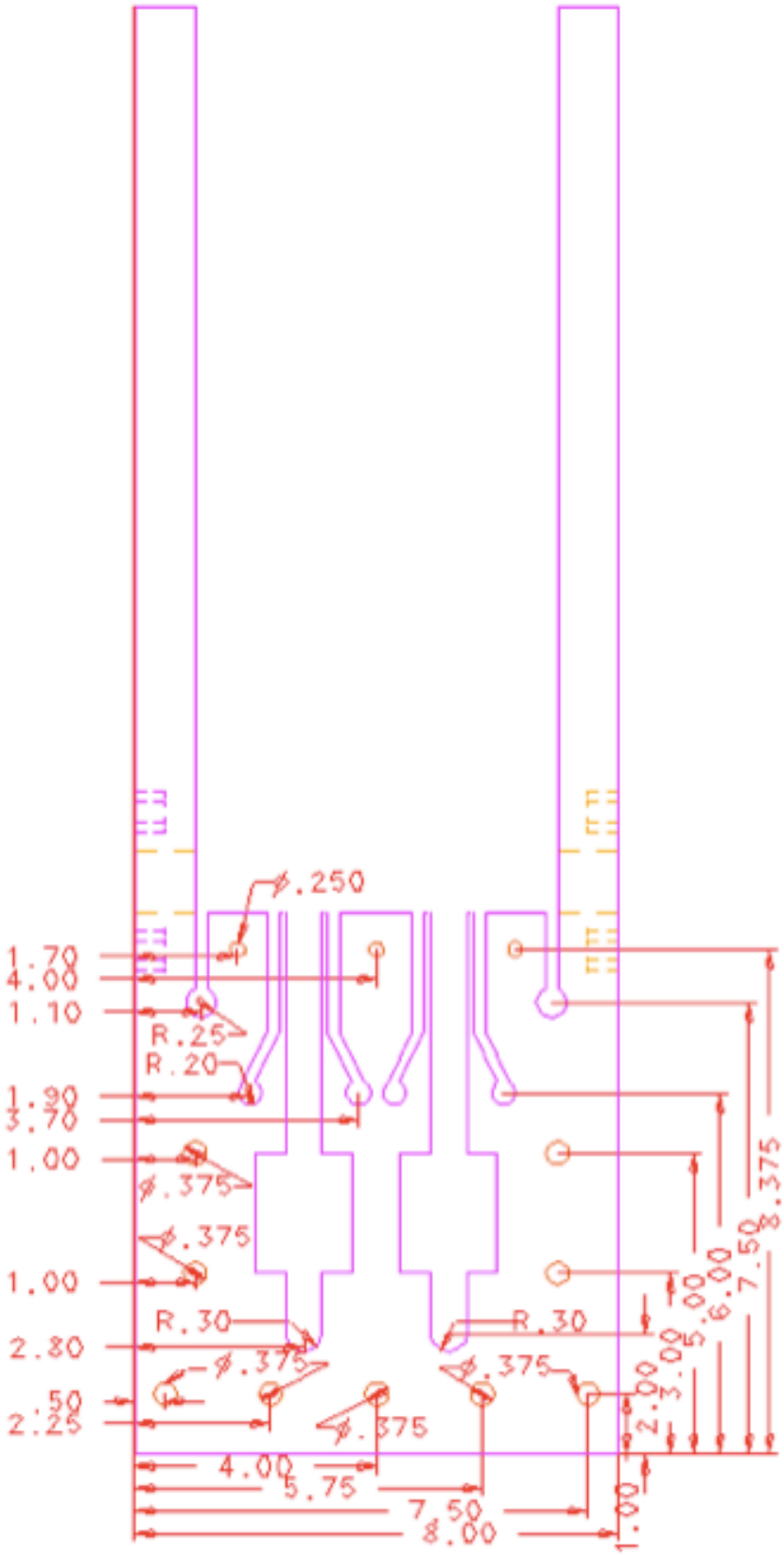

Figure 4.8: Schematic view of the double-injector shear coax combustor for oxidizer and fuel inlet. Unit:inch.

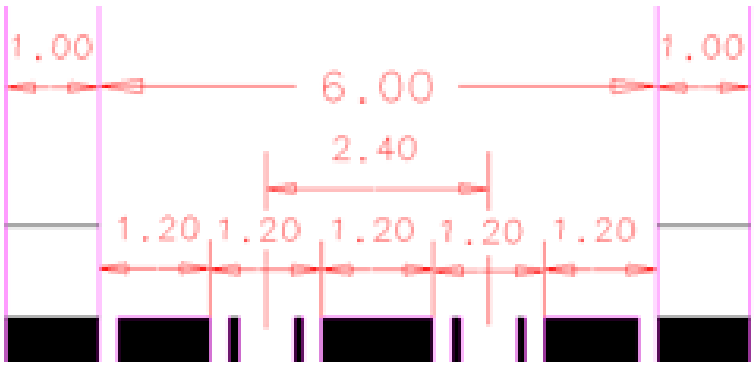

Figure 4.9: Dimensions of the injectors in the double-injector shear coax combustor, Unit:inch.

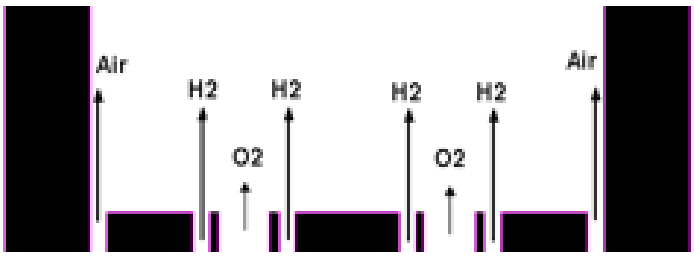

Figure 4.10: Flow configuration for H_2 and O_2 flames in the double-injector combustor.

Chapter 5

Flame-Acoustic Interaction in Single-Injector Combustor

5.1 Introduction

Experimental investigations of acoustic characteristics and flame-acoustic interaction in the single-injector model combustor are presented. Firstly, it was important to characterize the acoustic modes of the chamber so that interactions at different frequencies and amplitudes could be better interpreted. This is discussed in Section 5.2. The effect of fuel density on the acoustic resonance in the chamber was studied by introducing CH_4 as a secondary fuel, mixing it with H_2, as discussed in Section 5.3. Section 5.4 describes the ignition characteristics with H_2-CH_4 blended fuel. To gain insight into the physical mechanisms that affect acoustic stability, flames were excited using periodic forcing at a frequency not connected with acoustic resonances, as detailed in Section 5.5. The effect of the fuel density on the flame

response to traveling acoustic waves was studied. Both steady-states with different fuel compositions and transition processes were investigated.

5.2 Acoustic Characterization of Chamber

5.2.1 Non-Reacting Flow

A confined combustion chamber can be considered an acoustic resonator. Combustion instability is associated with the resonant coupling of the chemical heat release process and the chamber acoustic fluctuations, leading to growth of the hot gas pressure oscillations in one or more acoustic wave modes within the chamber. The experimental approach to find the dominant frequencies of a combustor is to excite it acoustically with broad-band white noise forcing and take pressure oscillation measurements. The resulting pressure spectra inside the chamber can be used to understand the resonance behavior by examining local maxima and minima in pressure spectral intensity. This method is very effective in obtaining the acoustic resonant frequencies of the chamber.

The acoustic characteristics of the chamber without flow were studied with white noise excitation in the single-element injector model combustor, shown in Figure 4.1. Figure 5.1 shows the resulting pressure spectra at various locations under a no-flow condition (quiescent air). Taps #1-4 are the tap locations near the injector across the combustor, as indicated in Figure 4.5. For each tap location, about 400 spectra were averaged to obtain these results, which show distinctive spectral peaks

corresponding to various acoustic resonance modes. While these spectra have many spectral peaks, usually there are only a few dominant acoustic modes interacting with the fluid injection. The coupling resonant modes are the key modes which can interact with combustion oscillation in the reacting tests. Thus the acoustic modes were identified with fluid injection experiments in these non-reacting flow tests.

With fuel and oxidizer injected, non-reacting experiments were conducted to identify the various acoustic modes in the single-element injector model combustor at room temperature. For the baseline case, involving only H_2 and O_2, the center jet was O_2, and the co-flowing jets were the fuel H_2, as illustrated in Figure 4.4(a). The flow conditions for all experiments in the single-injector combustor are summarized in Table 5.1. For this set of experiments, the reactants injected are marked as flow conditions A in Table 5.1. The fuel-oxidizer ratio was stoichiometric, and the velocity of O_2 was 4.5 m/s, which gave turbulent flow with a Reynolds number of approximately 5500. Local pressure oscillations were also measured at Taps #1-4, shown in the single-element combustor setup in Figure 4.2. The resulting pressure spectra at these four tap locations are shown in Figure 5.2. These pressure spectra show distinctive spectral peaks corresponding to various acoustic resonance modes which couple with the fluid in the chamber. These modes have potential to interact with the flame oscillation in the reacting flow cases. There are up to three distinctive spectral peaks worth noting and they are denoted as f_1, f_2, and f_3 in ascending order of frequency.

For estimating these three acoustic resonance modes, a simple analytical mixing model was used, as shown in Figure 5.3. The basic idea was to model distribution

Table 5.1: Flow conditions for the tests in this chapter.

Flow conditions	A	B	C	D	E	F	G
H_2 mole fraction (%)	100	99	99	94	82	37	0
CH_4 mole fraction (%)	0	1	1	6	18	63	100%
H_2 flowrate (g/s)	0.130	0.125	0.108	0.104	0.070	0.018	0
CH_4 flowrate (g/s)	0	0.015	0.013	0.058	0.126	0.231	0.265
Fuel velocity (m/s)	13.5	13.0	11.3	11.3	8.7	4.6	3.8
O_2 flowrate (g/s)	1.06	1.06	0.92	1.06	1.06	1.06	1.06
O_2 velocity (m/s)	4.5	4.5	3.9	4.5	4.5	4.5	4.5
O_2 Reynolds number	5500	5500	4700	5500	5500	5500	5500
Density ratio ρ_o/ρ_f	16.0	14.5	14.5	11.0	7.0	3.0	2.0
Velocity ratio u_f/u_o	3.0	2.9	2.9	2.5	1.9	1.0	0.8
Rate of heat release (kW)	16.1	15.9	13.8	15.5	14.9	13.8	11.9

of the fuel, the oxidizer and the fuel-oxidizer mixture within the combustor in a physically meaningful way in different regions of the combustor. The speed of sound in a given region's medium along with the boundary conditions could thus be obtained. With the known dimensions of the combustor, the resonant frequencies could be evaluated for various acoustic modes. The products were simply assumed to be a stoichiometric mixture of fuel and oxidizer as dictated by initial flow rates. For the cold flow tests, the temperature was considered room temperature. For instance, since acoustic waves travel through different media in the transverse direction, the quarter-wave mode in the transverse direction is evaluated as follows:

$$f_{\lambda/4} = \frac{1}{4\left[\left(\frac{W_o}{a_o}\right) + 2\left(\frac{W_f}{a_f}\right) + \left(\frac{W - W_o - 2W_f}{a_p}\right)\right]} \tag{5.1}$$

where a_o, a_f, and a_p denote the speed of sound as it travels through oxidizer, fuel and products respectively, and where W, W_o and W_f denote the chamber width, width of the oxidizer jet and width of the individual fuel jet respectively. In this equation, the frequency of the transverse mode depends on the assumptions for product composition and the regions of the fuel, oxidizer and product. For the baseline case being considered here, the products were simply the stoichiometric H_2 and O_2 mixture as dictated by the initial flow rates. Both longitudinal and transverse modes were calculated by this methodology. Comparing the calculated results and experimental data allowed identification of these acoustic modes.

On the basis of the isothermal flow investigations, the following findings were made:

- The observed frequency f_1 appears to be the quarter-wave mode of the oxi-

dizer post. The calculated frequency is in good agreement with the measured frequencies.

- The observed frequency f_2 appears to be the longitudinal three-quarter-wave mode of the combustion chamber. While the accuracy of the frequency calculation depends on how well the mixture composition can be predicted as a function of spatial location, a full-mixing assumption results in a close approximation of the frequency.

- The observed frequency f_3 appears to be the transverse quarter-wave mode of the combustor at the measured axial location. Assuming that this is the transverse mode, the mode shape is also well predicted.

Table 5.2 lists and compares various spectral peaks obtained at these four tap locations from the experimental data and the model analysis. The comparison of the measured and calculated resonance frequencies is in good agreement and supports the suggested physical mechanisms.

5.2.2 Reacting Flow

In a similar manner as in the non-reacting flow tests, reacting flow experiments were conducted with band-limited white noise excitation. Again, the same flow condition resulted in well-defined spectral peaks at Tap #1-4 as shown in Figure 5.4. In these experiments, only two spectral peaks are worth noting and they are marked as f_1 and f_2, while in the non-reacting flow tests, there are three spectral peaks. Although the actual frequencies are obviously different from those in the isothermal

Table 5.2: Comparison of measured spectral peak frequencies and calculated resonance frequencies.

Location	Mode	Measured (Hz)	Calculated (Hz)
Tap #1	f_1	434 ±10	430
	f_2	900 ±10	980
	f_3	1508 ±10	1430
Tap #2	f_1	434 ±10	430
	f_2	933 ±10	980
	f_3	1508 ±10	1430
Tap #3	f_1	433 ±10	430
	f_2	1017 ±10	980
	f_3	1580±10	1430
Tap #4	f_1	438 ±10	430
	f_2	1011 ±10	980
	f_3	1528 ±10	1430

experiments due to the temperature change, the nature of the two dominant modes appears to be the same. More precisely, the frequency f_1 appears to be related to the longitudinal quarter-wave mode of the oxygen post and the frequency f_2 appears to be the longitudinal three-quarter-wave mode of the combustion chamber. The combustion temperature can be calculated from the difference between the speed of sound in the isothermal case and reacting case. The estimated temperature is within reasonable bounds.

Another interesting observation for the reacting flow spectra is that the spectral peak shapes and frequencies are more dependent on the measurement location than the non-reacting flow spectra. A likely explanation is the high sensitivity of product temperature on reactant composition. Because different amounts of thermal energy can be added to the flow at different locations, the product temperature will not be uniform within the combustion chamber. Thus, a large variation in speed of sound is expected.

5.3 Blended Fuel Effect on Acoustic Characterization of Chamber

5.3.1 Non-Reacting Flow

In these experiments, the effect of the fuel density on the flame-acoustic interaction in the flowfield near the injector was examined by introducing CH_4 as a secondary fuel and mixing it with H_2. By tailoring the CH_4 mole fraction in the

blended H_2-CH_4 fuel, the density of the fuel changes substantially, which of course alters the density ratio between fuel and oxidizer commensurately. The chamber's acoustic impedance depends on the injected fluid within a fixed geometry. Modifications of the acoustic impedance resulting from different fuel compositions were studied using white noise excitation. Non-reacting experiments were conducted with the three different flow conditions D, E, and F shown in Table 5.1. For each flow condition, about 400 averaged pressure spectra corresponding to the first four tap locations, Tap #1-4, are presented. Figure 5.5, 5.6 and 5.7 show the local pressure spectra under flow conditions D, E and F. From these plots under the flow conditions D and E, it is obvious that the acoustic resonance characteristics of the model injector remained qualitatively similar under fuel composition variation. However, for the flow condition F with 37% mole fraction of H_2 in the blended fuel, both the density ratio and velocity ratio between the fuel and oxidizer were small, and the resulting spectra had numerous spectral peaks, which was similar to the case without flow injected, shown in Figure 5.1.

The acoustic impedance is affected by the fuel density change due to the speed of sound at given temperature. The frequency shift associated with different fuel densities for the isothermal case is shown in Figure 5.8. From the plot, it can be seen that the resonance at the lowest frequency f_1 was relatively unaffected by both tap location and flow conditions, as it only shifted 7% within the tested range. This frequency is considered the quarter-wave mode of the oxidizer post. Since the O_2 flow rate was held constant, this frequency would not be affected by fuel mixture modulation. Resonance at the second lowest frequency f_2 changed substantially

between the different flow conditions, but relatively little between the tap locations. Only 18% CH_4 addition (by mole fraction) causes this modal frequency to change 19%. As discussed before, this frequency was identified to be the longitudinal three-quarter-wave mode of the chamber. Resonance at the third lowest frequency f_3 also changed substantially amongst different flow conditions but was practically constant across the tap locations, which agrees with the hypothesis that it was related to the transverse mode. This transverse mode frequency shifted 18% with the flow conditions in these tests.

The trends of the resonant frequencies decreasing with increasing CH_4 mole fraction in the H_2-CH_4 blended fuel are in good agreement with the physical explanation. Each fuel composition represents a particular molecular weight of the fuel, which in turn means each fuel mixture has a different speed of sound at room temperature. With more CH_4 in the blended fuel, the density of the fuel increases, resulting in a lower speed of the sound in the medium and lower resonant frequencies within the same geometry. Acoustic impedance therefore changes due to the CH_4 addition. This suggests a potential method to control the combustion instability is to modify the acoustic impedance in the combustor by the injection of a different fuel composition.

An analytical model, similar to the one discussed in Section 5.2 was used to calculate the resonant frequencies for the different flow configurations. The products in each case were the stoichiometric fuel-oxidizer mixture as dictated by the initial flow rates of the H_2-CH_4 blended fuel and O_2. The temperature was assumed to be room temperature. The speed of sound in each flow configuration was calculated.

Table 5.3 lists and compares various spectral peaks obtained from the experimental data and the model analysis at flow conditions D and E. The calculated frequencies agree well with the experimental results for each case, and the model analysis predicts the trend as well. This simple model doesn't include the effect of the acoustic excitation, thus it cannot predict the variation between the tap locations.

5.3.2 Reacting Flow

For the same flow conditions D, E, and F, as the non-reacting tests, reacting flow experiments were conducted to study the effect of fuel composition on the acoustic impedance in the combustor. The results are shown in Figure 5.9-5.11. For flow conditions D and E, two well-defined peaks, similar to the H_2-O_2 flames, appear in the pressure spectra. However, for the case with 37% H_2 mole fraction, there are more peaks due to the smaller density and velocity ratios between the oxidizer and blended fuel. This is also observed in non-reacting flow.

In Figure 5.12, the shift in frequencies associated with the two dominant spectral peaks are plotted as a function of density ratio between oxidizer and fuel. Again, the quarter-wave mode associated with the oxygen post shifts only slightly, presumably due to the same mass flowrate of O_2 and minor changes in heat transfer into the oxygen post. However, the other identified spectral peak for the longitudinal three-quarter-wave mode of the combustion chamber goes through a significant 15% shift in frequency. This is related to the fuel density change and combustion heat release due to different reactants and combustion products. When more CH_4 is involved in

Table 5.3: Comparison of measured spectral peak frequencies and calculated resonance frequencies.

Location	Mode	Flow conditions D		Flow conditions E	
		Measured (Hz)	Calculated (Hz)	Measured (Hz)	Calculated (Hz)
Tap #1	f_1	423 ±10	430	423 ±10	430
	f_2	868 ±10	928	752 ±10	843
	f_3	1453 ±10	1370	1270 ±10	1269
Tap #2	f_1	434 ±10	430	423 ±10	430
	f_2	868 ±10	928	770 ±10	843
	f_3	1453 ±10	1370	1269 ±10	1269
Tap #3	f_1	434 ±10	430	423 ±10	430
	f_2	889 ±10	928	791/900 ±10	843
	f_3	1518 ±10	1370	1400 ±10	1269
Tap #4	f_1	434 ±10	430	423 ±10	430
	f_2	911 ±10	928	781/900 ±10	843
	f_3	1453 ±10	1370	1399 ±10	1269

the blend, the density of the fuel increases and the heat release of combustion decreases, both of which cause the speed of sound to decrease, leading to lower acoustic resonance frequencies in the chamber. Note that the pressure spectra at Tap #2 and 3 are omitted because the taps were located directly on the flame fronts, causing thermally induced errors in the transducers even with water cooling. The accuracy of the data for each test depends on the flame locations. Another observation is that the difference between the tap locations seems to increase with density ratio, which is related to the acoustic excitation from one side of the combustor causing slightly variance of the flowfield at two sides of the flames. The entrainment of the center O_2 jet determines the difference between the tap locations across the combustor.

To investigate the effect of total heat release magnitude on the combustor acoustic response, another set of tests were performed in which the total heat release level was varied while maintaining the fuel mixture ratio. This was accomplished by decreasing all reactant mass flow rates by the same proportion. The corresponding flow configurations for these tests are B and C in Table 5.1. The effect on flame-acoustic interaction associated with heat release can be separated from the fuel density. The results are given in Figure 5.13, which shows that except for the amplitude at frequency f_2, the pressure spectra are insensitive to the level of the total heat release. The modification of the pressure spectra, especially the frequency shift, shown in Figure 5.12, is mainly due to the change of the acoustic resonance in the chamber caused by the variation of fuel density corresponding to the different blended H_2-CH_4 fuel compositions.

5.4 Blended Fuel Effect on Flame Ignition Characteristics

When the fuel was exclusively CH_4, corresponding to flow conditions G in Table 5.1, the flame was lifted because the ignition time of CH_4 is longer than that of H_2. Thus for the same fuel and oxidizer velocities, the location of ignition of pure CH_4 is farther from the injector than H_2. This effect is illustrated in Figure 5.14, showing the flames are lifted from the injector. The general flame characteristics in terms of unforced flame shape and heat release behavior were relatively unaffected by a moderate amount of CH_4 addition. As long as there is a small quantity of H_2 in the blended fuel, the flame ignition characteristics are dominated by the faster response of the H_2 gas. In this set of tests, there was no acoustic excitation.

5.5 Blended Fuel Effect on Flame-Acoustic Interaction with Single Frequency Forcing

Acoustic forcing at one of the resonant frequencies will set up a standing wave pattern inside the combustion chamber resulting in a spatially varying amplitude pattern known as the mode shape. To study the potential interaction between flames and traveling acoustic waves, the flames were forced at frequencies sufficiently far away from the resonant modes. By avoiding resonant frequencies, the behavior of flames interacting with imposed traveling waves could be isolated. The results could provide additional insight into the physical mechanisms that affect acoustic

stability of the fuel mixture. The frequency of the spectral minimum between the two spectral peaks at Tap #4 for the flow condition A case, 1150 Hz, was considered a non-resonant forcing frequency f_f as indicated in Figure 5.15. This single forcing frequency was used for all the experiments in this section. The acoustic forcing level was fixed at 12.5 watts (40 V peak-to-peak).

5.5.1 OH* Chemiluminescence

Periodic single frequency (1150 Hz) forcing was used to excite flames with both pure H_2 and H_2-CH_4 blended fuel. The flow conditions for O_2/H_2 are listed in Table 5.1, denoted as A. The blended fuel mixture is marked as flow condition D in Table 5.1. Figure 5.16 shows the direct comparison of OH* chemiluminescence between O_2/H_2 flames and O_2/H_2-CH_4 flames under the same amount of acoustic excitation at 1150 Hz.

The O_2/H_2 flames show interesting asymmetric flame-acoustic interaction. The left side flame, closer to the acoustic driver, was wrinkled severely due to flame-acoustic coupling, while the right side, farther away from the acoustic excitation, was relatively unaffected. The origin of such asymmetric response was investigated and it was determined that intermittent baroclinic torque made the left side unstable while the right side was stable [94]. The density ratio between oxidizer and fuel plays a key role in the flame-acoustic interaction. When a blended H_2-CH_4 fuel was used, with an oxidizer-fuel density ratio of 3, marked as flow condition D, the interaction became much weaker as shown in Figure 5.16(b). This is a clear indication

that the flames from a blended H_2-CH_4 fuel are more stable against acoustic excitation at this single forcing frequency than those from a pure H_2 fuel. These results suggest that using a blended H_2-CH_4 can reduce the susceptibility to combustion instability at some single forcing frequency. By changing the acoustic impedance in the combustor, the blended H_2-CH_4 fuel can modify the flame response to the acoustic traveling wave at specific frequency.

5.5.2 Rayleigh Index

The Rayleigh index is a mathematical way to quantify the coupling between unsteady heat release and acoustic pressure fields. The local Rayleigh index at different spatial locations in the combustor and at various points in time with respect to the injection of blended fuel have been detailed to provide a better understanding regarding acoustically-driven combustion instability and how it is impacted by using a blended fuel. Localized simultaneous measurements of pressure and OH* chemiluminescence were made at selected tap locations along the two flame fronts, Tap #5-11, as summarized in Table 4.1. These specified sensor locations were carefully selected to probe various regions of interest, including the immediate wake of the injector post where the flames first ignite, the intermediate wake region where the flame brush starts thickening, and a region further downstream where flame wrinkling can be severely affected. In the last region, an additional sensor was placed to probe the external edge of the wrinkled flames. From these measurements, the spatial distribution of the local Rayleigh index was obtained. The Rayleigh in-

dex measurements can be evaluated to reveal various regions of flame-acoustic interaction, including instability-driving, instability-damping and instability-neutral regions within the injector flowfield. The local Rayleigh index at different spatial locations in the combustor and at various points in time with respect to the injection of blended fuel have been examined in detail to provide a better understanding regarding acoustically-driven combustion instability and how it is impacted with the use of blended fuel.

Tests were initially conducted to study combustion without acoustic excitation. The pressure oscillation, heat-release oscillation and corresponding local Rayleigh index at the three spatial locations, Tap #9-11, are shown in Figure 5.17 - 5.19 (marked as Natural). Without acoustic excitation, both sides of flames show similar response. Thus measurements were taken with the left flame. For all three locations, the pressure oscillation and heat release fluctuation were very small, and the Rayleigh index is almost zero without acoustic excitation. This shows this combustion system is not self-excited. Without external forcing, the combustion is stable, and it does not go to an unstable state by itself. Only when acoustic excitation is superimposed to the system does it have potential to develop combustion instability.

When the H_2 composition of 99% was forced at 1150 Hz, pressure oscillations and OH* chemiluminescence fluctuations were simultaneously observed from the flames on the driver and wall sides. These are shown in Figure 5.20. In Figure 5.20(a) and 5.20(b), although both flames are responding to a similar level of acoustic excitation, the amplitude of flame response is much larger on the driver side of the flames than on the wall side. Even near the injector exit, shown in Figure 5.20(c),

the driver side flames exhibit a more unstable response than the wall side flames. The density ratio associated with these flames is high, at 14.5. Figure 5.21 presents a comparison of the identical forcing configuration but at a lower density ratio of 3, with more CH_4 mole fraction. Again, the flame on the driver side exhibits a stronger response than the wall side flame to the same amount of pressure oscillation. However, the amount of OH* chemiluminescence fluctuation is much lower than in the 14.5 density ratio case.

The local Rayleigh index measurements also demonstrated an intriguing phenomenon in that neither the driving nor the damping of the instability took place continuously, but rather in a more sporadic fashion. Figure 5.22 shows time traces for locations corresponding to acoustically damping, driving, and neutral regions, respectively. One typical aspect seen is the appearance of high forcing frequency (1150 Hz) components of heat release riding on selective edges of a low frequency (97 Hz) heat release component. Both driving and damping regions experience extended periods of acoustic energy build-up and reduction that spans over 10-12 oscillation cycles. When flame-acoustic interaction is occurring, it can be seen that most of such interactions actively change the acoustic energy balance in one direction. This selective occurrence of high forcing frequency components on falling edges in Figure 5.22(a) and rising edges in Figure 5.22(b) of the underlying low frequency component are stimulated by the local Rayleigh-Taylor instabilities arising from accelerations of heavier oxidizer into lighter fuel. In the neutral regions, there appears to be no effect of acoustic excitation on flame or pressure oscillations.

A graphical summary of the category to which each tap belonged (instability-

damping, driving, or neutral) is presented in Figure 5.23, which shows the sensor locations with respect to a time-averaged OH* chemiluminescence image on the background. From the measurements, it appears that the ignition zone close to the injector post (Tap #5) was stable, while further downstream the flames became highly unstable (Tap #7, #10). Also near the combustor wall on the driver side (Tap #9), it appears that the flame-acoustic interaction was once again suppressed. The flames on the wall side seemed to be unaffected at the present level of acoustic excitation. In contrast to the pure H_2 case, which resulted in highly unstable flames on one side, blended H_2-CH_4 fuel yielded instability-neutral regions everywhere. This demonstrates that acoustic stability response to the travelling wave at this frequency was improved with the blended H_2-CH_4 fuel.

5.5.3 Transition Process

In order to gain insight into the transient behavior of the combustion process due to the addition of CH_4, experiments were performed using two fast-response R-DDV (rotary direct-drive valve) as actuators and a high speed camera for diagnostics. Both H_2 and CH_4 mass flow were controlled by two solenoid valves. These experiments started with the combustor operating at an equivalence ratio of unity with virtually all the fuel as H_2. The acoustic driver was turned on for excitation of the instability mode at 1150 Hz. After operating for a predetermined amount of time with no commanded CH_4 fuel, valve control signals were generated from the PC to instantaneously command the servo-valves to reduce the H_2 mass flow while

simultaneously introducing CH_4. The commanded mass flows were chosen to replace a portion of H_2 fuel with CH_4 while holding the fuel-oxygen ratio stoichiometric. The experimental configurations for the two fuel flow settings, hereafter referred to as flow conditions B and F are detailed in Table 5.1. Note that even for the desired zero CH_4 mass flow case, leakage through the servo-valve prevented a total cut-off of the CH_4 fuel, as shown for flow condition B. The level of acoustic excitation remained constant during these tests.

The results are shown in Figure 5.24 and 5.25. At the moment that the first image was taken, the flow condition was switched. The time interval between the images was 30 msec. From Figure 5.24, it can be seen that the flame farther away from the acoustic driver started to wrinkle more after 30 ms and the settling time for switching from flow condition B to flow condition F was 180 ms, whereas the settling time was 150 ms for the reverse state transition. It shows that the combustion system needs more time to stabilize than to to destabilize with CH_4 addition. This indicates that the application of dynamic control using CH_4 may not be feasible to the combustion system.

A closer investigation of this event using a PMT for diagnostics was conducted. This experiment showed the heat-release changes of the left side flame which was close to the excitation during the transient process from flow condition B to flow condition F. The heat-release history at Tap #9 is shown in Figure 5.26. Time t = 0 is the moment that the flow condition is commanded from B to F. Some reduction in the PMT voltage will naturally occur due to the decreased quantity of OH^* radicals when CH_4 is introduced in place of some H_2. However the amplitude of

flame perturbations decreases due to the favorable density tailoring, leading to less visibility of the perturbed flame to the PMT sensor, resulting in further decreases of the sensed chemiluminescence intensity. Moreover, not only does the sensed intensity go down in amplitude, but the fluctuating component of heat release is also diminished, as is evident in Figures 5.27 - 5.29. The settling time is 180 ms for the flame portion close to the excitation. This time delay is mainly due to the flow time from the servo-valves to the location in the combustor where the PMT sensor is located. It is not practical to apply active fast response control to this system because of this time delay. Most active combustion control requires high frequency response actuators to catch the unstable modes.

5.6 Summary and Discussions

Experimental investigations were conducted to explore the effect of fuel density on the flame-acoustic interaction with a combination of O_2 and H_2-CH_4 fuel mixture as propellants. Two different types of acoustic characterization experiments were conducted. The first utilized band-limited white noise forcing to obtain acoustic response spectra, from which resonance characteristics were evaluated. This method was shown to be very effective in obtaining resonant frequencies for both non-reacting flow and reacting flow. A simple analytical model was developed to identify the acoustic modes. Three dominant acoustic modes observed in non-reacting flow were the quarter-wave mode of the oxygen post, the three-quarter-wave longitudinal mode of the combustion chamber and the transverse first-quarter

wave mode of the chamber, while only two of them were observed in the reacting flow case: the quarter-wave mode of the oxygen post and the three-quarter-wave longitudinal mode of the combustion chamber. The resonant frequencies of these modes compared well with analytically obtained values. The acoustic resonance characteristics of the model injector remained qualitatively similar under blended fuel composition variation, but some of the resonant frequencies shifted to lower values with increasing CH_4 content, most likely due to the density of the fuel and product of combustion. Total heat release was not a key factor in this modification of the acoustic characteristics.

The second type of experiment was based on acoustic forcing at a fixed frequency different from the resonant modes. The interaction between the flame front and acoustic traveling wave was studied. Both global and local measurements of OH* chemiluminescence were made that indicated periodic heat release modulation with this single frequency forcing. Furthermore, simultaneous measurements of local pressure fluctuations showed that acoustic pressure oscillations were responsible for spatial fluctuations in OH* chemiluminescence. The general flame characteristics in terms of unforced flame shape and heat release behavior were relatively unaffected by a moderate amount of CH_4 addition. However, the flames from a hydrogen-methane blended fuel and oxygen were much more stable against acoustic excitation than those from a pure H_2 fuel and O_2 at this forcing frequency. It was shown in this experiment that the blended fuel flames wrinkled very little under acoustic forcing while the hydrogen flames wrinkled heavily under the same intensity of acoustic forcing. To further assess the active control potential of real-time

in-situ CH_4 addition, both transient and steady state characteristics of CH_4 addition into primary H_2 flow were investigated using high speed imaging and simultaneous dynamic pressure and chemiluminescence measurements. Local Rayleigh indices at selected points on the flame oscillation path before and after CH_4 addition were tracked. In the present experiment, the settling time for suppressing flame oscillations completely was as large as 180 ms, most likely due to convection delays caused by the control valve location. If this delay could be further shortened, it may be possible to consider an active control strategy using high-density fuel as an acoustic shield for preventing flame-acoustic interaction.

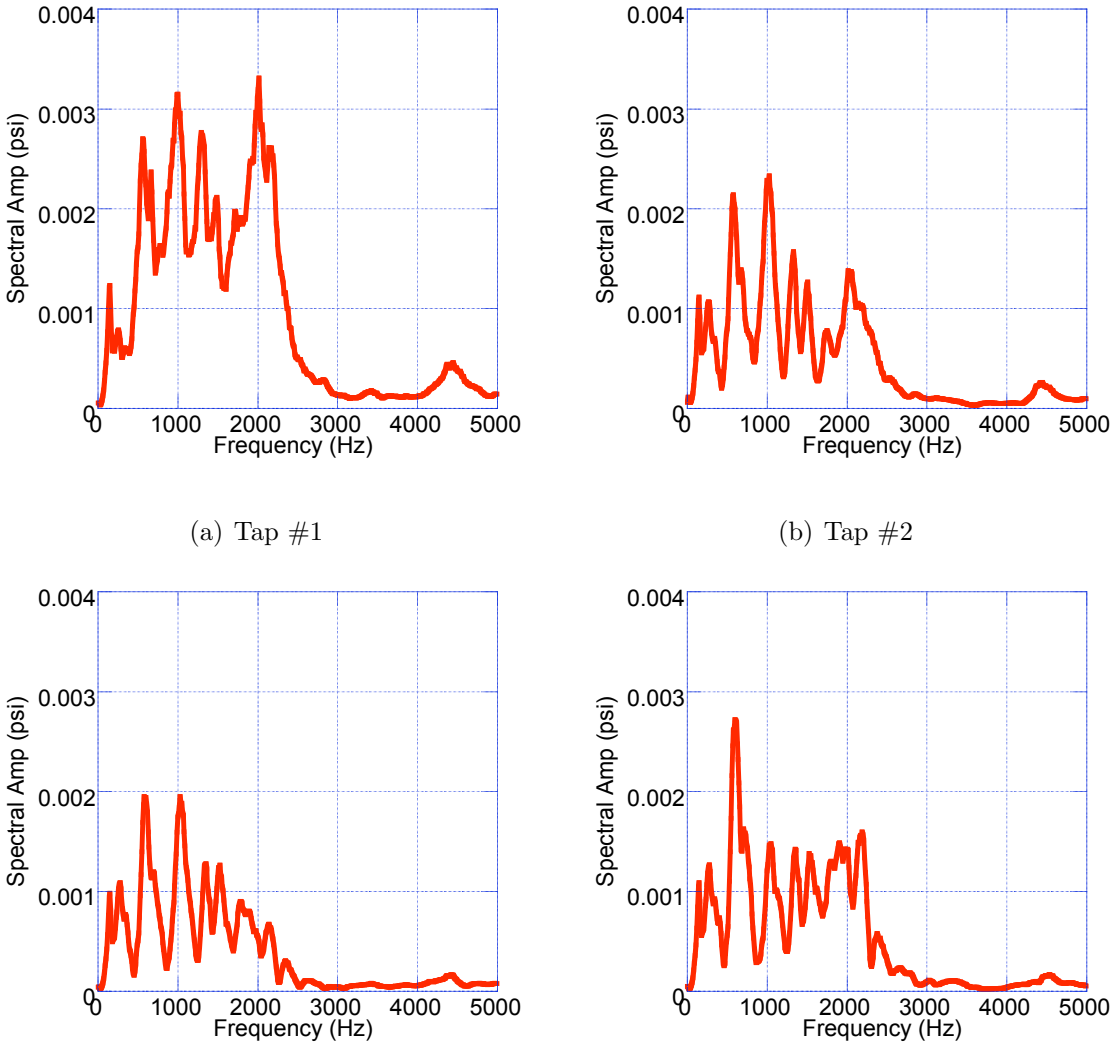

(a) Tap #1

(b) Tap #2

(c) Tap #3

(d) Tap #4

Figure 5.1: Dynamic pressure spectrum of the "no-flow" case under white noise acoustic excitation

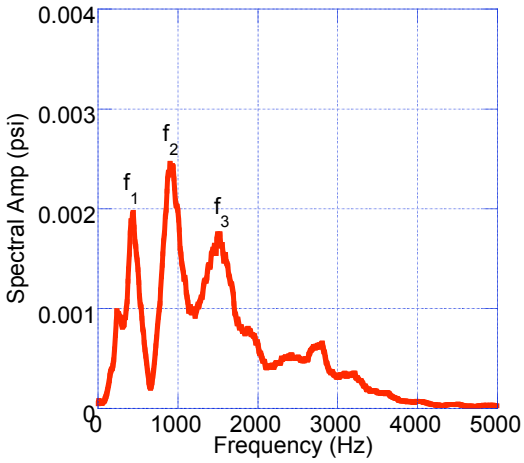

(a) Tap #1

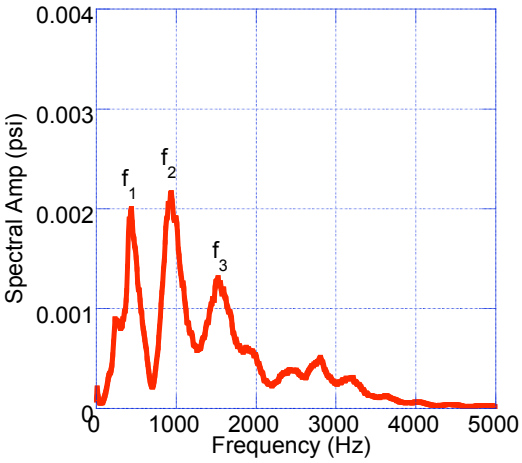

(b) Tap #2

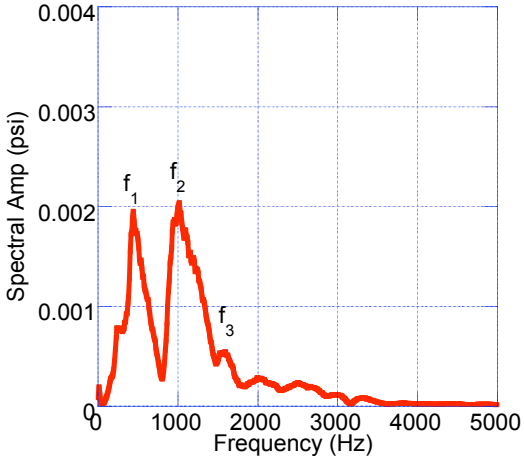

(c) Tap #3

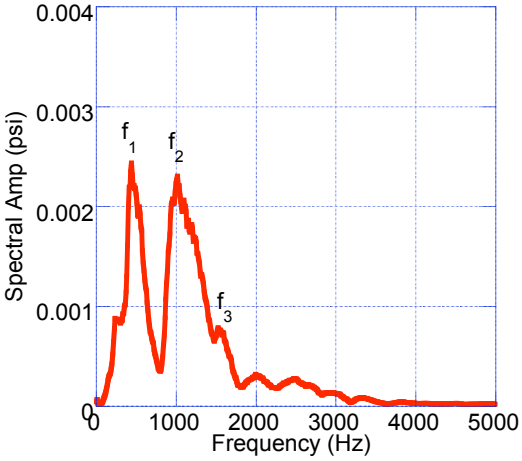

(d) Tap #4

Figure 5.2: Pressure spectrum of H_2-O_2 non-reacting case excited with white noise.

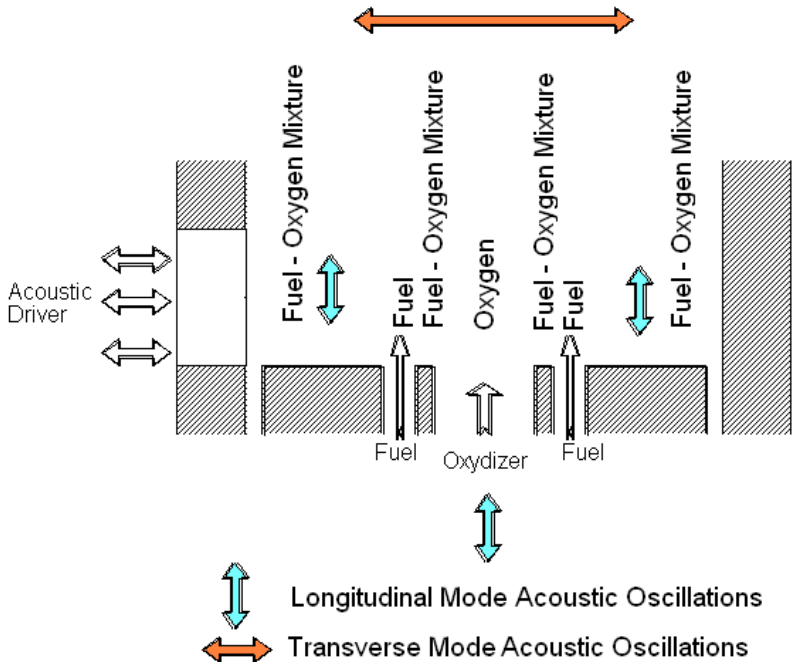

Figure 5.3: Schematic illustration showing distribution of acoustic media in the combustor.

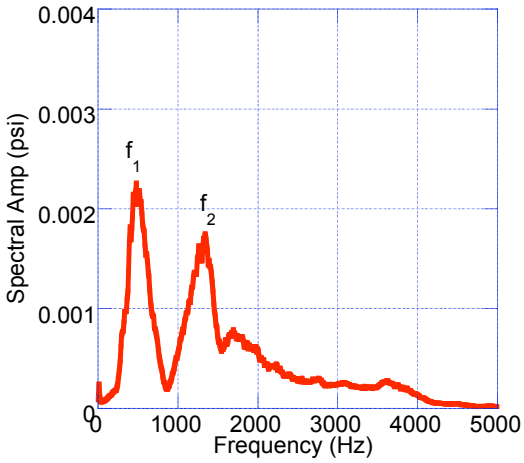

(a) Tap #1

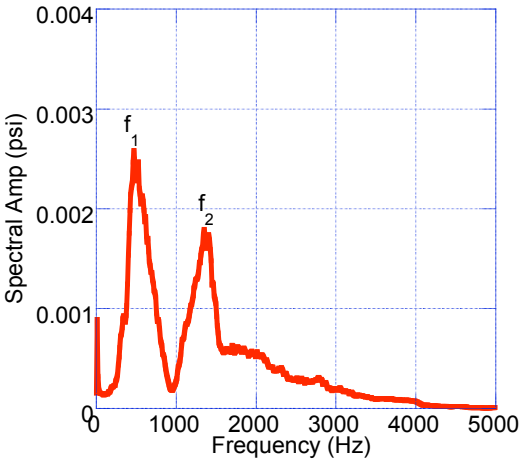

(b) Tap #2

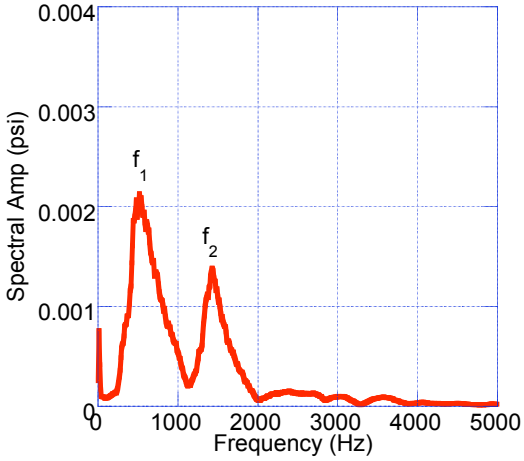

(c) Tap #3

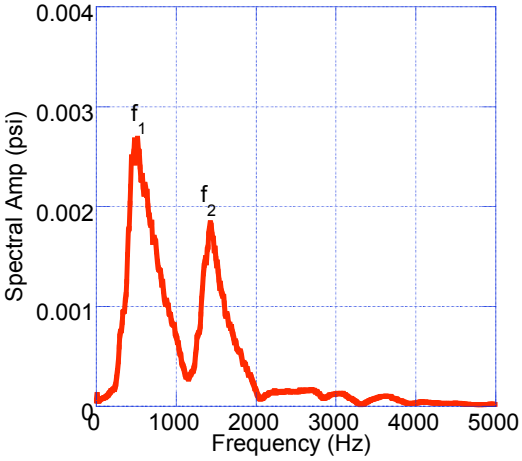

(d) Tap #4

Figure 5.4: Pressure spectrum of H_2-O_2 reacting case excited with white noise.

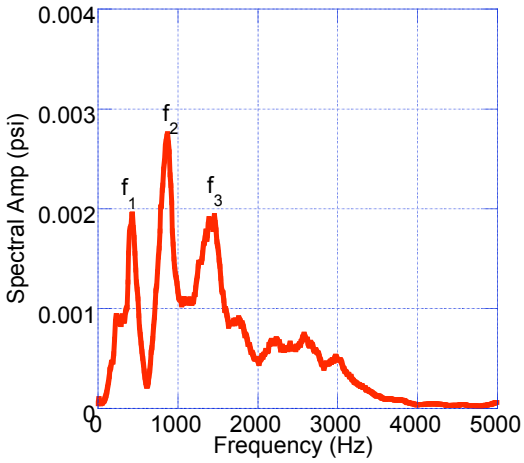

(a) Tap #1

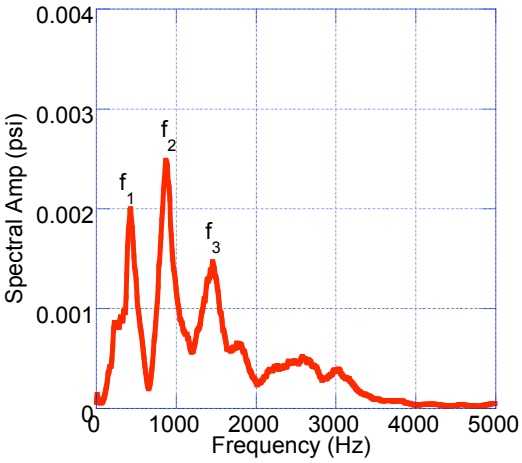

(b) Tap #2

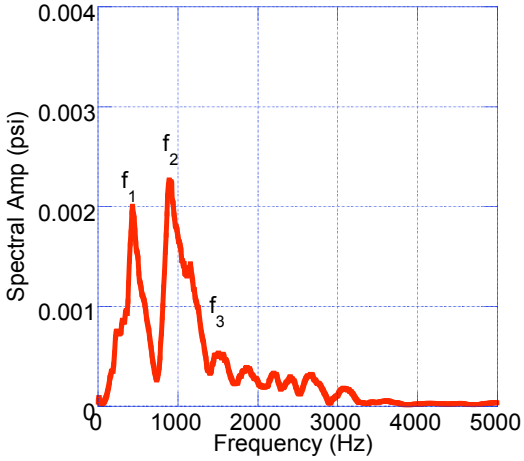

(c) Tap #3

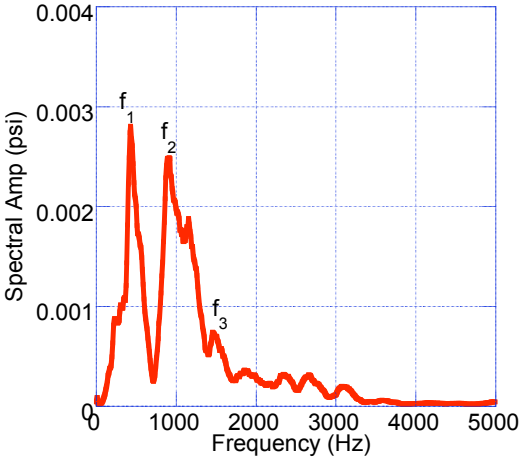

(d) Tap #4

Figure 5.5: Pressure spectrum of non-reacting case excited with white noise. H_2 mole fraction = 94%

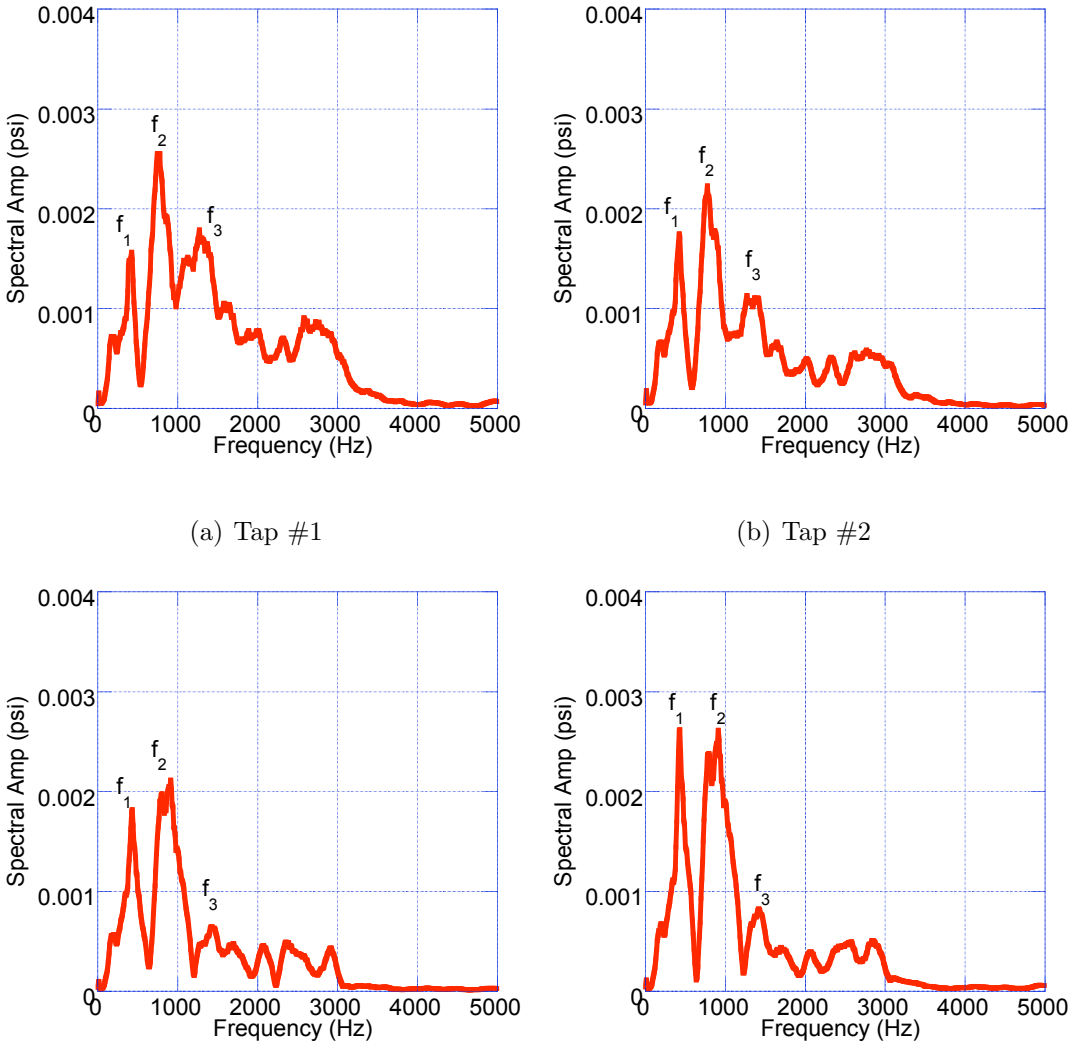

(a) Tap #1

(b) Tap #2

(c) Tap #3

(d) Tap #4

Figure 5.6: Pressure spectrum of non-reacting case excited with white noise. H_2 mole fraction = 82%

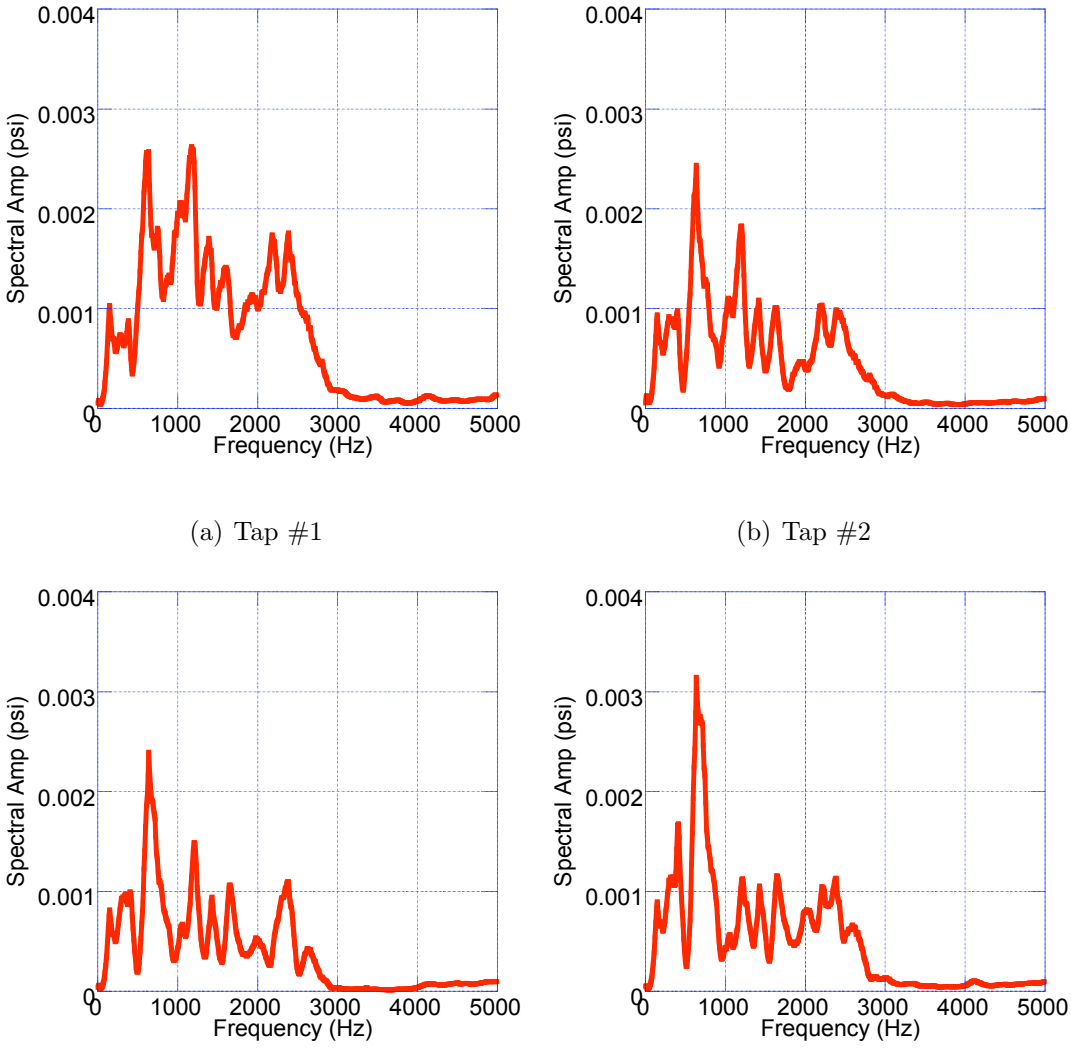

(a) Tap #1

(b) Tap #2

(c) Tap #3

(d) Tap #4

Figure 5.7: Pressure spectrum of non-reacting case excited with white noise. H_2 mole fraction = 37%

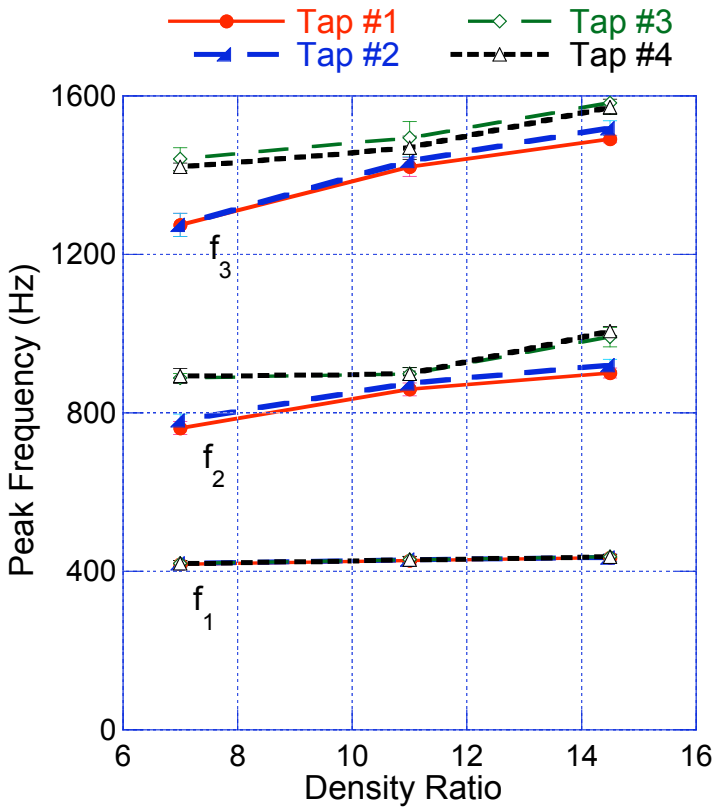

Figure 5.8: The effect of fuel mixture composition on the frequency shift in the non-reacting case.

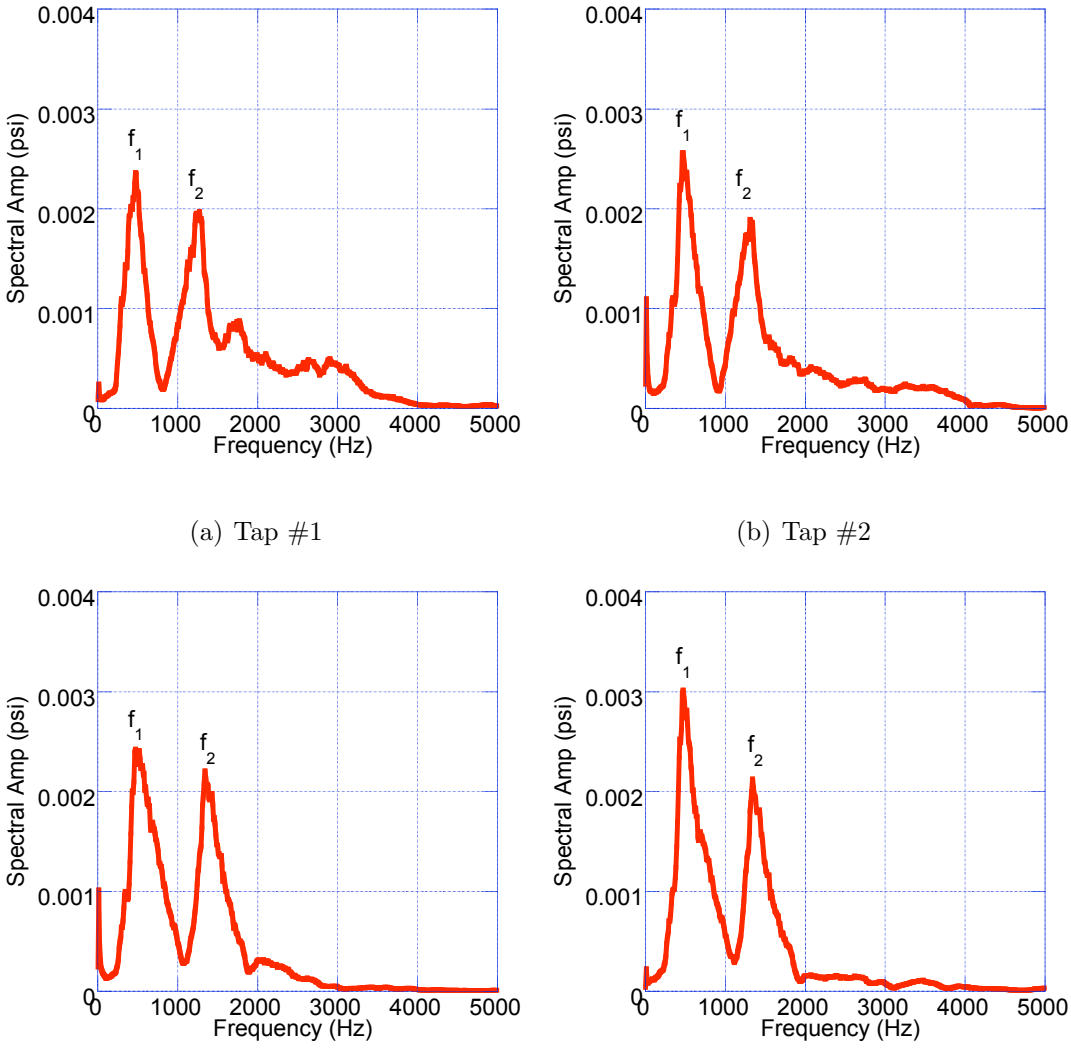

(a) Tap #1

(b) Tap #2

(c) Tap #3

(d) Tap #4

Figure 5.9: Pressure spectrum of reacting case excited with white noise. H_2 mole fraction = 94%

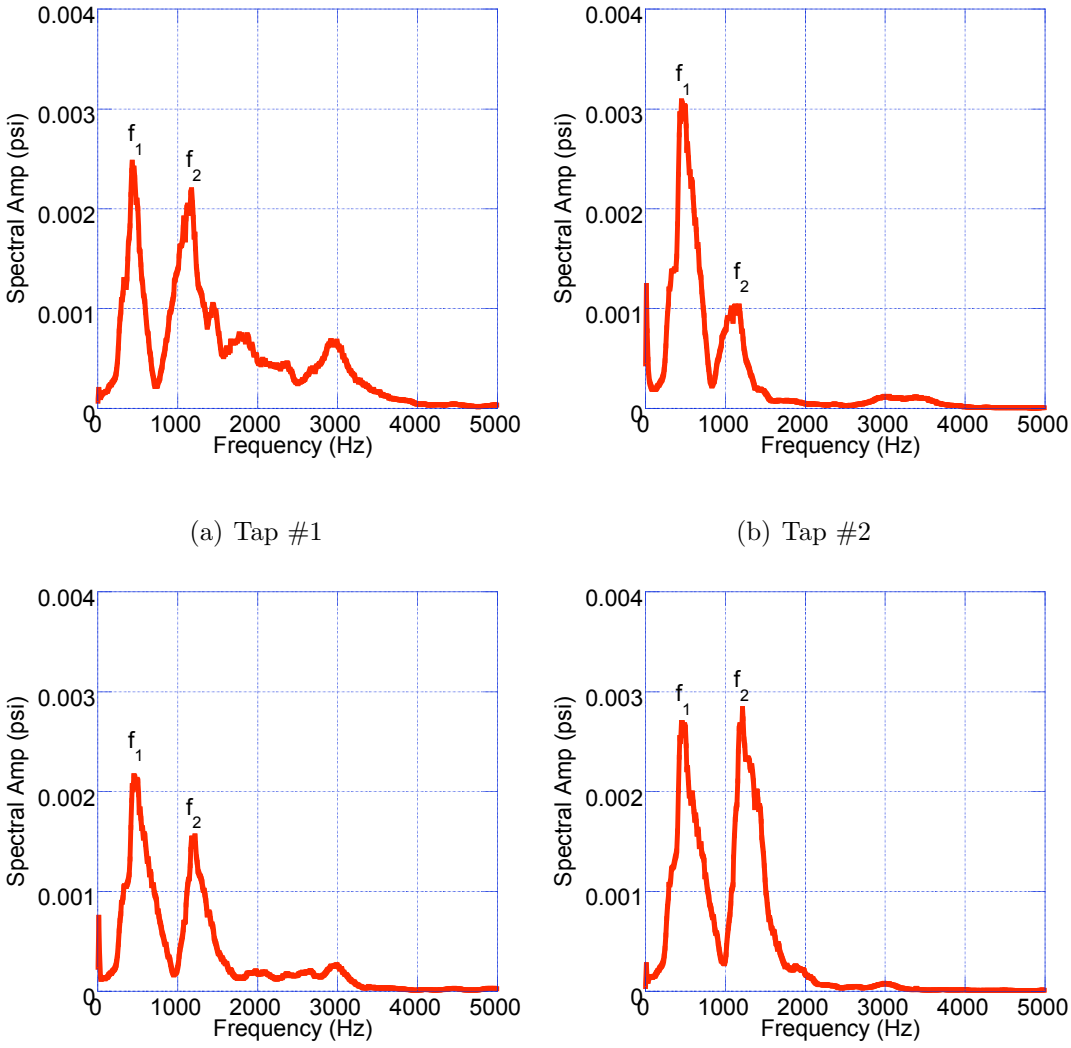

(a) Tap #1

(b) Tap #2

(c) Tap #3

(d) Tap #4

Figure 5.10: Pressure spectrum of reacting case excited with white noise. H_2 mole fraction = 82%

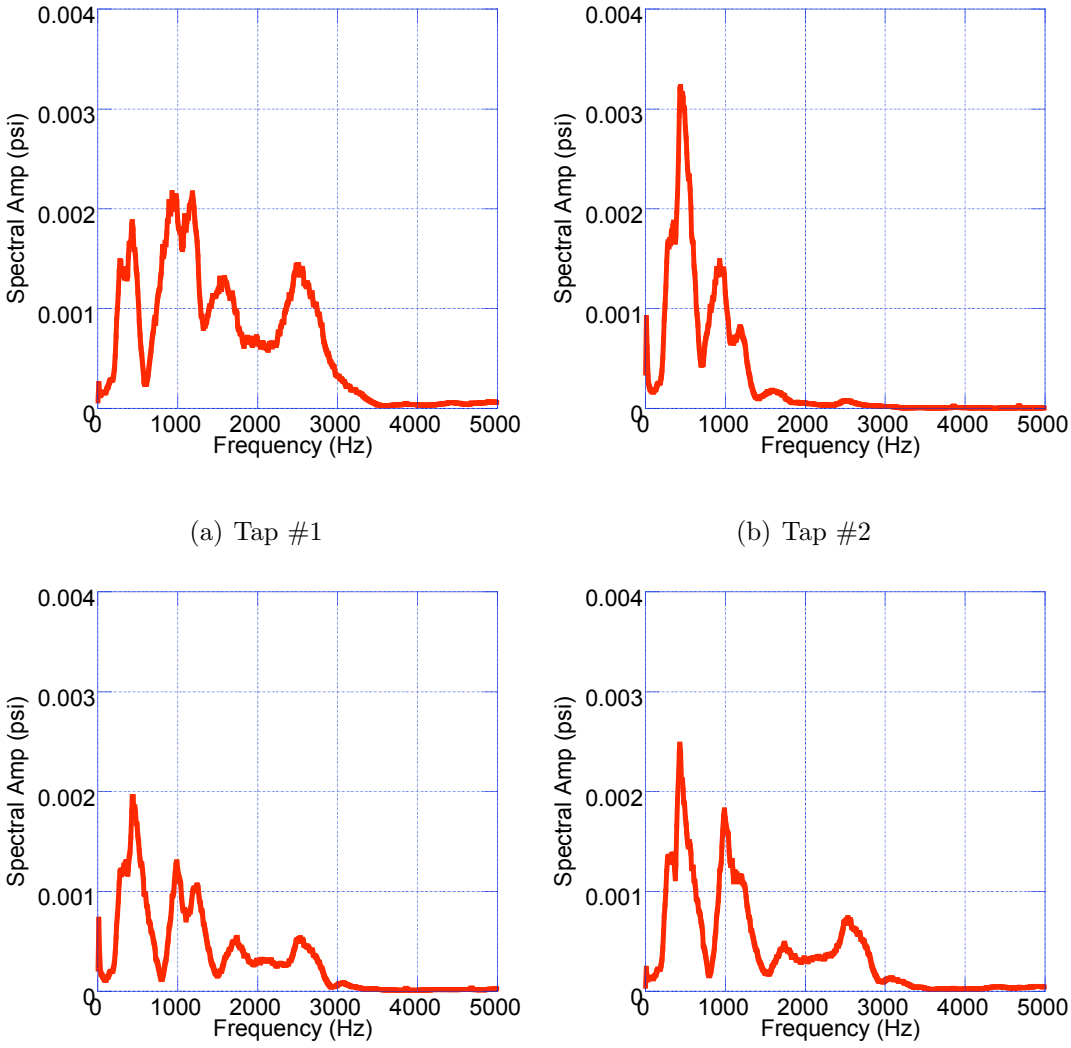

(a) Tap #1

(b) Tap #2

(c) Tap #3

(d) Tap #4

Figure 5.11: Pressure spectrum of reacting case excited with white noise. H_2 mole fraction = 37%

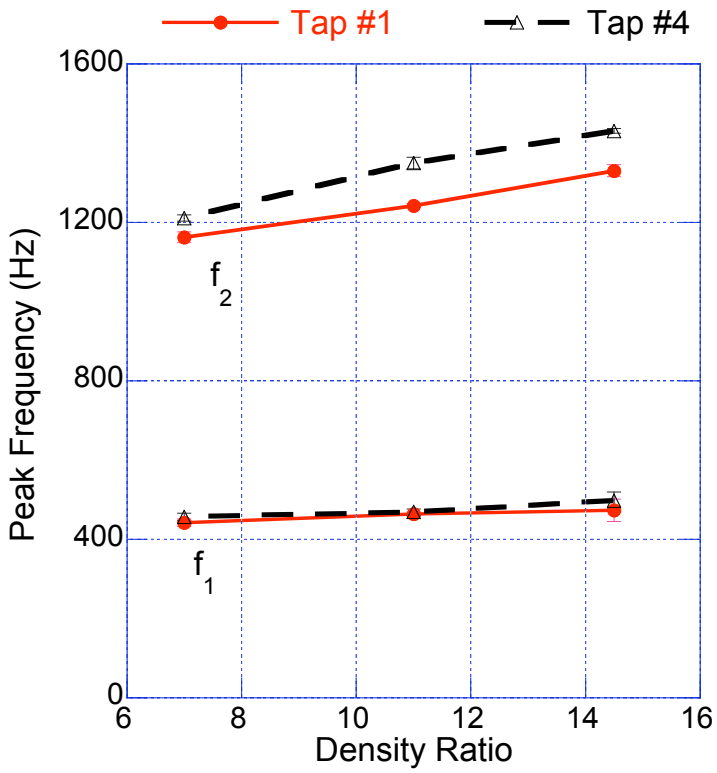

Figure 5.12: The effect of fuel mixture composition on the frequency shift in the reacting case.

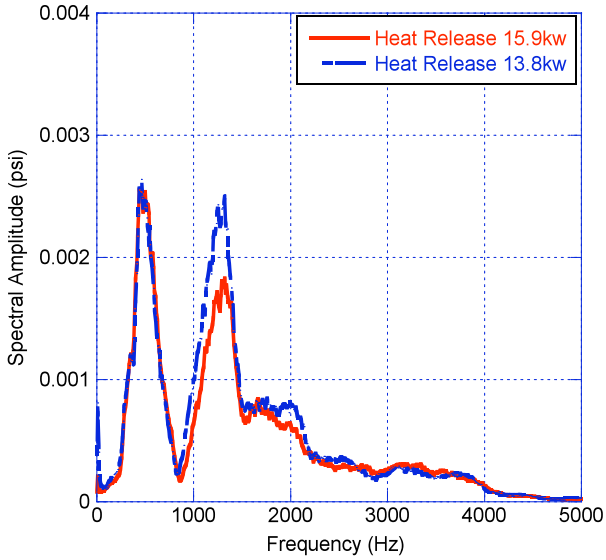

(a) Tap #1

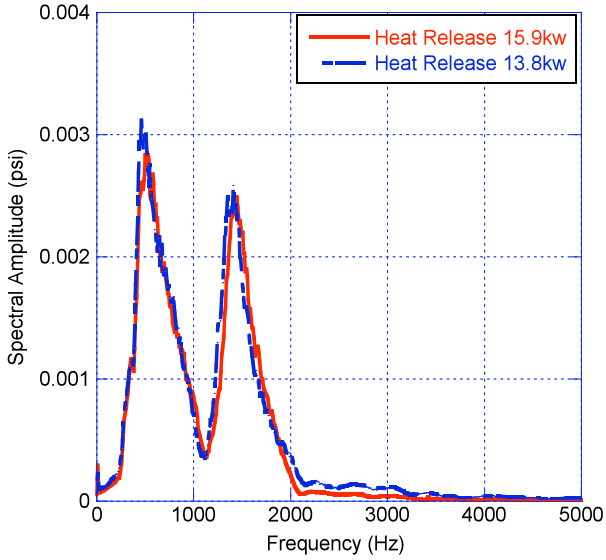

(b) Tap #4

Figure 5.13: The effect of total heat release on pressure spectrum. H_2 mole fraction = 99%.

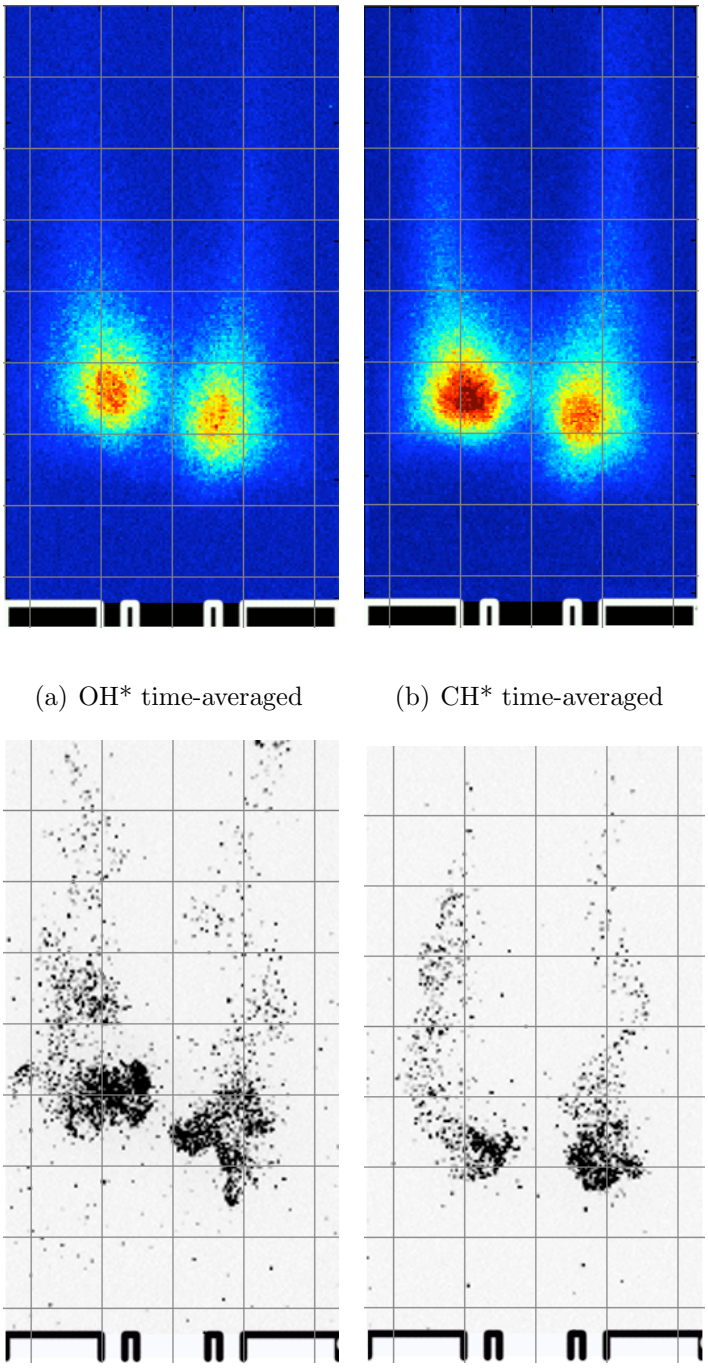

(a) OH* time-averaged (b) CH* time-averaged

(c) OH* instantaneous (d) CH* instantaneous

Figure 5.14: Chemiluminescence images of lifted flames using only CH_4 as fuel without acoustic excitation.

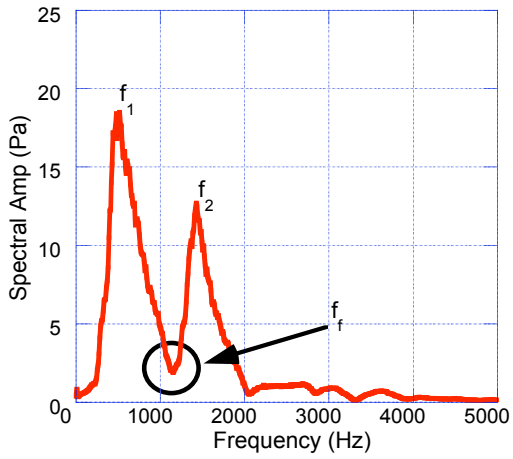

Figure 5.15: Choice of single forcing frequency from pressure spectrum.

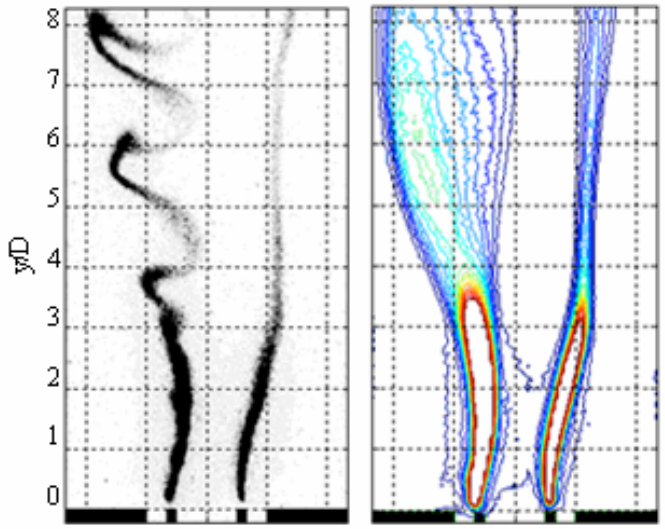

(a) O_2/H_2 flames

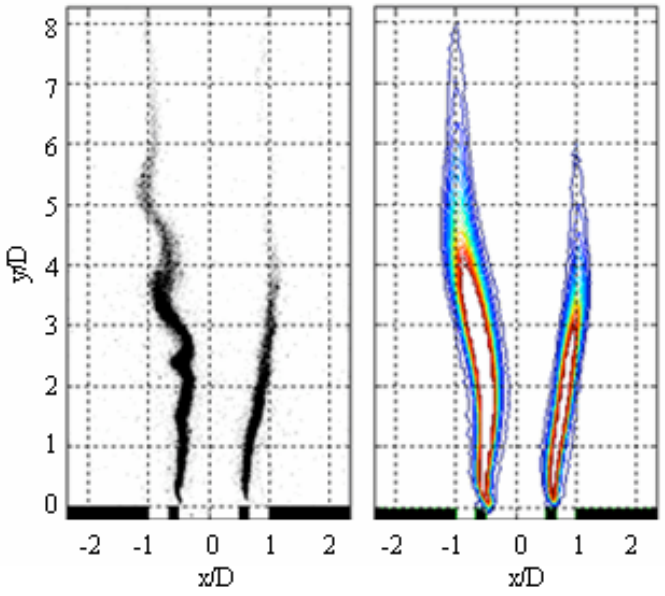

(b) O_2/H_2-CH_4 flames

Figure 5.16: OH* chemiluminescence images showing stability of acoustically forced flames. Left columns are instantaneous images, right columns are time-averaged images

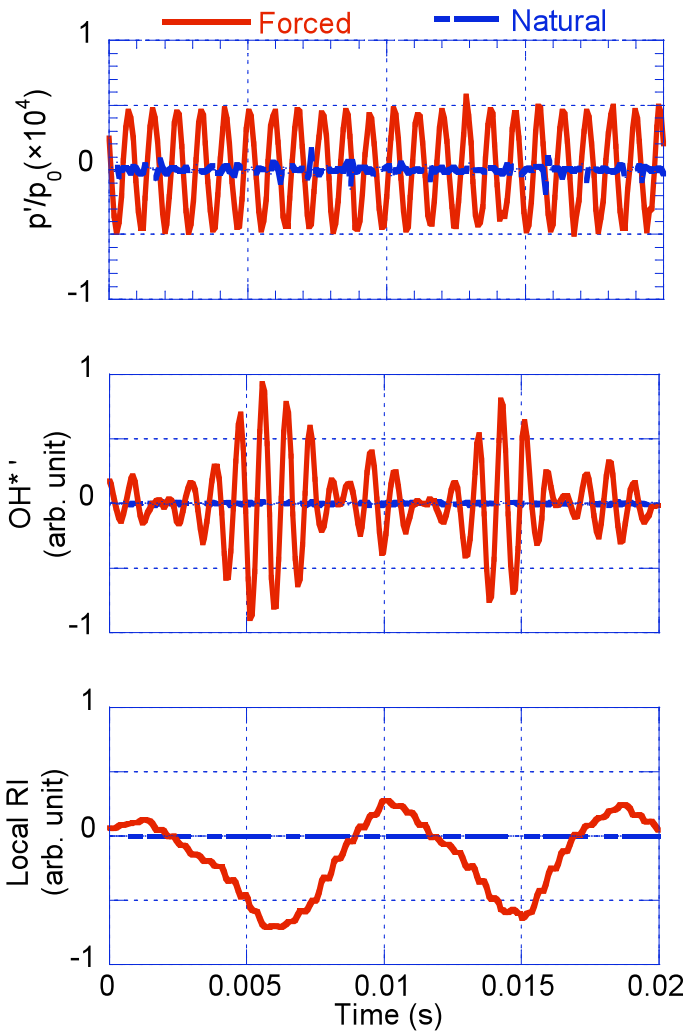

Figure 5.17: Comparison of behavior between forced at 1150 Hz and natural case at Tap #9. H_2 mole fraction = 99%.

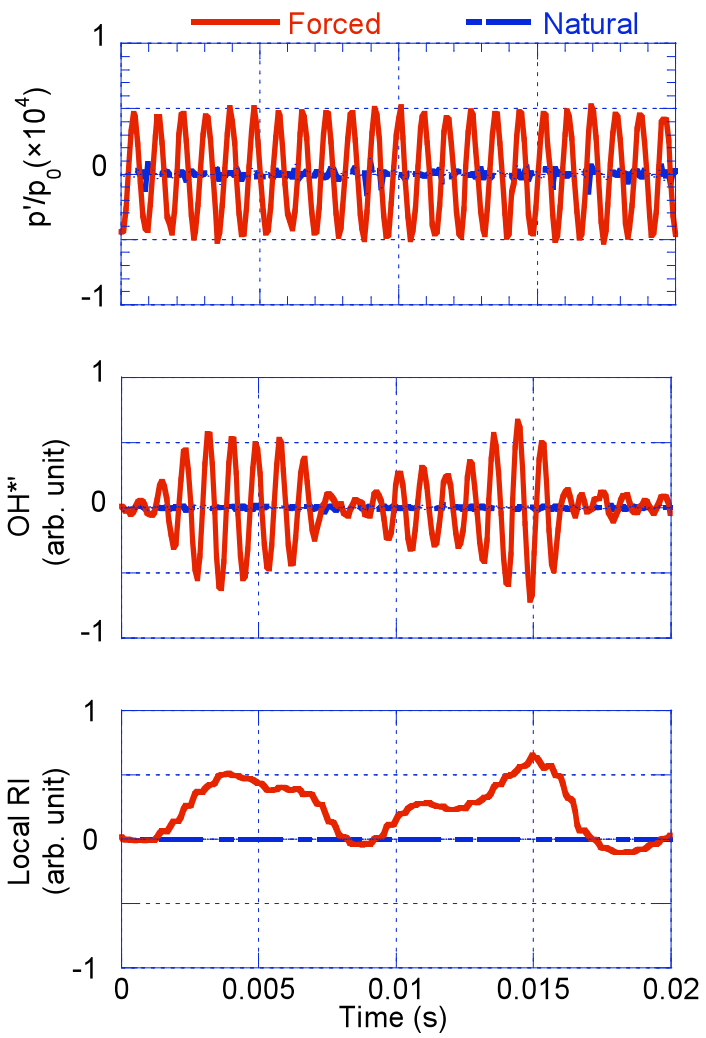

Figure 5.18: Comparison of behavior between forced at 1150 Hz and natural case at Tap #10. H_2 mole fraction = 99%.

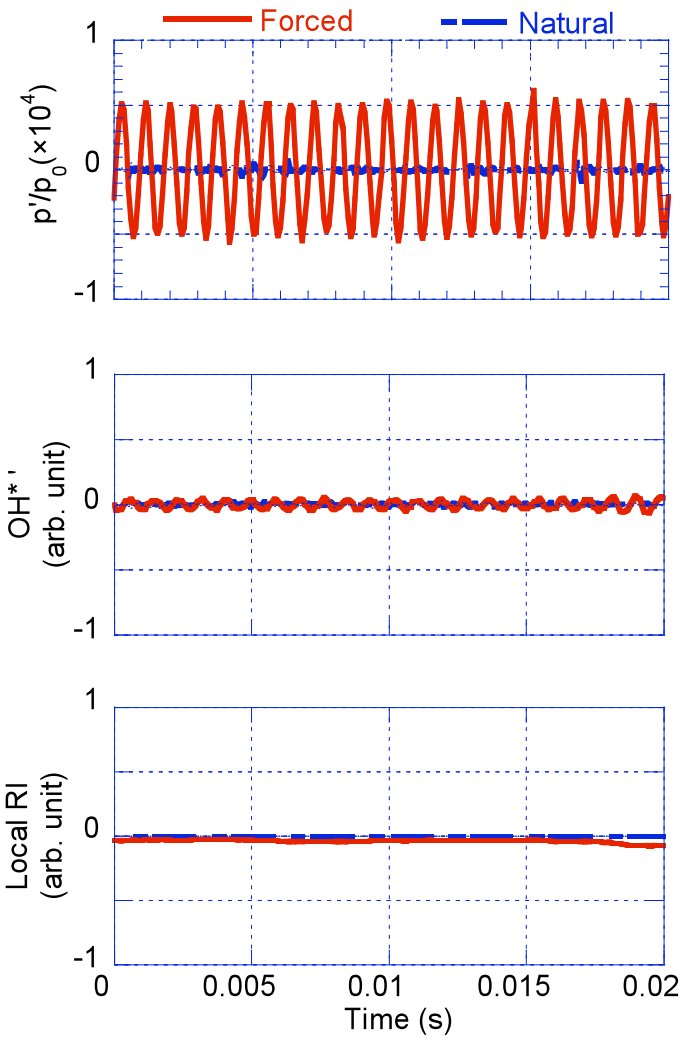

Figure 5.19: Comparison of behavior between forced at 1150 Hz and natural case at Tap #11. H_2 mole fraction = 99%.

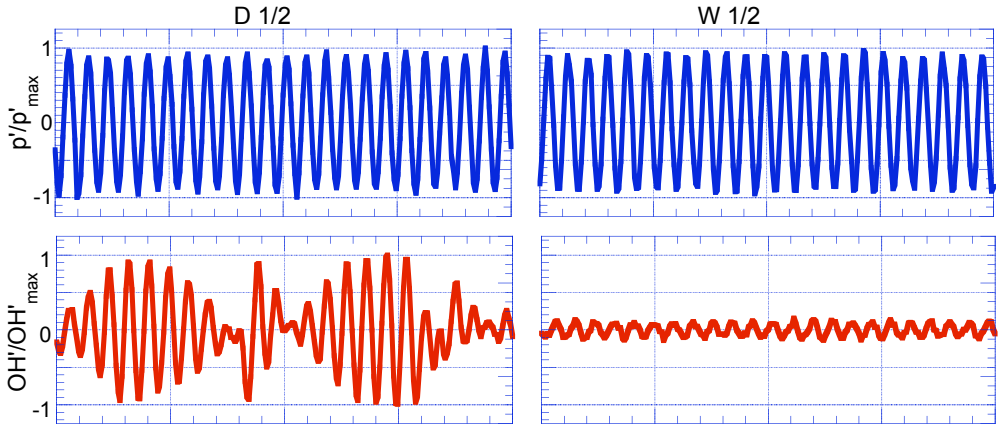

(a) Tap #10 and 11

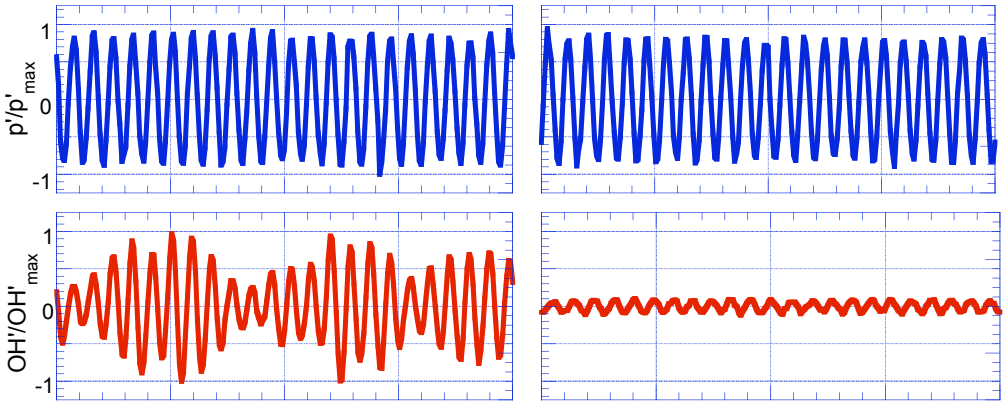

(b) Tap #7 and 8

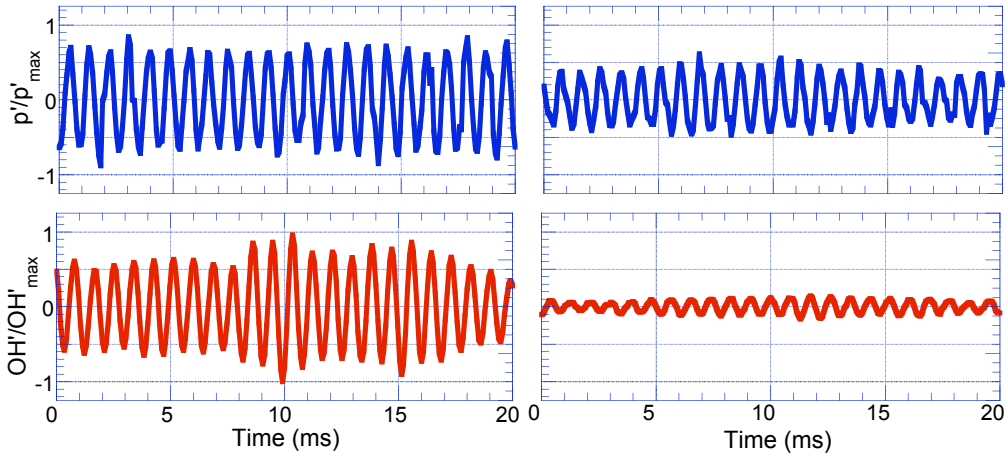

(c) Tap #5 and 6

Figure 5.20: Comparison of local OH* chemiluminescence fluctuations responding to pressure oscillation. H_2 mole fraction = 99%

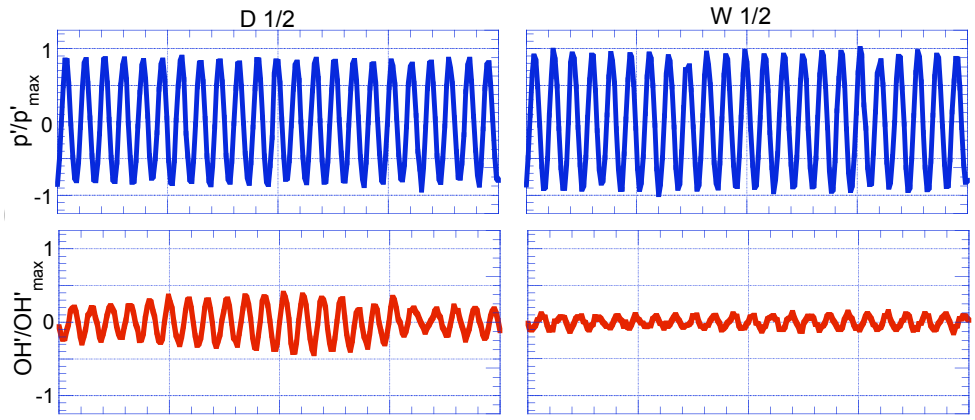

(a) Tap #10 and 11

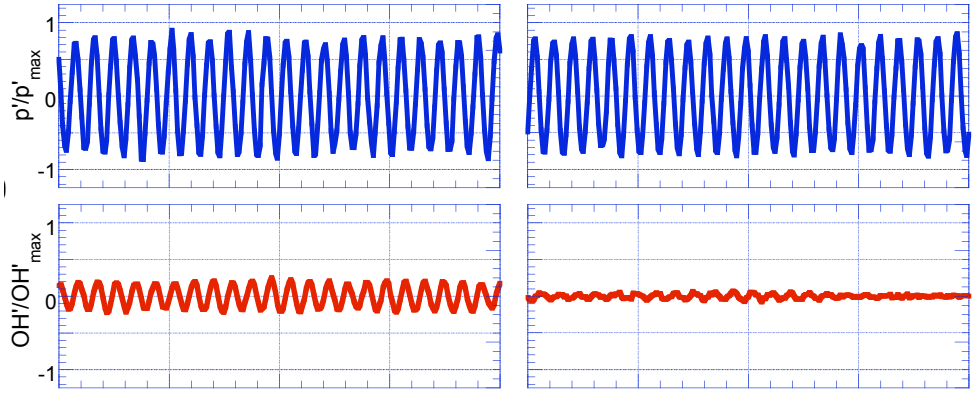

(b) Tap #7 and 8

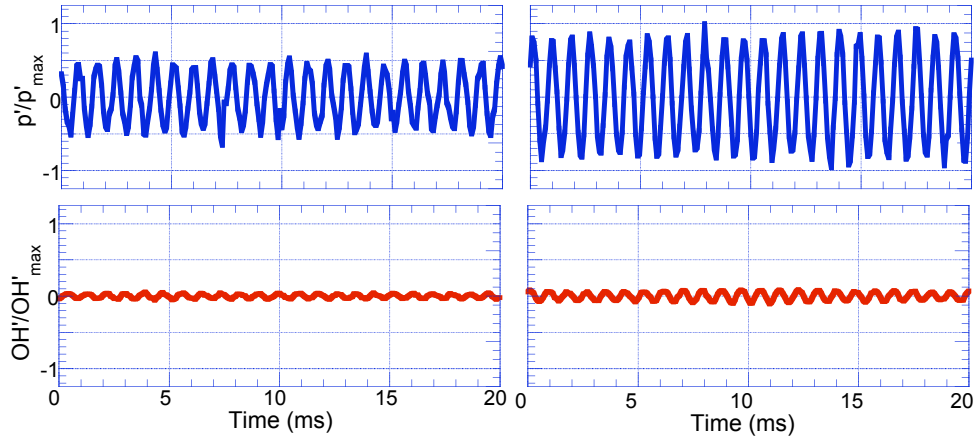

(c) Tap #5 and 6

Figure 5.21: Comparison of local OH* chemiluminescence fluctuations responding to pressure oscillation. H_2 mole fraction = 37%

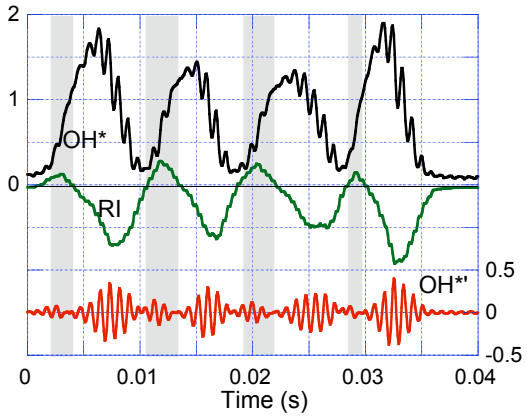

(a) Tap #9

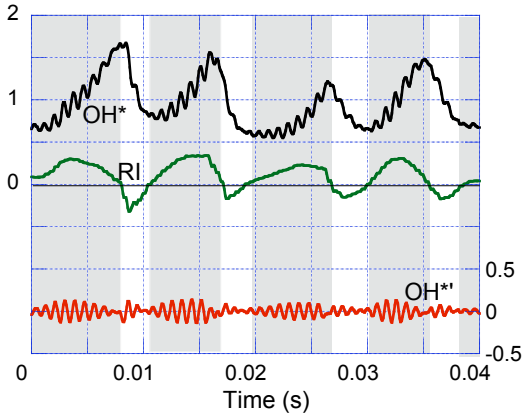

(b) Tap #10

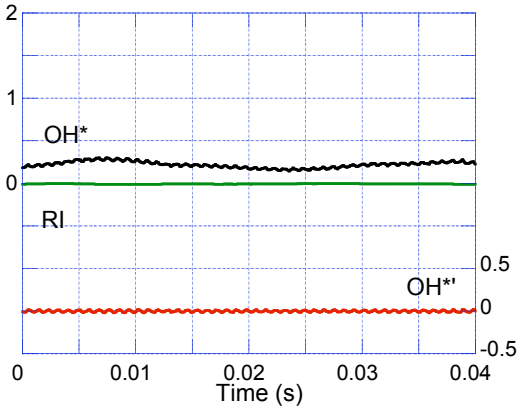

(c) Tap #11

Figure 5.22: Time traces of OH* chemiluminescence intensity, oscillation and local Rayleigh index. Shaded region is positive Rayleigh index.

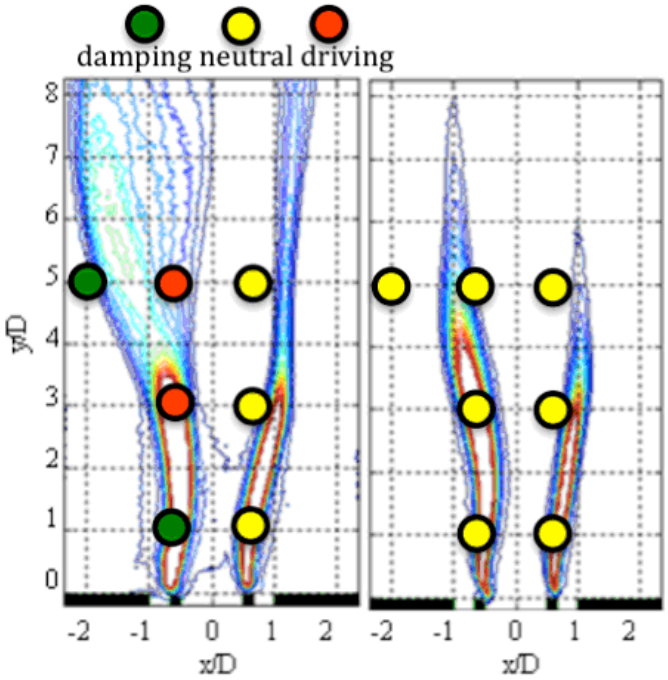

Figure 5.23: Rayleigh index measurements showing stability of acoustically forced flames for pure H_2 and H_2-CH_4 blended fuel.

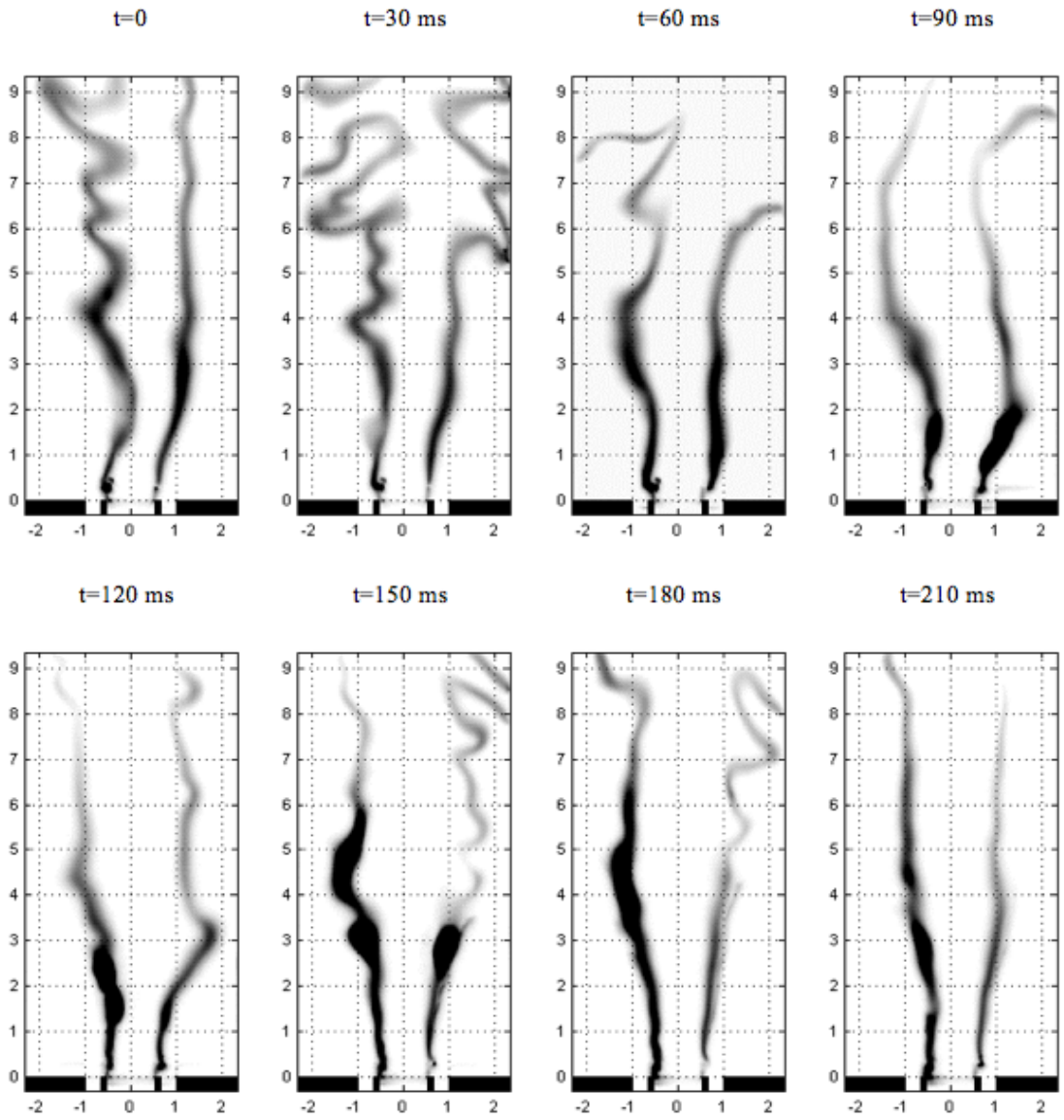

Figure 5.24: Transient behavior of flames with H_2 mole fraction from 99% to 37%.

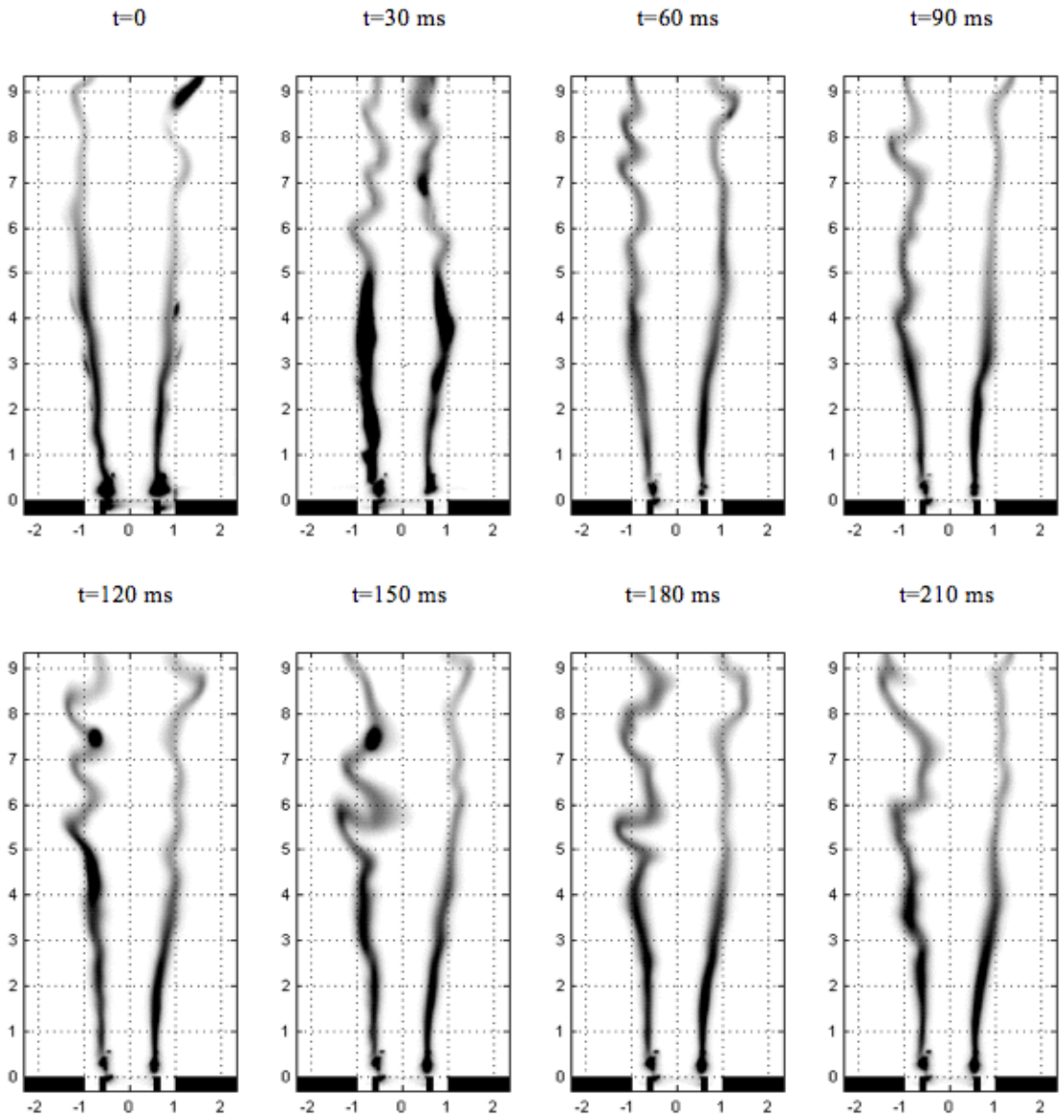

Figure 5.25: Transient behavior of flames with H_2 mole fraction from 37% to 99%.

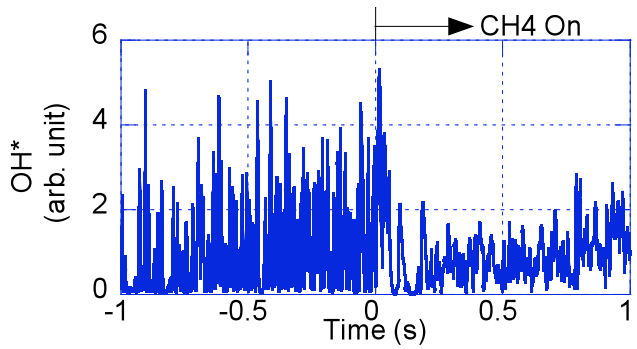

Figure 5.26: Time trace of heat release at Tap #9 associated with CH_4 injection at t = 0.

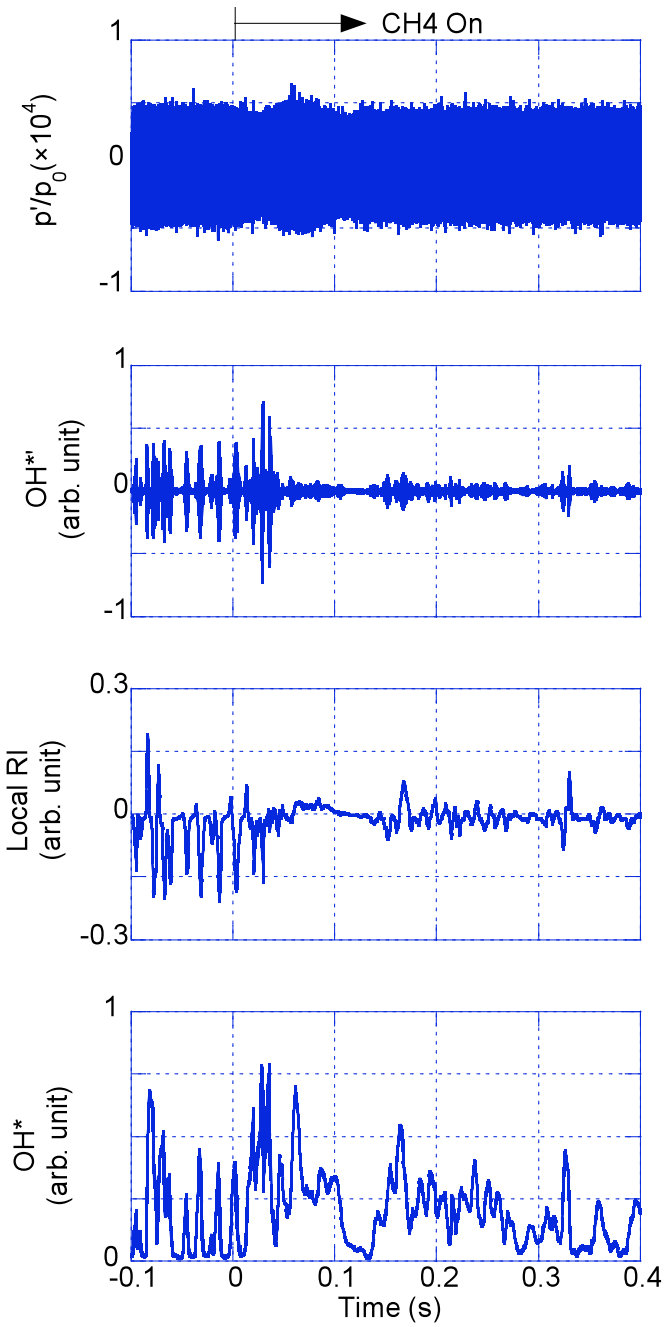

Figure 5.27: Transient behavior at Tap #9 associated with CH_4 injection at t = 0.

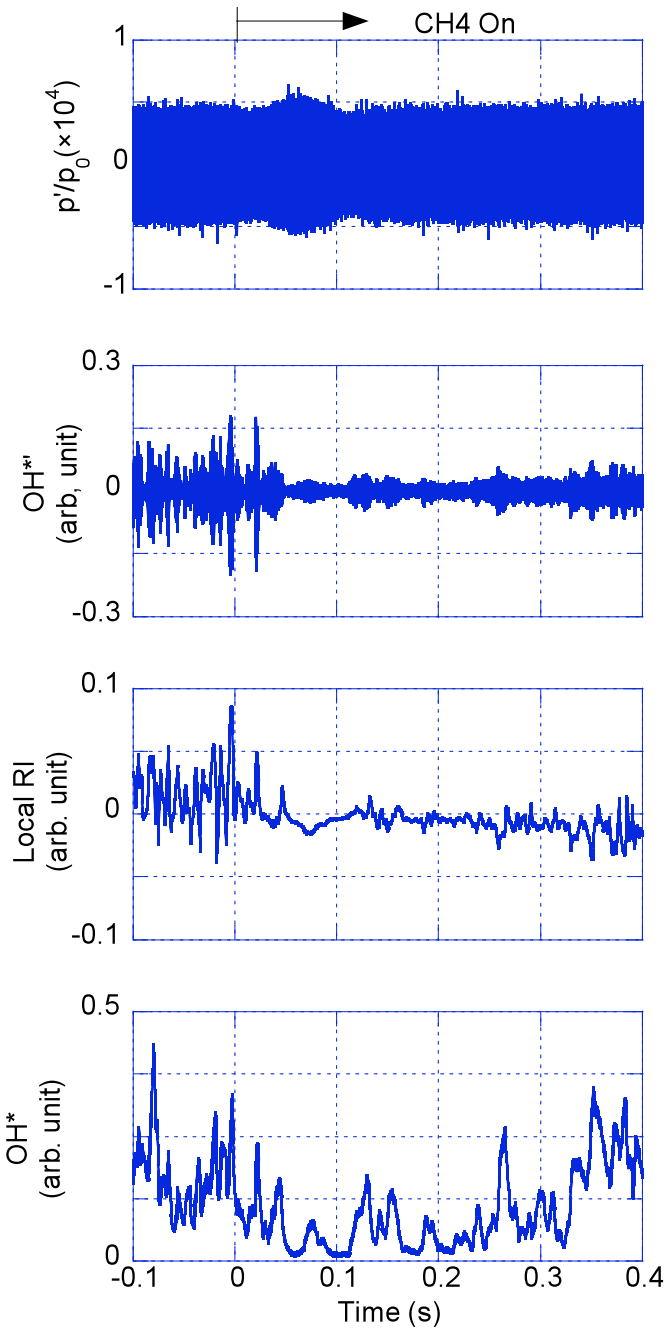

Figure 5.28: Transient behavior at Tap #10 associated with CH_4 injection at t = 0.

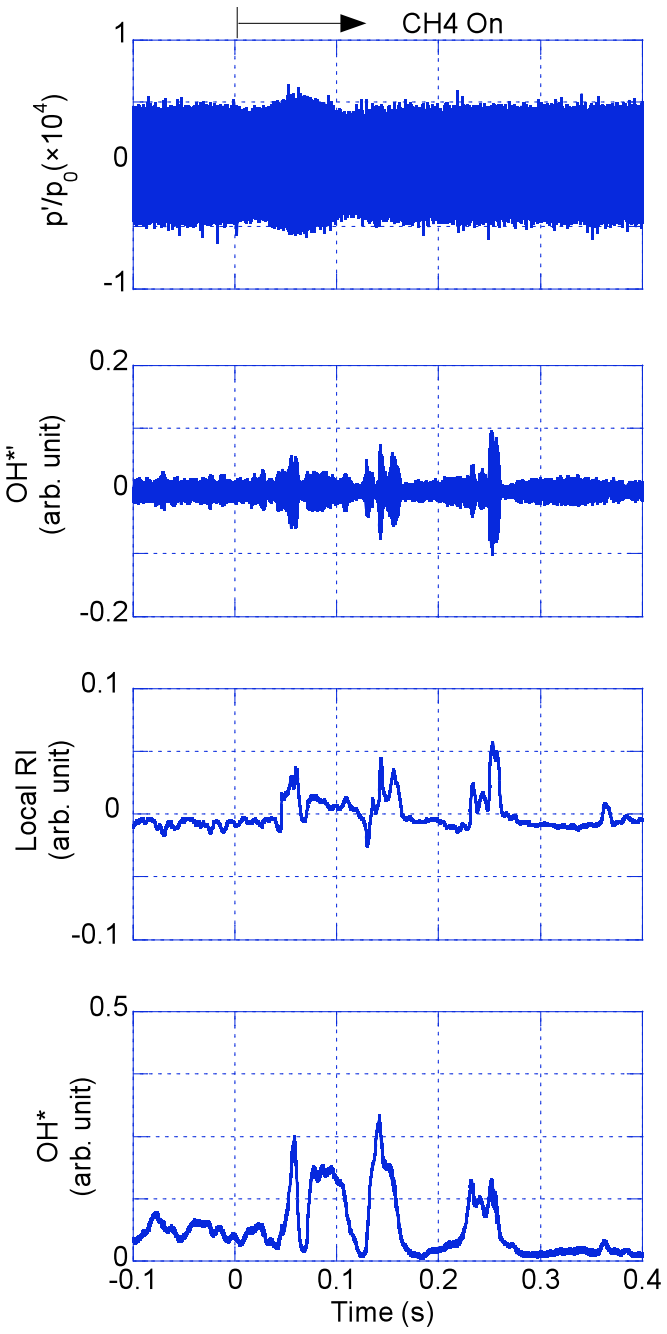

Figure 5.29: Transient behavior at Tap #11 associated with CH_4 injection at t = 0.

Chapter 6

Control Demonstration in Double-Injector Combustor

6.1 Introduction

In order to study the effectiveness of different reactant injection configurations on the acoustic characteristics in the combustion chamber, tests were conducted in the double-injector model combustor. Similar to the studies in the single-injector combustor, the chamber was first acoustically characterized as discussed in Section 6.2 with transverse white noise acoustic excitation. Experiments were performed to examine how changes in flow conditions at individual injectors could affect the overall resonance characteristics of the combustor. Two ways of changing the fluid injection were investigated. In Section 6.3, the effect of CH_4-H_2 blended fuel is discussed. In Section 6.4, a potentially more practical method, modifying the equivalence ratio while retaining the H_2 and O_2 reactants exclusively, is investigated.

6.2 Acoustic Characterization of Chamber

As described previously, band-limited white noise forcing was utilized to obtain the acoustic response spectrum, from which resonance characteristics are evaluated. In this test, the acoustic response of diffusion flames formed between a stoichiometric H_2 and O_2 mixture ratio for both injector elements was studied. This is considered the baseline case. The flow conditions for the baseline case are listed in Table 6.1. Reacting experiments were conducted in the baseline configuration to identify various acoustic resonance modes. Dynamic pressure measurements were taken at the three tap locations #1-3, shown in Figure 4.6, while the combustor was operating. About 400 spectra were averaged to obtain these results, which show distinctive spectral peaks corresponding to various acoustic resonance modes. The results are shown in Figure 6.1. At Tap #1 and 3, there are up to three distinctive spectral peaks worthy of mention. At Tap #2, only two of them show up as peaks while the middle one is the spectral minimum.

To estimate acoustic resonance modes, Loci-CHEM, a finite volume flow solver that uses high-resolution approximate Riemann solvers [95], was used to compute the speed of sound profile for the reacting flow in the combustor. The resonant frequencies were then calculated based on the speed of sound results from the simulation. Table 6.2 lists and compares various spectral peaks obtained from the experimental data and the numerical model analysis. The comparison of the measured and calculated resonant frequencies leaves little doubt about the nature of the dominant resonant modes.

Table 6.1: Flow conditions for fuel mixture tests

Oxidizer-fuel Density Ratio	16 (baseline)	11	7	3
O_2 flow rate (g/s)	1.13	1.13	1.13	1.13
O_2 velocity (m/s)	4.5	4.5	4.5	4.5
H_2 flow rate (g/s)	0.142	0.111	0.075	0.019
CH_4 flow rate (g/s)	0	0.062	0.134	0.246
H_2 mole fraction (%)	100	94	82	37
CH_4 mole fraction (%)	0	6	18	63
Fuel velocity (m/s)	13.5	11.3	8.7	4.5
Velocity Ratio	3.0	2.5	1.9	1.0
Rate of Heat Release (kW)	17.1	16.5	15.8	14.8

Table 6.2: Comparison of measured spectral peak minimum frequencies and calculated resonance frequencies

Location	Tap #1			Tap #2		Tap #3		
Mode	$L1_o$	T1	L3	$L1_o$	L3	$L1_o$	T1	L3
Measured (Hz)	580	1440	1950	580	2060	580	1320	1865
Calculated (Hz)	590	1548	1968	590	1968	590	1548	1968

On the basis of the baseline flow investigations, the following findings can be made:

- The first observed frequency appears to be the quarter-wave mode of the oxidizer post, denoted as $L1_o$.
- The second observed frequency appears to be the transverse quarter-wave mode of the combustion chamber at the measured axial location, denoted as T1.
- The third observed frequency appears to be the longitudinal three-quarter-wave mode of the combustion chamber, denoted as L3.

6.3 Blended Fuel Effect on Acoustic Characterization of Chamber

In Chapter 5, it was found that the acoustic resonance characteristics of the model injector remained qualitatively similar under fuel composition variation in the

single-injector configuration, but some of the resonant frequencies shifted to lower values with increasing CH_4 content due to the change of the acoustic impedance. For these tests, the fuel mixture ratio effect was also examined in the double-injector model combustor rig to show the effectiveness of the altered reactant injection within one injector on the acoustic characteristics of the entire combustor. The first tangential mode in full-scale rocket engines was simulated by the quarter-wave transverse mode (T1) in the experimental rig. If the frequency of this mode could be substantially shifted with controlled fluid injection, the control method would be considered effective in changing acoustic resonance characteristics. It is even better if this control method can affect other modes or change the pressure spectrum over a wide frequency range.

Four different blended fuel compositions, each corresponding to a stoichiometric fuel-oxidizer mixture ratio, were tested for their flame stability characteristics in the controlled injector. The standard injector was still operated at a baseline flow condition. The reactant compositions and flow conditions are summarized in Table 6.1. For each flow condition tested, the acoustic excitation was applied from both the side corresponding to the specially-controlled injector as well as from the side corresponding to the standard injector. This is illustrated in Figure 6.2.

The blended fuel mixture tests were conducted with acoustic excitation on each side with reacting flow. From the controlled element side, in Figure 6.3, the shifting frequencies associated with the three dominant spectral peaks are plotted as a function of density ratio. Figure 6.4 shows the results with the compression driver mounted on the standard element side. Both cases have similar tendencies.

All the peak frequencies shift to lower frequencies with lower density ratio, which corresponds to more CH_4 in the fuel, since the speed of sound is strongly influenced by the quantity of H_2 in the mixture. By increasing the CH_4 mole fraction, H_2 is proportionally replaced by CH_4, leading to an overall reduction in the mixture speed of sound. This effects a change in the local acoustic impedance, in addition to the reduced product temperatures, resulting in the peak frequency shifts. The trends were the same as was observed in the previous single injector combustor studies. It is also observed that the second peak is not dominant at Tap #2, which is the same behavior as the baseline case. The blended fuel mixture can potentially affect other modes as well.

6.4 H_2-O_2 Equivalence Ratio Effect

The effect of equivalence ratio between fuel and oxidizer of a selected injector on the flame-acoustic characteristics of the chamber was examined. The baseline case was a stoichiometric mixture. The fuel-oxidizer ratio was modified in two ways. One way was to keep the fuel H_2 mass flow rate the same as the baseline case while changing the O_2 mass flow rate. The other was the opposite, changing the O_2 mass flow rate while keeping H_2 mass flow rate the same. Both methods were applied to see the effects under differing directions of acoustic excitement as described previously.

Five different fuel-oxidizer equivalence ratios, including the baseline case, were characterized for flame stability. They are summarized in Table 6.3. There are two

Table 6.3: Flow conditions for equivalence ratio tests

Case	Baseline	H_2	Modification		O_2	Modification	
Equivalence Ratio	1.0	0	0.5	1.5	0.5	1.5	∞
O_2 flow rate (g/s)	1.13	1.13	1.13	1.13	2.27	0.76	0
O_2 velocity (m/s)	4.5	4.5	4.5	4.5	9.0	3.0	0
H_2 flow rate (g/s)	0.142	0	0.071	0.212	0.142	0.142	0.142
H_2 velocity (m/s)	13.5	0	6.75	20.25	13.5	13.5	13.5
Velocity Ratio	3.0	0	1.5	4.5	1.5	4.5	∞
Rate of Heat Release (kW)	17.1	0	8.56	20.3	5.60	11.4	0

extreme cases. One extreme is only injecting O_2 without any H_2, which corresponds to an equivalence ratio (ER) of zero. In contrast, the other extreme is to shut down the O_2 completely, only injecting H_2. This scheme gives an infinite local equivalence ratio. The injector with these two flow conditions can affect the flame structure as well.

6.4.1 Effect on Acoustic Characterization of Chamber

H_2 Mass Flow Rate Modulation Effect

In this series of tests, the effect of equivalence ratio on the flame-acoustic characteristics was examined by changing the mass flow rate of H_2. The first sequence of tests involved acoustic excitation from the side of the modulated injector. Figure 6.5 shows the pressure spectra with equivalence ratios from 0.5 to 1.5. The first

spectral peak frequency, the quarter-wave mode of the oxygen post, was relatively unaffected by both measurement (tap) location and fuel-oxidizer ratio. This is to be expected since the oxygen flow rate was being held constant. Within the range of equivalence ratios tested, the transverse mode of interest was slightly affected by the fuel-oxidizer ratio. The frequency of this mode did not shift substantially. Figure 6.6 shows the comparison between the H_2 completely-off case and the baseline case. When the fuel was off, the mode shape of the pressure spectrum was drastically changed. The speed of sound in H_2 is almost four times that in O_2. Thus, the overall speed of sound in this controlled injector region is decreased due to the lack of H_2 as well as lower temperatures from the lack of flames. The acoustic impedance near this injector is therefore substantially different from the standard injector. This suggests that turning off the fuel of the specially-modulated injector is a promising control method for combustion instability by modifying the acoustic characteristics near the injector regions.

The same fluid configurations were applied in the second set of tests as well, but with acoustic excitation provided on the side of the standard injector. The results are shown in Figure 6.7 and Figure 6.8. It can be seen that similar results were obtained as with the previous excitation configuration. Turning off the fuel is still the most effective control method, since it gives the greatest difference in pressure spectrum as compared with the baseline case. Not only did this shift the transverse mode by 40%, but it changed the shape of the pressure spectrum over a wide frequency range as well. Another observation is the other modes are also affected by the fuel modulation to some extent, which implies the potential for

additional instability-suppressing benefits.

O_2 Mass Flow Rate Modulation Effect

In a similar manner to the previous set of experiments, reacting flow tests were performed in which the O_2 mass flowrate was modulated, rather than H_2. Figures 6.9 and 6.11 show the results of equivalence ratios from 0.5 to 1.5 with acoustic excitation from the controlled injector side and standard injector side, respectively. The results are qualitatively similar amongst these cases, and do not show appreciable mode frequency shifts. Even for the case with no O_2, shown in Figures 6.10 and 6.12, the spectra were not as drastically changed as in the case with no H_2. When the O_2 was off, the speed of sound in the vicinity of the injector was similar to its value with nonzero O_2 mass flow. Despite the reduced temperature from the lack of flame, the pressure spectrum was not affected to a substantial extent. This implies the major reason for the change in the acoustic environment is the content of the flow rather than its temperature.

Figure 6.13 shows the summary of the first-quarter-wave transverse mode frequency shift associated with equivalence ratio at Tap #1 and 3. The pressure spectrum at Tap #2 does not show this frequency as a dominant peak. It can be seen that the case without fuel (ER=0) shifts this frequency by 40%. The cases other than the fuel-off configuration only affect the frequency of this mode slightly, up to 8% or so. This suggests that completely turning off fuel has the best control authority when modulating only the original fuel and oxidizer. This control method appears to be a practical method for application in a full-scale liquid rocket engine.

6.4.2 Effect on Flame Structure

The effects of turning off fuel or oxidizer on the flame structure are examined. For the baseline case, stoichiometric H_2-O_2 flow injected at both injectors, there are four flames in the combustor, as shown in Figure 6.14. When the fuel is completely shut down, which corresponds to ER=0, the number of flames reduces to three. Figure 6.15 shows the flame structure without H_2 in the injector closest to the acoustic driver. Two of the flames form between the fuel and oxidizer in the standard injector, while the third one forms between the oxidizer in the specially-controlled injector and some of H_2 from the coflow jet close to the controlled injector. This is also observed in the case of turning off H_2 in the controlled injector which is farthest away from the acoustic excitation, shown in Figure 6.16. Shutting down O_2 causes two of the flames to vanish compared to the baseline case due to the lack of oxidizer. These corresponding flame structures are shown in Figure 6.17 and 6.18. It is concluded that turning off fuel or oxidizer can change the flame structure substantially; however, turning off oxidizer affects the flame structure the most. A practical issue requiring consideration is that injection with only O_2 may corrode the walls of the combustor.

6.5 Summary and Discussions

The effect of injector flow modification on acoustic resonance characteristics was examined using a two-dimensional model combustor featuring a pair of shear-coaxial injector elements. White noise acoustic forcing was utilized to excite a pair

of turbulent GO_2-GH_2 diffusion flames and dynamic pressure measurements were taken at three locations across the combustor, by which flame acoustic characteristics were studied. With stoichiometric H_2-O_2 flames on both injectors, the chamber was characterized and three dominant acoustic modes were identified: the quarter-wave mode of the oxidizer post, transverse quarter-wave mode of the combustion chamber and longitudinal three-quarter-wave mode of the combustion chamber. The experimental results agree with the computational fluid dynamics (CFD) analytical results well.

Another set of tests were conducted to quantify the changes in acoustic resonance characteristics and to explore the feasibility of replacing hard wall baffles with a series of controlled injectors. The double elements consist of one controlled injector placed next to a constant-flow GO_2-GH_2 injector. Flames from these injectors were subjected to band-limited white noise acoustic forcing from the side of controlled injector, and again from the side of the standard injector, and the pressure responses was analyzed for a possible shift in acoustic resonance. Two different approaches for the controlled injector were considered. One approach used a specialized fuel consisting of a CH_4-H_2 blend in the controlled injector, while the other used the same fuel H_2 as in the constant-flow injector but had different flow rates. For the first approach, the CH_4 mole fraction in the blended fuel was varied from 0 to 63%, resulting in up to 23% shift in the most-amplified frequencies. However, this approach may not be practical in a flight-grade rocket due to the requirement for an additional fuel tank to hold CH_4. For the second approach, only the equivalence ratio was varied at the controlled injector, causing up to 40% shift in the chamber

frequency. The results imply that strategically-placed controlled injectors could be an effective tool to prevent resonant oscillations. The results open up the possibility of using a small number of controlled injectors to replace baffles in liquid-fueled rockets.

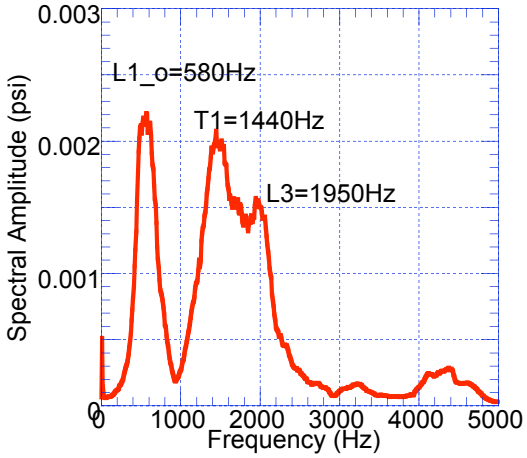

(a) Tap #1

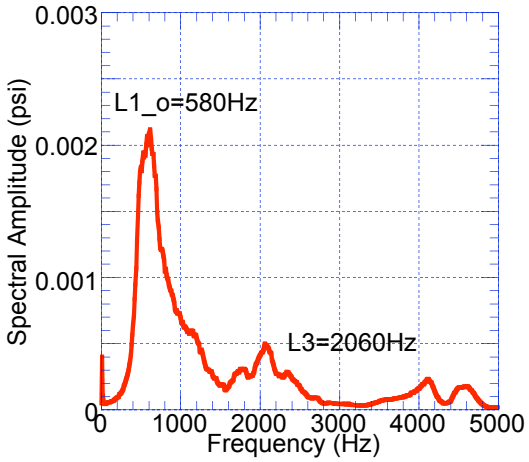

(b) Tap #2

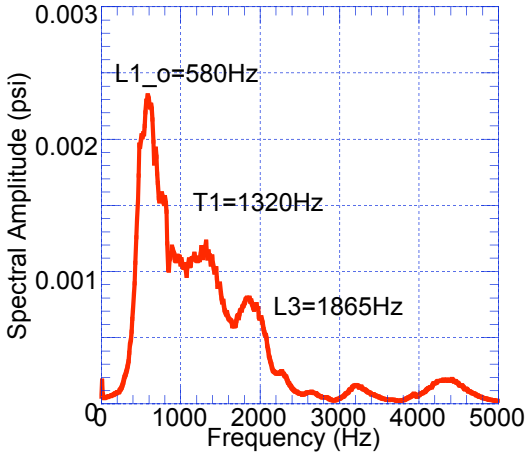

(c) Tap #3

Figure 6.1: Pressure spectrum for baseline case.

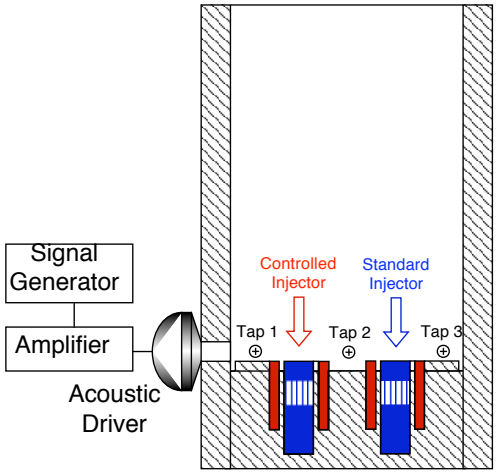

(a) Acoustic excitation directly against the controlled injector

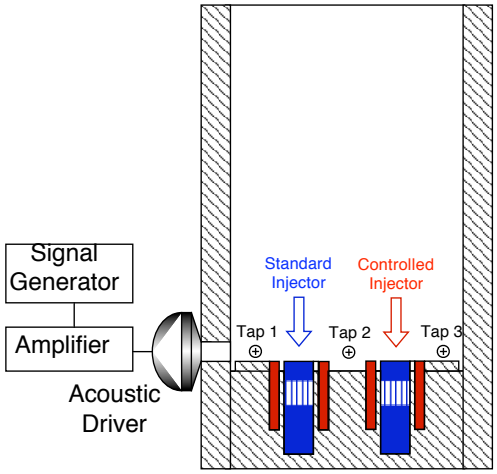

(b) Acoustic excitation directly against the standard injector

Figure 6.2: Direction of acoustic excitation and pressure tap locations.

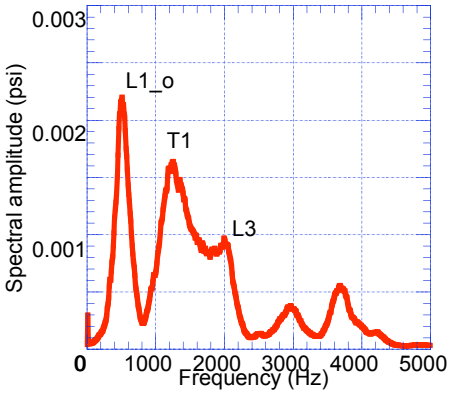

(a) Pressure spectrum

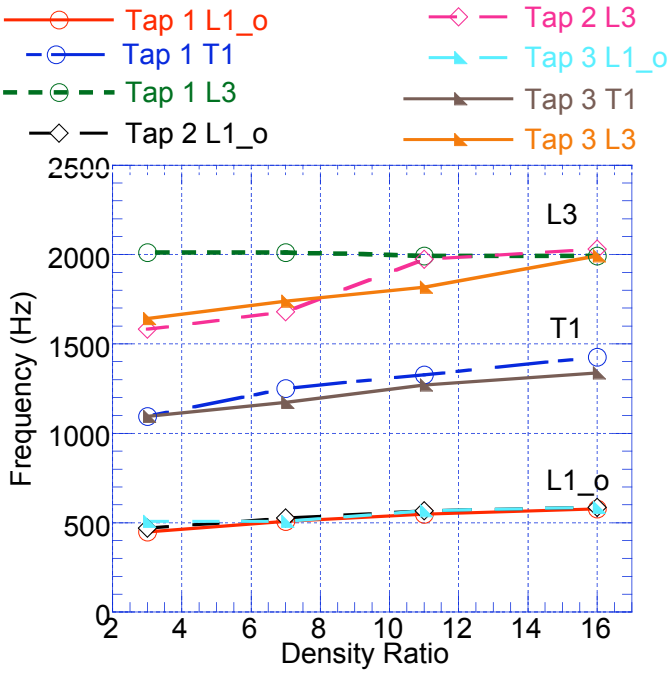

(b) Frequency shift associated with density ratio

Figure 6.3: Frequency shift from fuel mixture with acoustic excitation from the specially-controlled injector side.

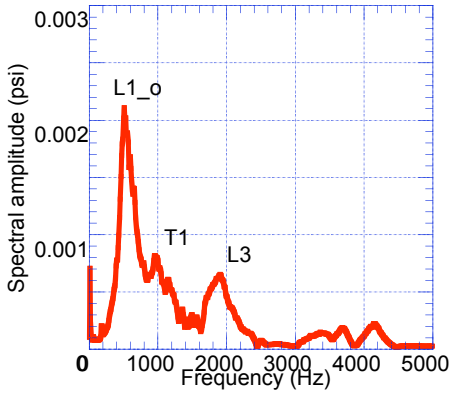

(a) Pressure spectrum

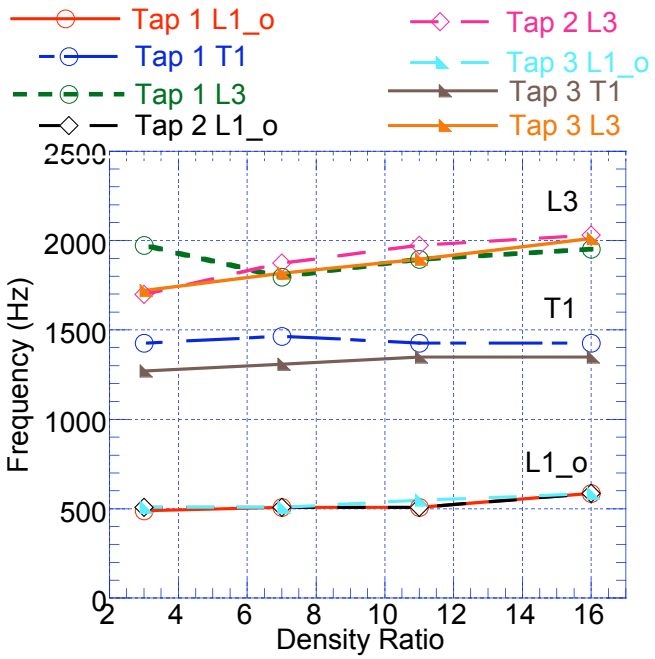

(b) Frequency shift associated with density ratio

Figure 6.4: Frequency shift from fuel mixture with acoustic excitation from the standard injector side.

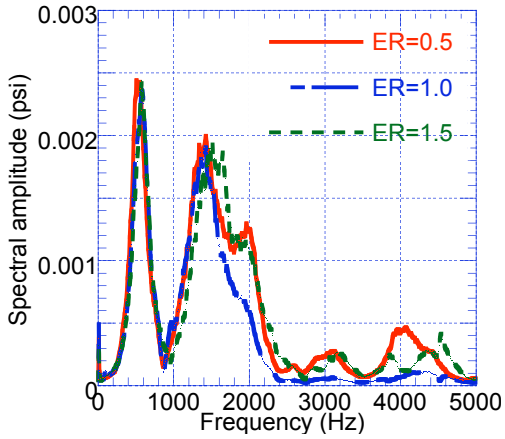

(a) Tap #1

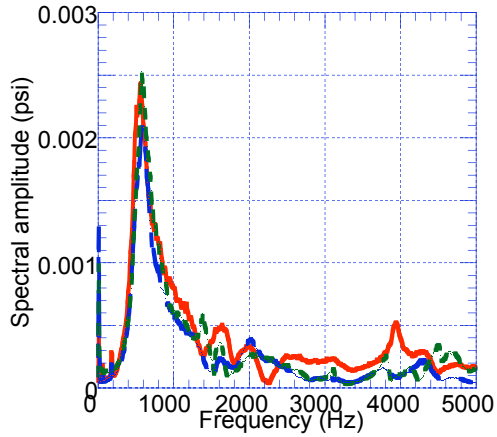

(b) Tap #2

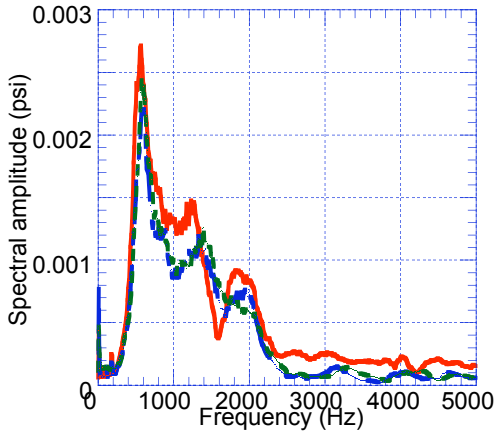

(c) Tap #3

Figure 6.5: Effect of equivalence ratio from modifying H_2 mass flowrate with acoustic excitation from the specially-controlled injector side.

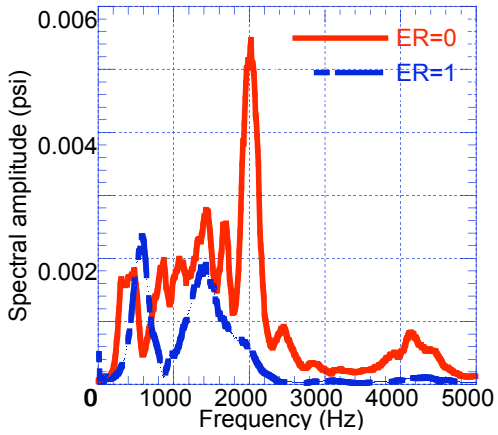

(a) Tap #1

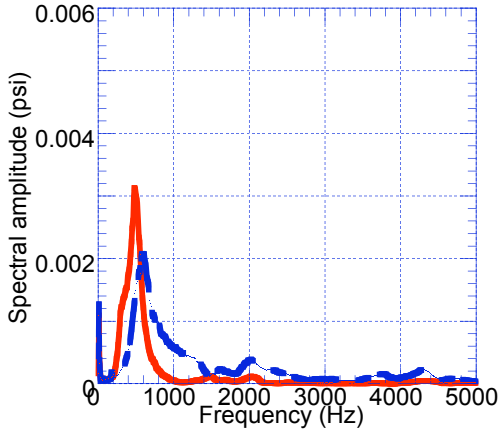

(b) Tap #2

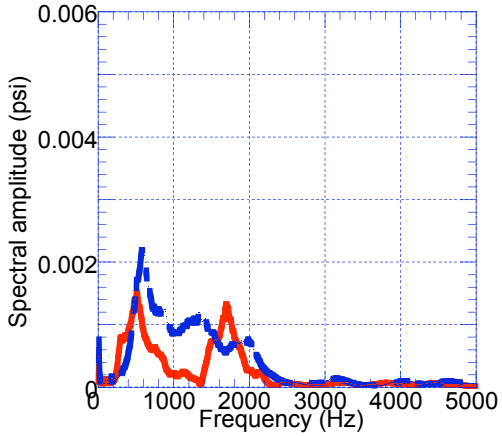

(c) Tap #3

Figure 6.6: Effect of equivalence ratio from shutting down H_2 mass flow with acoustic excitation from the specially-controlled injector side.

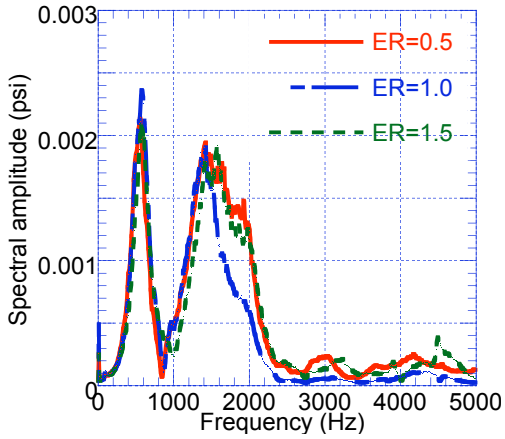

(a) Tap #1

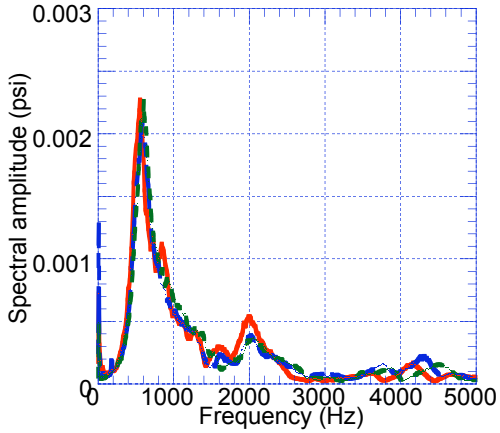

(b) Tap #2

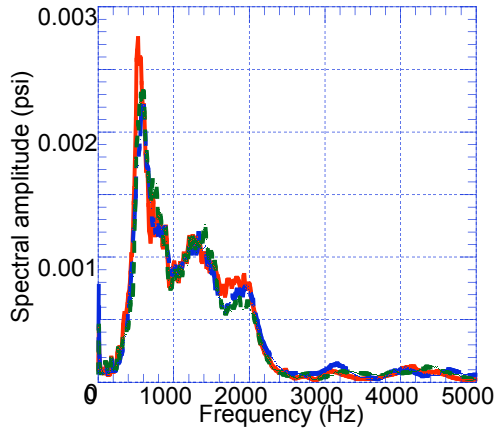

(c) Tap #3

Figure 6.7: Effect of equivalence ratio from modifying H_2 mass flowrate with acoustic excitation from the standard injector side.

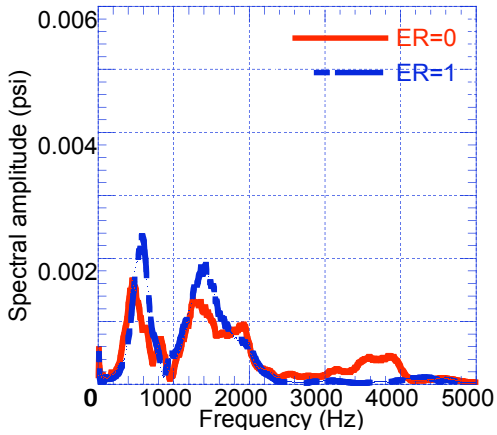

(a) Tap #1

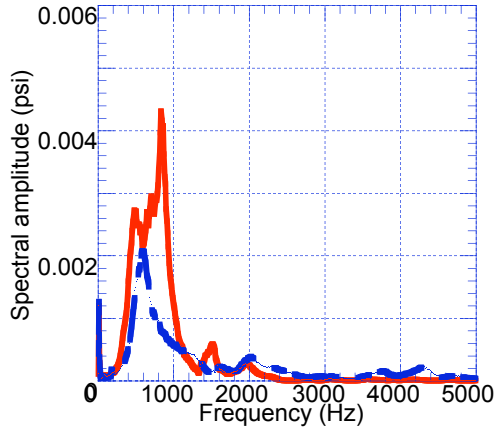

(b) Tap #2

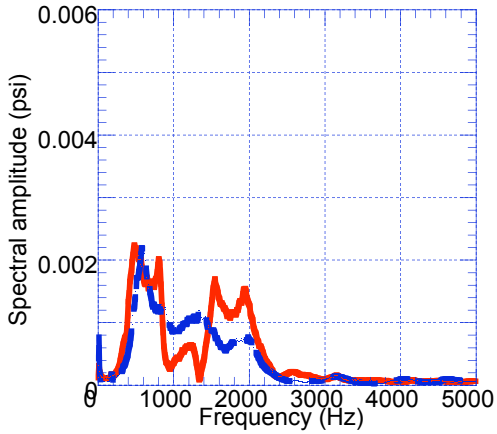

(c) Tap #3

Figure 6.8: Effect of equivalence ratio from shutting down H_2 mass flow with acoustic excitation from the standard injector side.

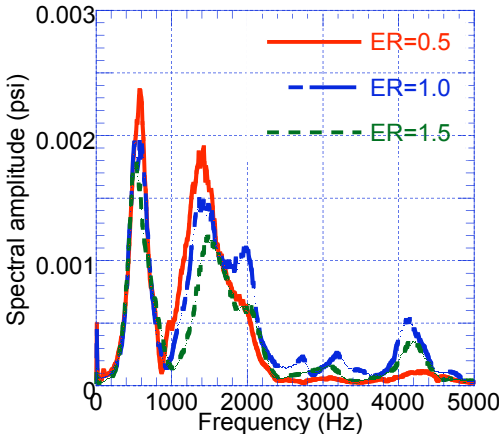

(a) Tap #1

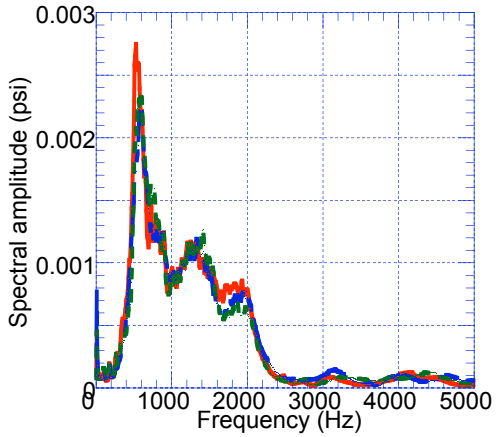

(b) Tap #2

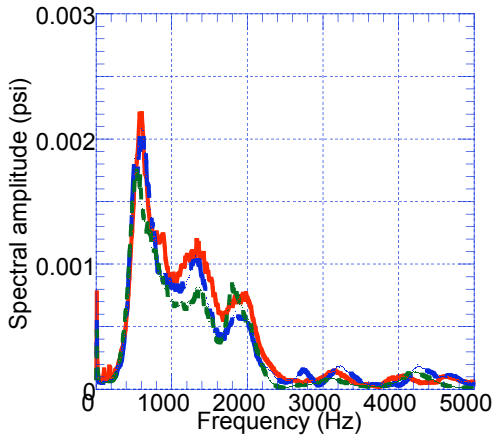

(c) Tap #3

Figure 6.9: Effect of equivalence ratio from modifying O_2 mass flowrate with acoustic excitation from the specially-controlled injector side.

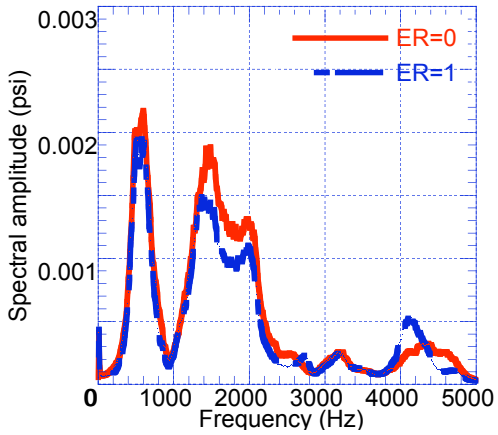

(a) Tap #1

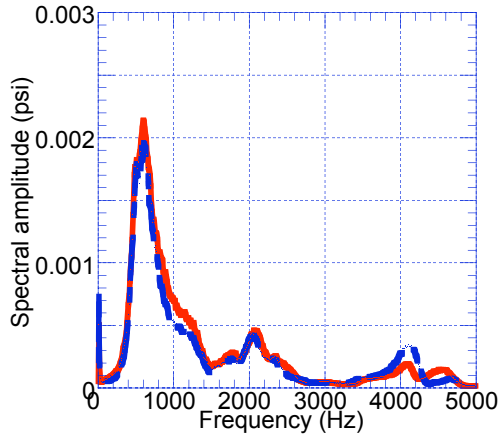

(b) Tap #2

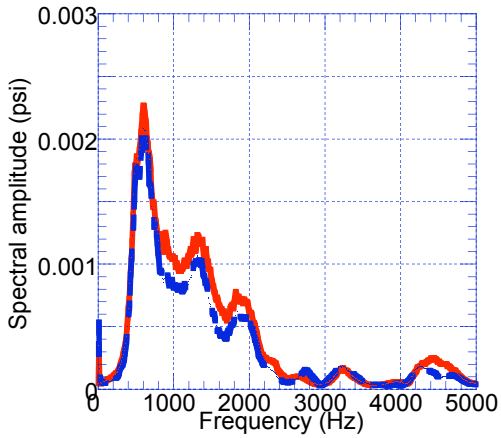

(c) Tap #3

Figure 6.10: Effect of equivalence ratio from shutting down O_2 mass flow with acoustic excitation from the specially-controlled injector side.

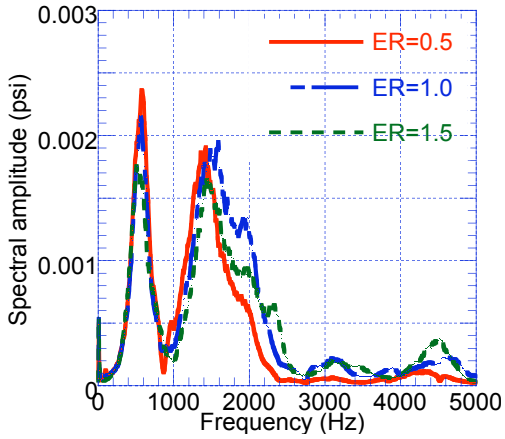

(a) Tap #1

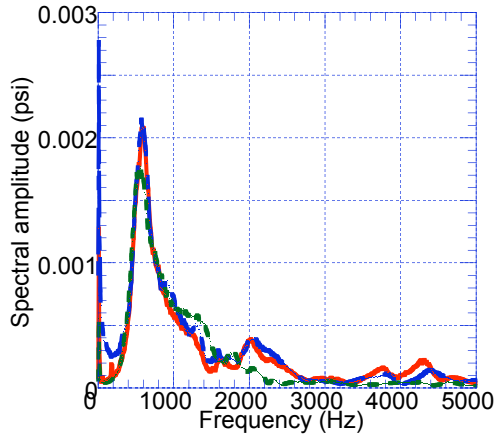

(b) Tap #2

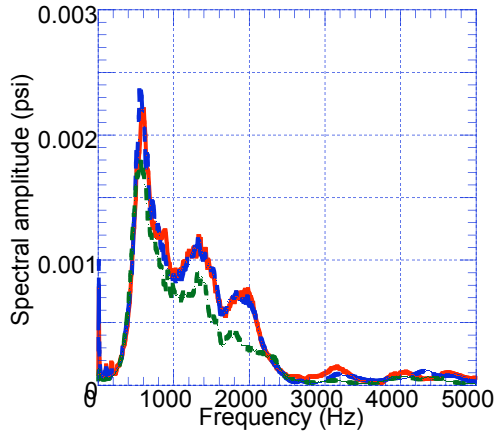

(c) Tap #3

Figure 6.11: Effect of equivalence ratio from modifying O_2 mass flowrate with acoustic excitation from the standard injector side.

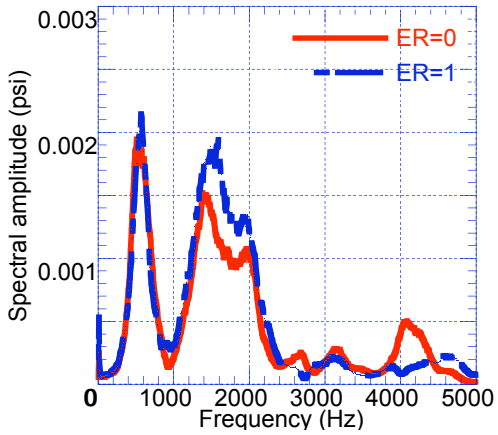

(a) Tap #1

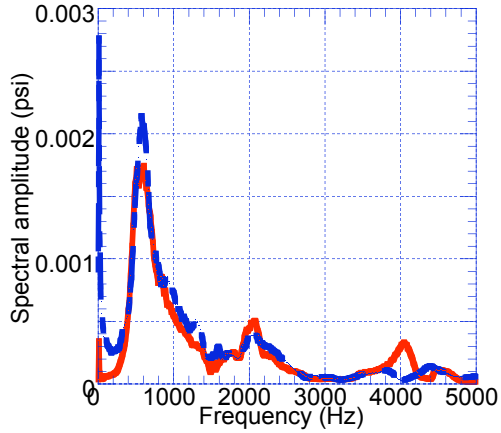

(b) Tap #2

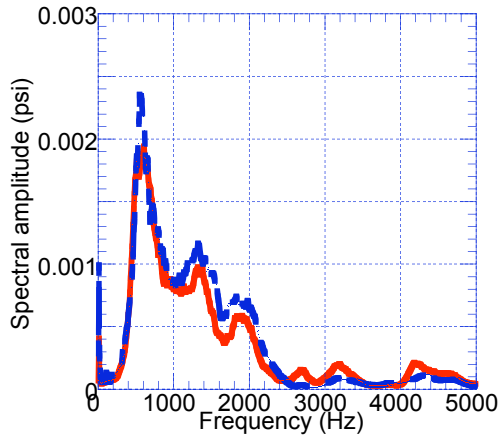

(c) Tap #3

Figure 6.12: Effect of equivalence ratio from shutting down O_2 mass flow with acoustic excitation from the standard injector side.

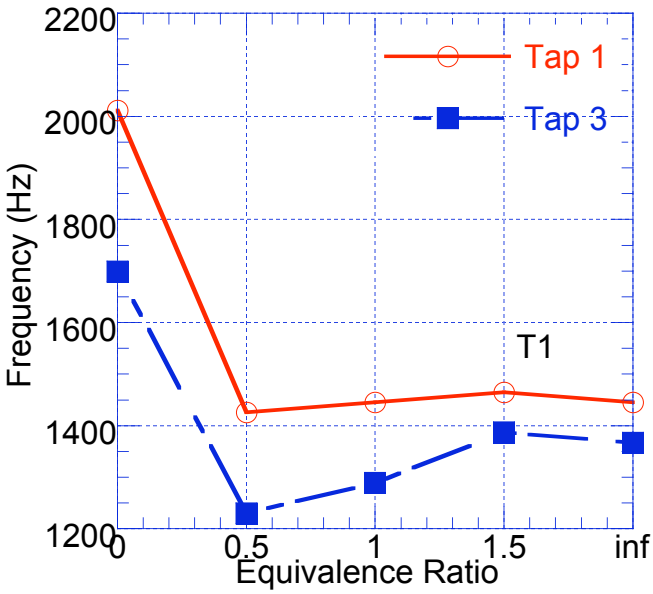

(a) Frequency shift with acoustic excitation from specially-controlled injector side

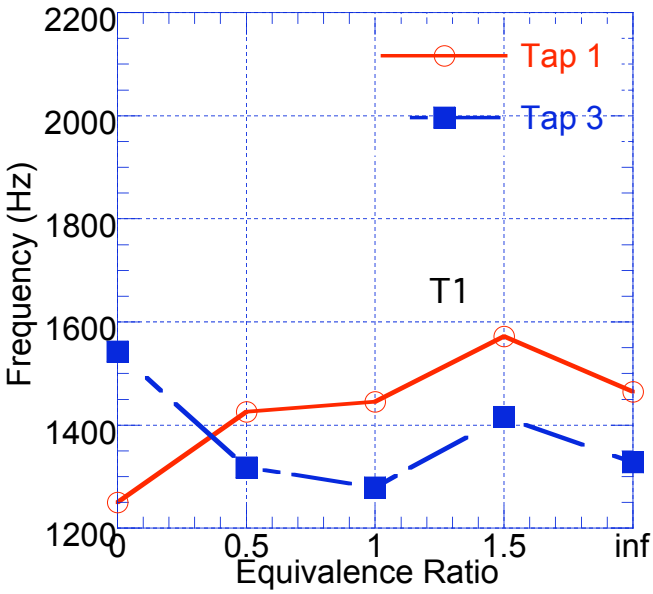

(b) Frequency shift with acoustic excitation from standard injector side

Figure 6.13: Frequency shift due to equivalence ratio between the fuel and oxidizer.

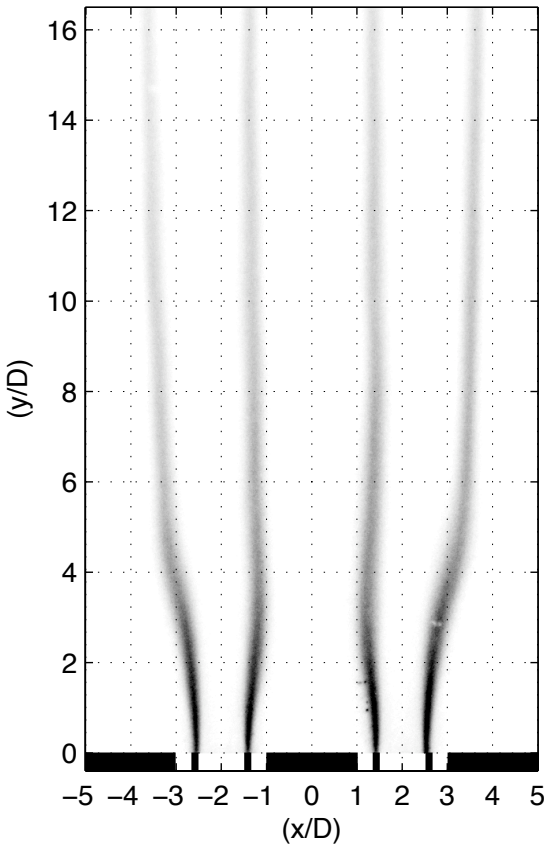

Figure 6.14: Flame structure for the baseline case. Acoustic driver is on the left side.

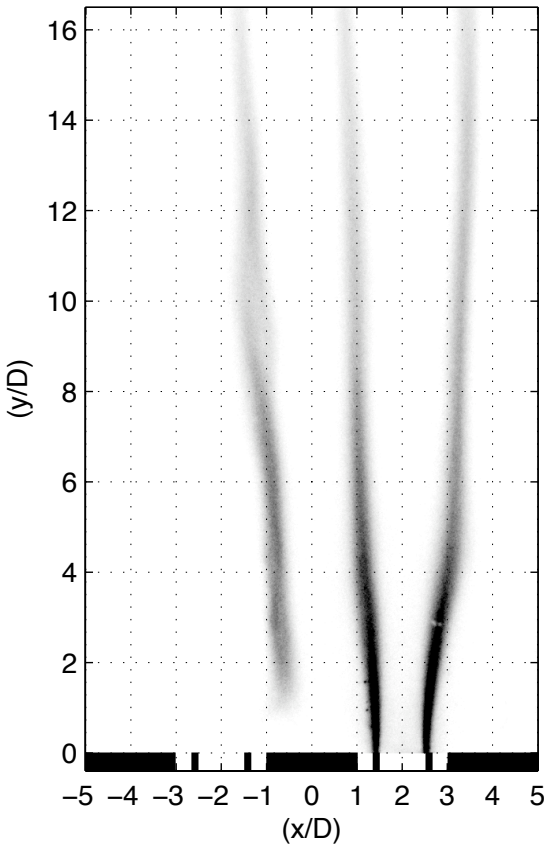

Figure 6.15: Flame structure with H_2 mass flow shut down and acoustic excitation from the specially-controlled injector side. Acoustic driver is on the left side.

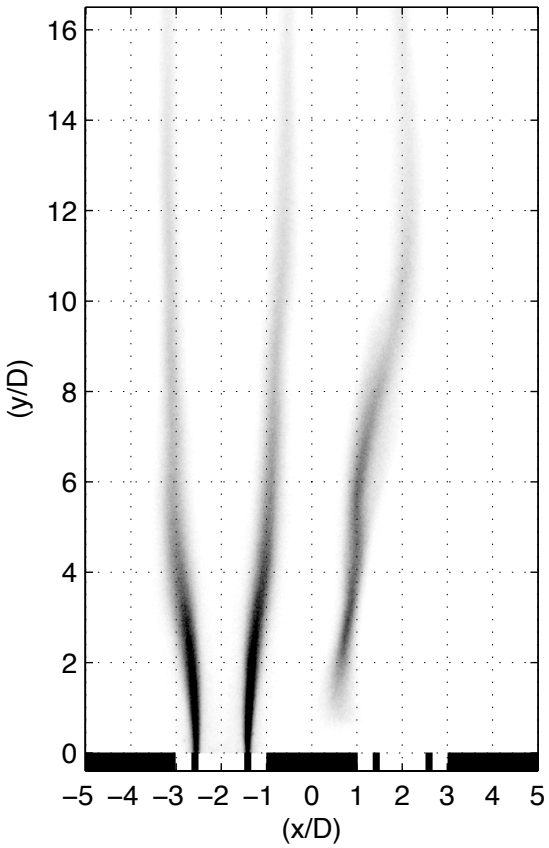

Figure 6.16: Flame structure with H_2 mass flow shut down and acoustic excitation from the standard injector side. Acoustic driver is on the left side.

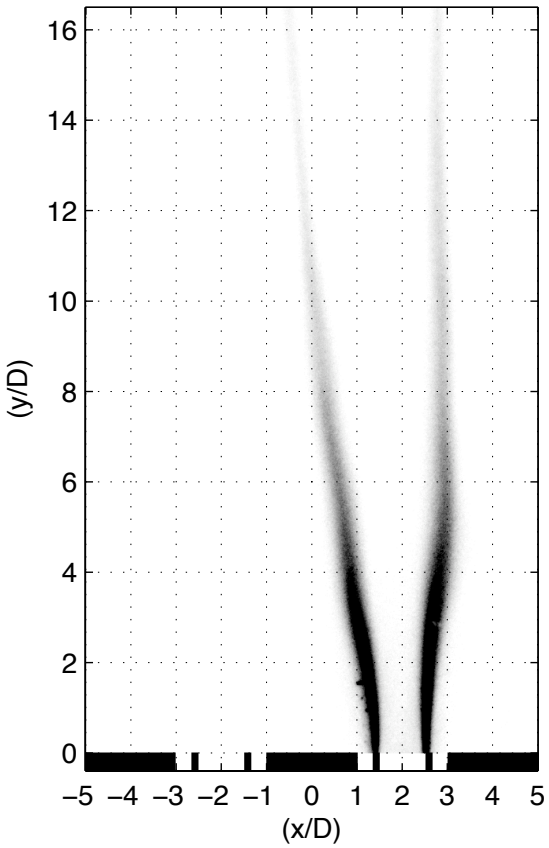

Figure 6.17: Flame structure with O_2 mass flow shut down and acoustic excitation from the specially-controlled injector side. Acoustic driver is on the left side.

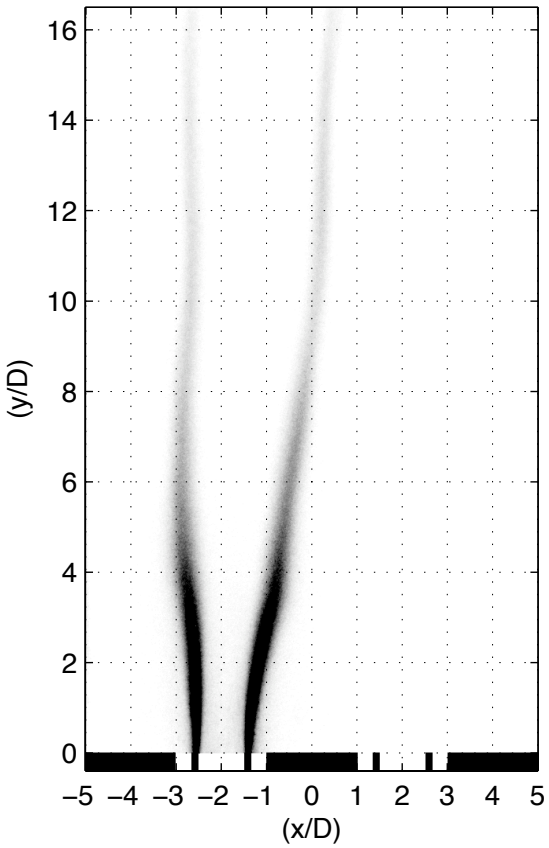

Figure 6.18: Flame structure with O_2 mass flow shut down and acoustic excitation from the standard injector side. Acoustic driver is on the left side.

Chapter 7

Conclusions and Future Work

7.1 Conclusions

In liquid rocket engine thrust chambers, particularly in the vicinity of the injector, flame-acoustic interactions may bring about large-amplitude self-sustaining combustion oscillations from small acoustic disturbances. Basic physical mechanisms of acoustically-driven combustion instabilities involving shear coaxial injectors were experimentally studied using gaseous H_2-O_2 turbulent diffusion flames in two-dimensional model combustors. Experiments were conducted in two different model combustors that were designed to capture the unit physics of the flame-acoustic interaction in a single-element injector configuration as well as in a double-element injector configuration. Also, the concepts and evidence supporting a novel combustion instability suppression strategy that could be analogous to acoustic baffles used in thrust chambers were presented.

The white noise excitation approach adopted in the present research proved to

be a valuable tool not only for identifying the dominant acoustic modes of the combustors but also for comparing combustion control effectiveness by measuring the quantitative shift in the local acoustic behavior. Flame-acoustic interaction experiments were conducted by establishing turbulent flames from each model injector and subjecting them to controlled acoustic excitation waves via the compression driver, mounted in the transverse direction. Band-limited white noise was utilized as the forcing input signal to the driver, and the forced combustor response was characterized by measuring the resulting pressure oscillations and the dynamic flame behavior. By comparing the spectral responses, any changes in acoustic resonance characteristics could be quantified and used for control performance evaluation as demonstrated in this thesis work.

A novel idea of mixing heavier CH_4 into the H_2 fuel to reduce flame-acoustic interaction was conceived and tested. It was recently noted that the large density difference between O_2 and H_2 could amplify the heat release disturbance when compression waves interacted with the diffusion flames, making the interface more susceptible to baroclinic torques. In an attempt to minimize this effect, the fuel was made denser while holding the same equivalence ratio, thus allowing limited control over the fuel-oxidizer density gradient. The results showed that the general characteristics of the unforced flames were unaffected by a moderate amount of methane addition. However, the effect on combustion oscillations turned out to be quite significant as the controlled flames became much more resistant to acoustic disturbances from the compression driver.

The quantitative effect of fuel density on the acoustic characteristics of the

chamber was investigated using the mixture of CH_4 and H_2 in the single-injector configuration. While the CH_4 mole fraction in the fuel was varied between 1% and 63% during the tests, the acoustic resonance characteristics of the model injector remained qualitatively similar. Some of the resonant frequencies decreased with increasing CH_4 concentration and the peak amplitudes were also affected due to changes in the local acoustic impedance. In non-reacting tests, the resonance of the quarter-wave mode associated with the oxidizer post was relatively unaffected, but the frequency of the three-quarter-wave chamber mode decreased by 15% with 18% CH_4 addition. Transverse-mode resonance was also altered significantly due to the changes in the speed of sound and the local acoustic impedances. In reacting tests, acoustic modes associated with the oxidizer post changed slightly with the fuel composition possibly due to the changes in product temperature and the heat transfer into the inlet. The dominant longitudinal mode of the chamber exhibited a frequency change of as much as 16% with the CH_4 addition.

Interaction between flames and traveling waves was simulated by acoustically forcing the combustion system at a fixed frequency far removed from any resonance. The selected frequency of 1150 Hz represented a local spectral minimum. It was expected that excitation at this frequency would not result in any standing wave pattern, thus establishing a distinct wave direction from the compression driver. Severe flame wrinkling was observed on one side of the flames in the H_2-O_2 case. Global and local measurements of OH* chemiluminescence indicated periodic heat release modulation at various frequencies including the forcing frequency. Simultaneous measurements of local pressure fluctuations and chemiluminescence showed

that acoustic pressure oscillations affected spatial fluctuations in OH* chemiluminescence. The selective presence of high frequency components of heat release riding on a low frequency component of heat release was observed indicating a possible case of local Rayleigh-Taylor instability.

Single frequency forcing tests were conducted also with the blended CH_4-H_2 fuel. Again, the flames from the blended fuel wrinkled much less than the H_2 flames under the same forcing conditions. These results suggested the possibility of using the blended H_2-CH_4 fuel to control the fuel-oxidizer density gradient which in turn affects the susceptibility to flame-acoustic interaction. To further assess the active control potential of real-time in-situ CH_4 addition, both transient and steady state characteristics of CH_4 addition into primary H_2 flow were investigated using high speed imaging and simultaneous dynamic pressure and chemiluminescence measurements. Local Rayleigh indices at selected points on the flame oscillation path before and after CH_4 addition were tracked. It was shown that the transient process typically took 150 - 180 ms of settling time, which was much longer than the oscillation period. This implies the fuel blending technique would not be suitable for high-speed real-time active instability control. Nonetheless it could be used to prevent instabilities from developing.

A novel strategy of preventing the combustion instabilities in liquid rocket engine is presented on the basis of the new understanding of the effect of fuel density on flame-acoustic interactions. Arrays of flow-controlled injectors arranged in a spatial pattern similar to the layout of baffles could be effective in modifying the local acoustic impedance as shown in this thesis. Both the fuel composition change and

the fuel-oxidizer ratio affected the local acoustic characteristics although by different amounts. Unlike a typical active control strategy in which high-frequency propellant modulation would be required, the present strategy relies on a quasi steady-state tailoring of the local acoustic characteristics similar to the mechanism underlying baffles. Demonstration experiments were conducted in the double-element injector configuration to assess the feasibility of the new control strategy. Use of the CH_4-H_2 blended fuel resulted in up to 18% modification in the spectral peak frequency. Another strategy, which involved using only the original H_2 and O_2 propellants but altering the equivalence ratio of the special injectors, also resulted in changes to pressure spectrum shape and amplitude. The current work opens up the possibility of developing a flexible combustion control methodology.

7.2 Findings and Key Contributions

7.2.1 New Control Strategies for Suppressing Combustion Instability

Novel flow-based strategies to suppress flame-acoustic instability in liquid rocket engines were established and demonstrated in the current research. These new control methodologies offer the potential for more thrust, eliminate the weight and cooling penalties, and reduce cut-and-try design cycles associated with hardware baffles. They can also mitigate systemic risk due to combustion instability and potentially extend the overall range of safe operating conditions. This opens up the

possibility for improved overall rocket system performance and greater flexibility.

- Specially-controlled reactant injectors are the basis for the methods developed. These injectors operate with different fluid configurations from the standard injectors when combustion instability tends to be a problem. The non-uniform injectant pattern results in a modified acoustic environment within the combustion chamber. The controlled injectors can be returned to flow configurations identical to the bulk of the injectors when the engine is no longer operating at or near critical conditions.

- Two different propellant control strategies were examined: the use of a blended fuel in specially-modulated injectors by introducing CH_4 as a secondary fuel to H_2, and modification of the equivalence ratio at specially-modulated injectors by altering the mass flowrate of H_2 or O_2.

7.2.2 Physical Mechanisms of the Strategies

The specially-controlled injectors are configured to perform a role analogous to hardware baffles by regulating the local acoustic impedance. These injectors are associated with a local acoustic impedance field that differs substantially from the injectors that are operating at the standard conditions (typically stoichiometric). When they were employed experimentally, substantial changes in the acoustic impedance environment were observed and dominant acoustic modes in the combustion chamber exhibited shifts in their associated frequencies.

- Variation of the speed of sound with local fuel composition, and corresponding

variation in acoustic impedances was one of the mechanisms underlying the effectiveness of the blended fuel approach. Mixing CH_4 with H_2 modified the fuel density and changed the speed of sound as well.

- Acoustic energy suppression by discouraging conditions favorable for thermo-acoustic instability was another physical mechanism when CH_4 was used. With more CH_4 in the blended fuel, the flame response to the acoustic traveling wave was suppressed due to the lessened density gradient between fuel and oxidizer.

- Acoustic speed was tailored through flame structure modification via propellant rate control, without the use of a secondary fuel. Mass flow rate modulation of the original H_2 and O_2 propellants was effective in this manner.

7.2.3 Effectiveness of the Strategies

The effectiveness of the two control methods was demonstrated in a double shear-coaxial injector element combustor. One element was specifically-modulated, while the other was operated using standard parameters. The mechanism focused on one of the transverse modes of the model combustor, which represented either a tangential or radial mode in a full-scale liquid rocket engine.

- In the experiments employing H_2-CH_4 blended fuel in the controlled injector, all peak frequencies were found to shift to a lower value with increasing CH_4 proportion. This was due to the changes in the acoustic impedance associated with the controlled injector.

- For the scheme in which the controlled injector's equivalence ratio was altered, the pressure spectrum across the chamber was not affected to a significant extent until the H_2 mass flow was turned off (zero equivalence ratio). Turning off the oxidizer mass flowrate (∞ equivalence ratio) was not as effective as turning off the fuel.

- From a practical perspective, turning off the fuel may not be optimal due to the potentially corrosive effect of oxygen flow in the thrust chamber. Turning off the oxidizer in certain injectors during operation in regimes of impending combustion instability may be one way to apply fluidic control to suppress the flame-acoustic instability.

7.3 Future Work

The current work provided the basic physical and control effectiveness demonstrations for suppressing flame-acoustic interaction through unit physics experiments. However there are still some issues that need to be addressed in order to fully understand the physical processes and apply the control methodology to liquid rocket engines. Firstly, it is important to examine the flame response in a three-dimensional two-phase flow configuration, as the current experimental setup is limited to two- dimensional single phase flow. Secondly, in this lab scale combustor the Reynolds number is scaled down to approximately 5500. More experimental studies at full-scale Reynolds numbers are required to obtain more insight. Finally, in flight-grade liquid rockets, both fuel and oxidizer are cryogenic fluids. Therefore

the fuel temperature is a key factor in the application of these experimental results. It is recommended to perform similar tests with cryogenic fuel and oxidizer to study the instability mechanisms associated with the atomization and vaporization processes.

The present research and most of the prior work have used single-element and double-element injectors to examine the flame behavior of propellants in order to predict the injector performance. However, there are hundreds of injectors element in actual rocket, as shown in Figure 3.5. It is necessary to extend experimental investigations to sub-scale combustors with multiple (20-40) injectors to verify the effectiveness of the strategies presented in this work in more representative configurations. These tests can also be used to determine optimal layouts of the specially-modulated injectors. The application of these propellant injection control methods to full-scale development engines is recommended if the sub-scale test results are promising. The layout pattern and mass flowrates of the specially-controlled injectors can be further tuned, as they would then be in the most realistic operating environments.

Computational Fluid Dynamics (CFD) tools are widely used to assist in the design of aerothermodynamic devices such as rocket engines. However, such tools are presently unable to accurately predict and model combustion instability because the physical and chemical mechanisms are still not well understood. The current lab-scale experimental data can provide verification and validation for reacting flow CFD solvers with respect to flame-acoustic interactions. It will be easier to start with the simple 2-D model configuration to validate CFD models. CFD codes should

be used to predict the reacting flow fields with acoustic excitation for sub-scale and full-scale tests once they are validated with the experimental data. Use of accurate CFD simulations can help reduce the need for expensive experiments.

Bibliography

[1] Harrje, D. and (eds.), F. R., "Liquid Propellant Rocket Combustion Instability," *NASA SP-194*, 1972.

[2] Crocco, L. and Cheng, S. I., *Theory of Combustion Instability in Liquid Propellant Rocket Motors*, AGARD monograph, Butterworths Scientific Publications, 1956.

[3] Price, E., *Combustion Instabilities in Solid Propellant Rocket Motors*, Astronautica Acta, 1959.

[4] Zinn, B. and Powell, E., "Nonlinear Combustion Instability in Liquid Propellant Rocket Engines," *Thirteenth Symposium (International) on Combustion, The Combustion Institute*, 1971, pp. 491–503.

[5] Culick, F. E. C. and Yang, V., "Overview of Combustion Instabilities in Liquid-Propellant Rocket Engines," *Liquid Rocket Engine Combustion Instability, Progress in Astronautics and Aeronautics*, Vol. 169, 1995, pp. 3–37, AIAA, Washintong DC.

[6] Hulka, J. and Hutt, J. J., "Instability Phenomena in Liquid Oxygen/Hydrogen Propellant Rocket Engines," *Liquid Rocket Engine Combustion Instability, Progress in Astronautics and Aeronautics*, Vol. 169, 1995, pp. 39–72, AIAA, Washintong DC.

[7] Yang, V. and Culick, F., "Analysis of Low Frequency Combustion Instabilities in a Laboratory Ramjet Combustor," *Combustion Science and Technology*, Vol. 45, 1986, pp. 1–25.

[8] Schadow, K. and Gutmark, E., "Combustion Instability to Vortex Shedding in Dump Combustors and Their Passive Control," *Progress in Energy Combustion and Science*, Vol. 18, No. 2, 1992, pp. 117–132.

[9] Hedge, U., Reuter, D., Daniel, B., and Zinn, B., "Flame Driving of Longitudinal Instabilities in Dump Type Ramjet Combustors," *Combustion Science and Technology*, Vol. 55, 1987, pp. 125–138.

[10] Yu, K., Lee, S., Trouve, A., Stewart, H., and Daily, J., "Vortex Nozzle Interactions in Ramjet Combustors," AIAA Paper No. AIAA-87-1871.

[11] Yu, K., Trouve, A., and Daily, J., "Low-Frequency Pressure Oscillation in a model ramjet combustor," *Journal of Fluid Mechanics*, Vol. 232, 1991, pp. 47–72.

[12] Schadow, K., Wilson, K., and Gutmark, E., "Characterization of Large Scale Structures in a Forced Ducted Flow with Dump," *AIAA Journal*, Vol. 25, No. 9, 1987, pp. 1164–1170.

[13] Langhorne, P., "Reheat Buzz: An Acoustically Coupled Combustion Instability. Part 1. Experiment," *Journal of Fluid Mechanics*, Vol. 193, 1988, pp. 417–443.

[14] Bloxsidge, G., Dowling, A., and Langhorne, P., "Reheat Buzz: An Acoustically Coupled Combustion Instability. Part 2. Theory," *Journal of Fluid Mechanics*, Vol. 193, 1988, pp. 445–473.

[15] Putnam, A., *Combustion-Driven Oscillations in Industry*, Elsevier, New York, 1971.

[16] Rayleigh, G., *The Theory of Sound*, Vol. 2, Dover Publications, 1945.

[17] Putnam, A. and Dennis, W., "A Study of Burner Oscillations of the Organ-Pipe Type," *Trans. A.S.M.E.*, Vol. 75, No. 1, 1953, pp. 15–28.

[18] Zinn, B., "Pulse Combustion: Recent Applications and Research Issure," *Twenty-Fourth Symposium (International) on Combustion, The Combustion Institute*, 1992, pp. 1297–1305.

[19] Culick, F., "Nonlinear Behavior of Acoustic Waves in Combustion Chambers Parts I and II," *Acta Astronautica*, Vol. 3, 1976, pp. 714–757.

[20] Culick, F., "A Note on Rayleigh Criterion," *Combustion Science and Technology*, Vol. 56, 1987, pp. 159–166.

[21] Sterling, J., *Longitudinal Mode Instabilities in Air Breathing Engines*, Ph.D. thesis, California Institute of Technology, 1987.

[22] Sterling, J. and Zukoski, E., "Nonlinear Dynamics of Laboratory Combustor Pressure Oscillations," *Combustion Science and Technology*, Vol. 77, 1991, pp. 225–238.

[23] Gaydon, A. and Wolfhard, H., *Flames, Their Structure, Radiation and Temperature*, Chapman & Hall, 1960, Chap. VII.

[24] Toong, T., Salant, R., Stopford, J., and Anderson, G., "Mechanisms of Combustion Instability," *Tenth Symposium (International) on Combustion, The Combustion Institute*, 1965, pp. 1301–1313.

[25] Price, E., "Recent Advances in Solid Propellant Combustion Instability," *Twelfth Symposium (International) on Combustion, The Combustion Institute*, 1969, pp. 101–113.

[26] Marxman, F. and Wooldridge, C., "Finite-Amplitude Axial Instability in Solid-Rocket Combustion," *Twelfth Symposium (International) on Combustion, The Combustion Institute*, 1969, pp. 115–127.

[27] Sirignano, W., "A Theory of Axial-Mode Shock-Wave Oscillations in a Solid Rocket Combustor," *Twelfth Symposium (International) on Combustion, The Combustion Institute*, 1969, pp. 129–137.

[28] Thring, M., "Combustion Oscillations in Industrial Combustion Chambers," *Twelfth Symposium (International) on Combustion, The Combustion Institute*, 1969, pp. 163–168.

[29] Kydd, P., "Analysis and Experiments on Unsteady Flow in Gas Turbine Main Combustors," *Twelfth Symposium (International) on Combustion, The Combustion Institute*, 1969, pp. 183–192.

[30] Williams, F., *Combustion Theory*, Benjamin Cummings, Menlo Park, CA, 1984, chapter 9, pp. 294-372.

[31] Laverdant, A., Poinsot, T., and Candel, S., "Mean Temperature Field Effect on Acoustic Mode Structure in Dump Combustor," *Journal of Propulsion and Power*, Vol. 2, 1986, pp. 311–316.

[32] Candel, S., "Combustion Instabilities Coupled by Pressure Waves and Their Active Control," *Twenty-Fourth Symposium (International) on Combustion, The Combustion Institute*, 1992, pp. 1277–1296.

[33] Kendrick, D., Zsak, T., and Zukoski, E., "An Experimental and Numerical Investigation of Premixed Combustion in a Vortex in a Laboratory Dump Comubstor," *Unsteady Combustion*, 1996, pp. 33–69, F.Culick et al. (eds.) Kluwer Academic Publishers.

[34] Sreenivasan, K. and Raghu, S., "The Control of Combustion Instability: A Perspective," *Current Science*, Vol. 79, No. 6, 2000, pp. 867–883.

[35] Chu, B., "On the Energy Transfer to Small Disturbances in Fluid Flow," *Acta Mechanica*, Vol. 1, 1965, pp. 215–234.

[36] Crocco, L., Grey, J., and Harrje, D., "Theory of Liquid Propellant Rocket Combustion Instability and its Experimental Verification," *ARS Journal*, Vol. 30, 1960, pp. 159–168.

[37] Crocco, L., "Theoretical Studies on Liquid Propellant Rocket Instability," *Tenth Symposium (International) on Combustion, The Combustion Institute*, 1965, pp. 1101–1128.

[38] Crocco, L., "Research on Combustion Instability in Liquid Propellant Rockets," *Twelfth Symposium (International) on Combustion, The Combustion Institute*, 1969, pp. 85–99.

[39] Summerfield, M., "A Theory of Unstable Combustion in Liquid Propellant Rocket Systems," *ARS Journal*, Vol. 21, No. 5, 1951, pp. 108–114.

[40] Gunder, D. and Friant, D., "Stability of Flow in a Rocket Motor," *Journal of Applied Mechanics*, Vol. 17, 1950, pp. 327–333.

[41] Yachter, M., "Discussion of the Paper by Gunder, D.F. and Friant, D.R." *Journal of Applied Mechanics*, Vol. 18, 1951, pp. 114–116.

[42] Crocco, L., "Aspects of Combustion Instability in Liquid Propellant Rockets," *Journ. Amer. Rocket Soc.*, Vol. 21, 1951, Part I.

[43] Crocco, L., "Aspects of Combustion Instability in Liquid Propellant Rockets," *Journ. Amer. Rocket Soc.*, Vol. 22, 1952, Part II.

[44] Berman, K. and Cheney, S., "Combustion Studies in Rockets Motors," *Journ. Amer. Rocket Soc.*, Vol. 23, No. 2, 1953.

[45] Ellis, H., Odgers, I., Stosick, A., Van, D., and Wick, R., "Experimental Investigation of Combustion Instability in Rocket Motors," *Fourth Symposium (International) on Combustion, The Combustion Institute*, 1953.

[46] Ellis, H., *Liquid Propellant Rocket Combustion Research*, Edwin G. Baetger, II Colloquium, 1960, Princeton University, Feb 9.

[47] Male, T., Kerslake, W., and Tischler, A., "Photographic Study of Rotary Screaming and Other Oscillations in a Rocket Engine," 1954, NACA-RM-E54A29.

[48] Maslen, S. and Moore, F., "On Strong Transverse Waves Without Shocks in a Circular Cylinder," *Journ. Aero Sci.*, Vol. 23, No. 6, 1956, pp. 583–593.

[49] Osborn, J. and Bonnell, J., "On the Importance of Combustion of Combustion Chamber Geometry in High Frequency Oscillations in Rocket Motors," 1960, ARS Semi-Annual Meeting, Los Angeles, California.

[50] Pickford, R. and Peoples, R., "The Inherent Stability of the Combustion Processes," 1960, ARS 15th Annual Meeting, Washington, D.C.

[51] Reardon, F., *An Investigation of Transverse Mode Combustion Instability in Liquid Propellant Rocket Motors*, Ph.D. thesis, Princeton University, 1961.

[52] Barsotti, R., Datsko, S., Louison, R., Kovach, R., Miller, D., and Pulliam, W., "Development of Liquid Oxygen/Liquid Hydrogen Thrust Chamber for the M-1 Engine," 1968, NASA-CR-54813.

[53] Culick, F. E. C., "Combustion Instabilities in Liquid-fueld Propulsion Systems: an Overview," *AGARD NATO*, 1988, Presented at AGARD Conf. Combust. Instabil. Liquid-Fueled Prop. Syst., Seuille-Sur-Sine.

[54] Mitchell, C., "Analytical Models for Combustion Instability," *Liquid Rocket Engine Combustion Instability, Progress in Astronautics and Aeronautics*, Vol. 169, 1995, pp. 403–430, AIAA, Washintong DC.

[55] Barrere, M. and Williams, F., "Combustion Oscillations in Industrial Combustion Chambers," *Twelfth Symposium (International) on Combustion, The Combustion Institute*, 1969, pp. 169–181.

[56] "Liquid Rocket Engine Combustion Stabilization Devices," *NASA SP-8113*, 1974.

[57] Baer, M. and Mitchell, C., "Theoretical Evaluation of Rigid Baffles in Suppression of Combustion Instability," *AIAA Journal*, Vol. 15, No. 2, 1977, pp. 212–217.

[58] Mitchell, C., Howell, D., Dodd, F., and Acker, T., "User's Manual for the Multidimensional Baffle Model Computer Programs," 1987, Mechanical Engineering Report.

[59] J.M. Wicker, M. Y. and Yang, V., "Linear and Nonlinear Pressure Oscillations in Baffled Combustion Chambers," *Journal of Sound and Vibration*, Vol. 184, 1995, pp. 141–171.

[60] Male, T. and Kerslake, W., "A Method for Prevention of Screaming in Rocket Engines," 1954, NACA-RM-E54F28A.

[61] Harrje, D., Stinger, W., and Sirignano, W., "Flow Behavior with Acoustic Liners," 1967, ICRPG 4th Combustion Conference, Menlo Park, California.

[62] Laudien, E., Pongratz, R., Pierro, R., and Preclik, D., "Experimental Procedures Aidding the Design of Acoustic Cavities," *Liquid Rocket Engine Combustion Instability, Progress in Astronautics and Aeronautics*, Vol. 169, 1995, pp. 377–399, AIAA, Washintong DC.

[63] Wanhainen, J., Bloomer, H., Vincent, D., and Curley, J., "Experimental Investigation of Acoustic Liners to Suppress Screech in Hydrogen-Oxygen Rockets," 1967, NASA-TN-D-3822.

[64] Sirignano, W., Crocco, L., and Harrje, D., "Acoustic Liner Studies," No. 138, 1967, ICRPG 3rd Combustion Conference, CPIA Publication.

[65] Gysling, D., Copeland, G., McCormick, D., and Proscia, W., "Combustion System Damping Augmentation with Helmholtz Resonators," *Journ. Eng. Gas Turbines Power-Trans. ASME*, Vol. 122, No. 2, 2000.

[66] Bellucci, V., Rohr, P., Paschereit, C., and Magni, F., "On the Use of Helmholtz Resonators for Damping Acoustic Pulsations in Industrial Gas Turbines." *Journ. Eng. Gas Turbines Power-Trans. ASME*, Vol. 126, No. 2, 2004.

[67] Pandalai, R. and Mongia, H., "Combustion Instability Characteristics of Industrial Engine Dry Low Emission Combustion System," 1998, AIAA Paper No. AIAA-1998-3379.

[68] Richards, G., Straub, D., and Robey, E., "Passive Control of Combustion Dynamics in Stationary Gas Turbines," *Journal of Propulsion and Power*, Vol. 19, No. 5, 2003, pp. 795–810.

[69] Tsien, H., "Servo-Stabilization of Combustion in Rocket Motors," *ARS Journal*, Vol. 22, 1952, pp. 256–263.

[70] Marble, F. and Cox, D., "Servo-Stabilization of Low-Frequency OScillations in a Liquid Bipropellant Rocket Motor," *ARS Journal*, Vol. 23, 1953, pp. 63–74.

[71] Lee, Y., Gore, M., and Ross, C., "Stability and Control of Liquid Propellant Rocket Systems," *ARS Journal*, Vol. 23, 1953, pp. 75–81.

[72] Ffowcs-Williams, J., "Anti-Sound," *Proceedings of Royal Society of London*, Vol. A395, 1984, pp. 63–88.

[73] Dine, P., *Active Control of Flame Noises*, Ph.D. thesis, Cambridge University, 1983.

[74] Heckl, M., *Heat Sources in Acoustic Resonators*, Ph.D. thesis, Cambridge University, 1985.

[75] Heckl, M., "Active Control of the Noise form a Rijke Tube," *IUTAM Symposium on Aero- and Hydro-Acoustics, Lyon 1985, Springer-Verlag*, 1986, pp. 211–216.

[76] Bloxsidge, G., Dowling, A., Hooper, N., and Langhorne, P., "Active Control of Reheat Buzz," AIAA Paper No. AIAA-87-0433.

[77] Bloxsidge, G., Dowling, A., Hooper, N., and Langhorne, P., "Active Control of an Acoustically Driven Combustion Instability," *Journal of Theoretical and Applied Mechanics*, Vol. 6, 1987, pp. 161–175.

[78] Lang, W., Poinsot, T., and Candel, S., "Active Control of Combustion Instability," *Combustion and Flame*, Vol. 70, 1987, pp. 281–289.

[79] Poinsot, T., Bourienne, F., Candel, S., Esposito, E., and Lang, W., "Suppression of Combustion Instabilities by Active Control," *Journal of Propulsion and Power*, Vol. 5, 1987, pp. 14–20.

[80] Poinsot, T., Veynante, D., Bourienne, F., Candel, S., Esposito, E., and Surget, J., "Initiation and Suppression of Combustion Instabilities by Active Control," *Proceedings of the 22nd Symposium (International) on Combustion*, 1988, pp. 1363–1370.

[81] Langhorne, P., Dowling, A., and Hooper, N., "Practical Active Control System for Combustion Oscillations," *Journal of Propulsion and Power*, Vol. 6, No. 3, 1990, pp. 324–333.

[82] Chu, Y., Dowling, A., and Glover, K., "Robust Control of Combustion Oscillations," Proc. 1998 IEEE, Int. Conf. Control Applications,Trieste, Italy.

[83] Moran, A., Steele, D., and Dowling, A., "Active Control and its Applications," 2000, Presented at Proc. RTO AVT Symp. Active Control Tech. Enhanced Performance Operational Capabilities Military Aircraft, Land Vehicles Sea Vehicles, Braunschweig, Germany. Neuilly-Sur-Seine, France:RTO, NATO.

[84] Seume, J., Vortmeyer, N., Krause, W., Hermann, J., Hantschk, C., and Zangl, P., "Application of Active Combustion Instability Control to a Heavy Duty Gas Turbine," *J. Eng. Gas Turbines Power*, Vol. 120, 1998, pp. 721–726.

[85] Hoffmann, S., Weber, G., Judith, H., Hermann, J., and Orthmann, A., "Application of Active Combustion Control to Siemens Heavy Duty Gas Turbines," 1998, Proc. RTO AVT Symp. Gas Turbine Engine Combust. Emiss. Altern. Fuels, Lisbon, Portugal. Neuilly-Sur-Seine, France:RTO, NATO.

[86] Cohen, J., Rey, N., Jacobson, C., and Anderson, T., "Active Control of Combustion Instability in a Liquid-Fueled Low-Nox Combustor," *J. Eng. Gas Turbines Power*, Vol. 121, 1999, pp. 281–284.

[87] Hibshman, J., Cohen, J., Banaszuk, A., Anderson, T., and Alholm, H., "Active Control of Combustion Instability in Liquid-Fueled Sector Combustor," 1999, Presented at ASME-99-GT-215 Indianapolis. New York: ASME.

[88] Neumeier, Y. and Zinn, B., "Experimental Demonstration of Active Control of Combustion Instabilities using Real Time Modes Observation and Secondary

Fuel Injection," *Twenty-sixth Symposium (International) on Combustion, The Combustion Institute*, 1996.

[89] Johnson, C., Neumeier, Y., Neumaier, M., Zinn, B., Darling, D., and Sattinger, S., "Demonstration of Active Control of Combustion Instability on a Full-Scale Gas Turbine Combustor," 1999, Presented at ASME Turbo. Expo., 2001-GT-0519 New Orleans, Louisiana. New York: ASME.

[90] Crocco, L., Grey, J., and Harrje, D., "Theory of Liquid Propellant Rocket Combustion Instability and Its Experimental Investigations," *ARS Journal*, Vol. 30, 1960, pp. 159–168.

[91] Sutton, G. P. and Biblarz, O., *Rocket Propulsion Elements*, A Wiley-Interscience publication, seventh ed., 2000.

[92] Oefelein, J. and Yang, V., "Comprehensive Review of Liquid Propellant Combustion Instabilities in F-1 Engines," *Journal of Propulsion and Power*, Vol. 9, No. 5, 1993, pp. 657–677.

[93] Docquier, N. and Candel, S., "Combustion Control and Sensors: A Review," *Prog. Energy Combust. Sci.*, Vol. 28, 2002, pp. 107–150.

[94] Ghosh, A., *The Role of Density Gradient in Liquid Rocket Engine Combustion Instability*, Ph.D. thesis, University of Maryland, 2008.

[95] Luke, E., *A Rule-Based Specification System for Computational Fluid Dynamics*, Ph.D. thesis, Mississippi State University, 1999.